UFBA

UNIVERSIDADE FEDERAL DA BAHIA
ESCOLA POLITÉCNICA
PROGRAMA DE PÓS GRADUAÇÃO EM
ENGENHARIA INDUSTRIAL - PEI

DOUTORADO EM ENGENHARIA INDUSTRIAL

RAONY MAIA FONTES

An MPC auto-tuning framework for tracking economic goals of ESP-lifted oil wells

PEI

Programa de Pós-Graduação em Engenharia Industrial

AN MPC AUTO-TUNING FRAMEWORK FOR TRACKING ECONOMIC GOALS OF ESP-LIFTED OIL WELLS

Raony Maia Fontes

Dissertation presented to PEI/UFBA as a partial fulfillment of the requirements for the degree of Doctor of Science (D.Sc.).

Orientador: Márcio André Fernandes Martins

Salvador

Agosto de 2023

AN MPC AUTO-TUNING FRAMEWORK FOR TRACKING ECONOMIC GOALS OF ESP-LIFTED OIL WELLS

RAONY MAIA FONTES

Tese submetida ao corpo docente do programa de pós-graduação em Engenharia Industrial da Universidade Federal da Bahia como parte dos requisitos necessários para a obtenção do grau de doutor em Engenharia Industrial.

Examinada por:

Prof. Dr. Márcio André Fernandes Martins _____
Doutor em Eng. Química, pela Universidade de São Paulo, Brasil, 2014

Documento assinado digitalmente
MARCIO ANDRE FERNANDES MARTINS
Data: 17/08/2023 11:36:58-0300
Verifique em https://validar.iti.gov.br

Prof. Dr. Antonio Carlos Zanin _____
Doutor em Eng. Química, pela Universidade de São Paulo, Brasil, 2001

Prof. Dr. Bruno Faccini Santoro _____
Doutor em Eng. Química, pela Universidade de São Paulo, Brasil, 2015

Profa. Dra. Luz Adriana Alvarez Toro _____
Doutora em Eng. Química, pela Universidade de São Paulo, Brasil, 2012

Prof. Dr. Luís Cláudio Oliveira Lopes _____
Doutor em Eng. Química, pela Lehigh University, USA, 2000

Documento assinado digitalmente
LUIS CLAUDIO OLIVEIRA LOPES
Data: 16/08/2023 07:15:15-0300
Verifique em https://validar.iti.gov.br

Salvador, BA - BRASIL
agosto/2023

Agradecimentos

Agradeço aos meus amigos, Anderson, Carine, Cibele, Daniel, Erbet, Reiner, Rodrigo, que são como as camadas de um modelo de rede neural, que se unem para formar um sistema poderoso e preciso. Juntos, compartilhamos conhecimentos, debatemos ideias e nos ajudamos em momentos de dificuldade. Sem dúvida, essa sinergia contribuiu para o meu sucesso.

A meu orientador, Márcio Martins, que também é meu amigo pessoal, que como um controlador preditivo me guiou na direção certa com sabedoria e conhecimento, atuando de maneira ótima para ajustar pensamentos e atenuar distúrbios.

Falando em distúrbios, agradeço imensamente a minha esposa Diana Souza, que, apesar de às vezes causar perturbações no processo, atuou na maior parte do tempo me sintonizando, fornecendo apoio, motivação e incentivo para alcançar meus objetivos.

Não posso esquecer de meus pais, Vera Maia e José Fontes, e minha irmã Aruanã Fontes, que são como os dados de entrada que alimentam um modelo de aprendizado de máquina, fornecendo a base sólida que me permitiu desenvolver e crescer, dando-me amor e apoio incondicional durante todo o momento.

Por último, mas não menos importante, temos mimhas cadelinhas Ava e Missy. Elas são como a otimização de processos, sempre buscando maneiras de melhorar e simplificar as coisas, me oferecendo alegria, companhia e uma pausa bem-vinda durante os momentos estressantes.

Em suma, todos mencionados são como os componentes essenciais de um sistema de aprendizado de máquina. Cada um deles desempenhou um papel crucial em minha jornada e contribuiu para o sucesso desta pesquisa.

"Todos os dias quando acordo não tenho mais o tempo que passou, mas tenho muito tempo. Temos todo tempo do mundo"

Renato Russo

Abstract of Dissertation presented to PEI/UFBA as a partial fulfillment of the requirements for the degree of Doctor of Science (D.Sc.)

The use of electrical submersible pumps (ESP) for oil lifting is a widely used method in the oil and gas industry to increase production. Therefore, controlling and optimizing this process to ensure stable and economical production is crucial, minimizing operational costs and maximizing production efficiency. A widely used technique to maximize performance, reduce costs, and define operational goals is real-time optimization (RTO). In order to adequately implement this technique, it is necessary that the control layer works appropriately and is aligned with the challenges and requirements of the process. Recently, the literature has found excellent results using the advanced model predictive control (MPC) technique due to its ease of incorporating constraints and economic requirements into its formulation. Although it is a powerful technique, a reasonable definition of MPC parameters is necessary for its good operation; otherwise, the system may operate at suboptimal or inefficient conditions. However, tuning the MPC controller is a complex problem requiring specialized knowledge to select controller parameters, such as prediction horizons, control horizons, and control weights. In addition, most of the literature tuning methods are dedicated to specific MPC formulations, performance, or robustness goals, not exploring the impact of tuning on economic indicators. So, it is a need for a generalized tuning method that works for different formulations, processes, and tuning requirements. Besides that, no studies in the literature investigate the effect of MPC tuning on the optimization and operation of ESP-lifted wells, whether by performance, robustness, or economic criteria. Therefore, a generalized MPC tuning method is presented, based on an online receding horizon optimization algorithm capable of encompassing different MPC formulations, constraints, and tuning criteria, from performance to economics. This method provides a new perspective for the online optimization of ESP-lifted oil wells, explicitly addressing the MPC tuning problem. The results show that the proposed approach has potential for the oil and gas industry since it was possible to test different case studies and control formulations in simulated results, achieving a 5.7% improvement in oil production or a 2.1% reduction in energy consumption, depending on the desired criteria.

Keywords: MPC controllers, MPC Tuning, Economic Tracking, ESP-lifted wells

Contents

List of Figures

xi

xiii

List of Tables

Nomenclature & Greek Symbols

Nomenclature and Greek Symbols for Chapter 1

ESP   Electrical Submersible Pump, page 2

MPC   Model Predictive Control, page 2

RTO   Real-time Optimization, page 2

SPDC   Smultaneous Process Design and Control, page 3

Nomenclature and Greek Symbols for Chapter 2

$\mathbf{Q_x}$ weighting matrix of the state variables, page 11

$\mathbf{Q_u}$ weighting matrix of the manipulated variables, page 11

$\mathbf{Q_y}$ weighting matrix of the controlled variables, page 11

$\mathbf{R}$ weighting matrix of the manipulated increments or supression matrix, page 11

$\mathbf{S}$ slack variables weighting matrix, page 11

m MPC control horizon, page 11

N MPC model horizon, page 11

p MPC prediction horizon, page 11

AS   Analytical Solution of unconstrained MPC, page 11

DMC   Dynamic Matrix Controle, page 11

FIHMPC   Fuzzy Infinite Horizon MPC, page 8

FIR   FInite Impulse Response, page 11

FIS   Fuzzy Inference System, page 12

GPC Generalized Predictive Control, page 11

IHMPC Infinite-Horizon-based MPC, page 7

MIMO Multiple Input Multiple Output, page 11

MV   Manipulated Variable, page 11

NMPC Nonlinear MPC, page 8

PID Proportional Integral Derivative, page 6

PV   controlled (Process) Variable, page 11

RPN Robust Performance Number, page 11

SISO Single Input Single Output, page 11

SS   State Space model, page 11

Nomenclature and Greek Symbols for Chapter 3

$\mathbf{q}_{\max}$ maximun values of the diagonal elements of the weithing matrix $\mathbf{Q_y}$, page 33

$\mathbf{q}_{\min}$ minimum values of the diagonal elements of the weithing matrix $\mathbf{Q_y}$, page 33

$\mathbf{r}_{\max}$ maximun values of the diagonal elements of the supression matrix $\mathbf{R}$, page 33

$\mathbf{r}_{\min}$ minimum values of the diagonal elements of the supression matrix $\mathbf{R}$, page 33

$\boldsymbol{\delta}_{y,k}$ vector of slack variables of the IHMPC, page 30

$\Delta\mathbf{q}_{\max}$ maximun increment values of the diagonal elements of the weithing matrix $\mathbf{Q_y}$, page 33

$\Delta\mathbf{q}_{\min}$ minimu increment values of the diagonal elements of the weithing matrix $\mathbf{Q_y}$, page 33

$\Delta\mathbf{r}_{\max}$ maximun increment values of the diagonal elements of the supression matrix $\mathbf{R}$, page 33

$\Delta\mathbf{r}_{\min}$ minimu increment values of the diagonal elements of the supression matrix $\mathbf{R}$, page 33

$y_{i,\min}(k+j)$ minimum tunnel limits of the "i-th" controlled variable at instant $k+j$, page 26

$\mathbf{q}(0)$ initial values of the diagonal elements of the weighting matrix $\mathbf{Q_y}$, page 32

$\mathbf{r}(0)$ initial values of the diagonal elements of the supression matrix $\mathbf{R}$, page 32

CLS Closed-Loop Simulation, page 21

CSTR Continuous Stirred Tank Reactor, page 41

IAE Integral of the Absolute Errors, page 25

IMVI Index of the sum of Manipulated Variable Increments, page 27

ISE Integral of the Square Errors, page 25

T tunnel performance objective, page 27

TISE Tunnel sum of the Squared Error, page 27

Nomenclature and Greek Symbols for Chapter 4

$\bar{A}$ the average cross-section area, page 54

$\bar{L}$ the average well length, page 54

β_2 the Bulk modulus, page 54

Δp_f hydrostatic pressure, page 54

Δp_p the differential pressure over the ESP, page 54

ρ the average density, page 54

A the cross-section area of the annulus, page 54

f the rotational frequency., page 54

f_i the friction factor of the "i-th" well section, page 54

H the pump head, page 54

h_i the height of the "i-th" well section, page 54

Chapter 1

Introduction

The petroleum industry has become increasingly complex, with environmental safety requirements and the need for validated methods to maximize profits in oil production systems. Optimizing oil production systems involves handling concurrent and multi-objective decisions to achieve profitability and success (Franklin et al. 2022). Among the various artificial lift methods available, the Electrical Submersible Pump (ESP) stands out for its ability to produce large volumes of oil, making it a popular choice for onshore and offshore applications.

Various studies have explored the economic efficiency of artificial lift-employing ESP installations in oil wells by applying Real-time Optimization (RTO) approaches. Khalid et al. (n.d.) implemented a real-time workflow that uses real-time data and well models to minimize ESP failure and downtime in an ESP-lifted oil wells grid. This system provides ESP performance and operation indicators that are helpful for monitoring, decision-making, and optimizing the wells. Sharma & Glemmestad (2013) presented a nonlinear steady-state optimization approach to maximize profits in a simulated environment of 5 ESP-lifted wells. The optimization problem considered factors such as oil production, energy consumption, separator operating costs and process constraints like flow rate window, bubble point pressure, and final control element limitations. Hoffmann & Stanko (2016) presented a Mixed-Integer Linear Programming with a Piecewise model approximation to maximize the oil production of a network with 15 ESP-lifted wells. The optimizer computed the optimal rotational frequency of each ESP and the wells' status (open/close) for different case studies evaluating constraints, operational failure, and operation conditions. Finally, Noorbakhsh & Khamehchi (2020) optimized oil field production using sequential quadratic programming using an integrated model simulation (i.e.,

reservoir, wells, and surface facilities model). The proposed optimization algorithm increased daily revenue and cumulative oil production in different scenarios.

One of the primary concerns with RTO implementations is the time required to execute the economic optimization process. This process involves static data analysis, which includes data reconciliation constrained by mass and energy balances and parameter estimation of a rigorous static model. Once these preliminary steps are completed, a nonlinear programming solver determines the optimal control targets to meet economic requirements (Engell 2007, Darby et al. 2011, Santos et al. 2021). In addition, RTO implementations require a well-functioning control layer, which means having a control system that can effectively track and lead the process towards the optimal steady-state target calculated by the RTO.

In the ESP-lifted oil field, Model Predictive Control (MPC) strategies have gained attention in recent years as a potential alternative control system for ESP operation due to their flexibility in incorporating constraints, such as the operational envelope and economic goals. Notable research efforts in this area include works that consider linear MPC formulations (Binder et al. 2014, Krishnamoorthy et al. 2016, Patel et al. 2019, Binder et al. 2019, Fontes et al. 2020), highlighting Pavlov et al. (2014), who proposed an MPC formulation that tracked ESP intake pressure and minimized power consumption by incorporating a production choke opening target in the controller's objective function while also explicitly considering operational envelope constraints. Traditional linear MPC formulations, on the other hand, may function ideally only under certain operating conditions or near the model linearization point. Some publications have proposed the usage of adaptive MPC (Delou et al. 2019, 2020, Santana et al. 2021, Matos et al. 2022) or nonlinear MPC (Osnes 2020, Hernes 2020, Santana et al. 2022) architectures to overcome this issue. These solutions may provide better flexibility and performance in more complicated and dynamic operational contexts.

While there have been significant advancements in the control and optimization techniques applied to ESP-lifted oil production, it is noteworthy that the problem of MPC tuning has yet to be widely explored. Although several tuning methods are available in the literature (Alhajeri & Soroush 2020), the lack of attention to this issue may be attributed to the application of expert knowledge or the inherent

2

difficulty in tuning MPC problems.

It is common to find MPC tuning strategies specifically designed for a particular MPC formulation and based solely on the performance of the system variables or robustness requirements (Garriga & Soroush 2010, Alhajeri & Soroush 2020). Several of these methods are based on guidelines and simple algebraic expressions to meet predetermined requirements for specific MPC formulations (Short 2016, Yamashita et al. 2016, Jabbour & Mademlis 2018, Klopot et al. 2018, He et al. 2020, Nebeluk & Ławryńczuk 2021). In contrast, some MPC tuning methods, denominated as auto-tuning, are described as optimization problems. Consequently, they do not require much knowledge about the system and can be systematically applied to different MPC formulations (Garriga & Soroush 2010, Alhajeri & Soroush 2020). Nonetheless, most auto-tuning methods are also based on performance or robustness indices. Due to their high computational cost, they are implemented offline (Francisco et al. 2010, Exadaktylos & Taylor 2010, Weber dos Santos et al. 2017, 2019) or based on algebraic simplifications of specific MPC formulations (Han et al. 2006, van der Lee et al. 2008) to facilitate the tuning optimization problem or online implementation Fan & Stewart (2009).

Furthermore, the aforementioned tuning methods can provide only implicit economic gains associated with a better process response (lesser oscillations, smoother response) since the respective tuning parameters are not evaluated using explicit economic criteria. There has recently been a growing interest in MPC design strategies based on detailed economic requirements. De Carvalho & Alvarez (2020) employed offline simultaneous process design and control (SPDC) to achieve desired dynamics and economic performance. De Schutter et al. (2020) developed an offline tool to provide a first-order feedback law equivalent for a nonlinear economic MPC by computing optimal steady states or periodic trajectories and cost matrices. However, as far as we know, there is a lack of research on MPC auto-tuning methods that explicitly track economic goals and are flexible enough to be used with different control formulations. In particular, there are no studies about MPC tuning methods applied to improve the ESP installations in terms of performance or economic requirements.

3

1.1 Objectives of the work

This thesis aims to track the economic requirements of oil wells lifted by ESP (Electric Submersible Pump) by proposing an economic-oriented Model Predictive Control (MPC) auto-tuning strategy. The proposed auto-tuning strategy should have a flexible structure incorporating various MPC formulations, tuning requirements, and process features. Additionally, it should be able to interact online with both the RTO (Real-Time Optimization) and MPC layers.

The contributions of the proposed method stand out as follows:

- To present a novel MPC auto-tuning framework based on a receding optimization problem, which is flexible in applying to different MPC formulations, different tuning criteria, and designed for online implementation.

- To derive a flexible receding horizon optimization framework that enables the process and control system monitoring, the optimal parameters computing, when necessary, the tuning requirements tracking, keeping the best parameters for the control system, composed of (i) a closed-loop simulation in the presence of model-plant mismatch; (ii) a sequence of tunable parameters; (iii) tuning requirements in a cost function form;

- To address the proposed framework flexibility in the face of different MPC formulations and some regulatory tuning requirements design (as cost functions), including the manipulated and controlled variables trade-off performance;

- To evaluate robustness of the technique in oil production systems with ESP installations considering the operation envelope with reasonable computational time and optimization feasibility

1.2 Publications

This thesis encompasses the idea and findings of the principal papers obtained by this research, namely

- Fontes, R. M., Martins, M. A. F., & Odloak, D. (2019). An Automatic Tuning Method for Model Predictive Control Strategies. Industrial & Engineering

Chemistry Research, 58(47), 21602–21613;

- Fontes, R. M., Santana, D. D., & Martins, M. A. F. (2022). An MPC auto-tuning framework for tracking economic goals of an ESP-lifted oil well. Journal of Petroleum Science and Engineering, 217(July), 110867.

1.3   Organization of this thesis

The overall structure of this work is organized into 5 chapters, including this introductory chapter. The remaining chapters present the findings of the research, focusing on the objective and contributions pointed out previously.

The second chapter concerns a systematic literature review of MPC strategies applied to artificial lifting by ESP and existent MPC tuning methods, presenting the main features of the MPC formulation applied to ESP operation and classifying the overall MPC tuning methods.

Chapter 3 presents an online automatic tuning method based on two steps: monitoring and optimal tuning. The flexibility and suitability of the technique are tested in the face of a Dynamic Matrix Control, an Infinite Horizon Model Predictive Control, different simulation scenarios, and performance tuning criteria.

The fourth chapter presents the research findings, focusing on the trade-off between economic and performance tuning requirements. Different economic goals for ESP-lifted well operation are employed in the auto-tuning layer, resulting in gains without compromising the process.

Chapter 5 summarizes the preliminary contributions of this work and suggests the future stages.

Chapter 2

Literature review

Implementing artificial lifting systems, specifically Electrical Submersible Pumps (ESPs), is essential for efficient oil production from reservoirs. Model Predictive Control (MPC) strategies have been widely applied to optimize the operation of ESPs, leading to significant improvements in oil production and reduced operating costs.

This chapter presents a systematic literature review of the various MPC strategies applied to artificial lifting by ESPs and existing MPC tuning methods, outlining the main features of the MPC formulation applied to ESP operation and classifying the overall MPC tuning methods.

By doing so, this chapter provides a comprehensive overview of the state-of-the-art MPC-based control strategies for ESPs and MPC tuning methods, which can aid in developing more effective optimization for artificial lifting systems in the oil and gas industry.

2.1 Advanced control in ESP-lifted oil wells

The classical PID framework can effectively execute control tasks and provide stable and safe ESP operations. In fact, it is possible to design a PID controller for each control variable in a single-input single-output structure. However, this classical solution does not explicitly consider process constraints, which are instead handled by other control layers (Haapanen & Gagner 2010, Sharma & Glemmestad 2013, Souza et al. 2014, Krishnamoorthy et al. 2019). Consequently, ESP operations could achieve better results in reaching optimal operations, such as maximizing oil production or minimizing power consumption, if process constraints were incorporated into the

control framework.

To address these challenges, MPC can systematically handle multivariable and constrained systems with associated economic goals. As a result, MPC-based solutions for oil production wells with ESP installations are recognized for their functional role in achieving optimal, stable, and safe ESP operations, including upthrust and downthrust operational envelope-type time-varying constraints, robust processes, and guaranteed feasibility.

Over the last several years, there has been an increasing focus on applying MPC strategies to optimize ESPs. Notable research efforts in this area include the work of Pavlov et al. (2014), who proposed an MPC formulation that tracked ESP intake pressure and minimized power consumption by incorporating a production choke opening target in the controller's objective function while also explicitly considering operational envelope constraints. Similarly, Binder et al. (2014) used the same MPC controller formulation and ESP dynamic model as Pavlov et al. (2014) to investigate the implementation of an embedded MPC on a programmable logic controller. However, the regulation of ESP power minimization relied on an ESP motor current target, and downthrust and upthrust force limits were explicitly omitted. Krishnamoorthy et al. (2016) designed an MPC controller for ESP installations producing heavy viscous crude oil using a linearized model obtained from a high-fidelity simulator and the same control objectives as Pavlov et al. (2014). Patel et al. (2019) implemented advanced control strategies that used a linear MPC with rotational speed, choke valve opening, and ESP voltage as manipulated variables. This approach achieved a 20% reduction in power consumption. Binder et al. (2019) explored several MPC formulations that included measured disturbances, such as reservoir pressure, to evaluate the control performance. More recently, Fontes et al. (2020) proposed an infinite-horizon-based MPC (IHMPC) that explicitly considered downthrust and upthrust constraints and maximized ESP oil production by tracking the economic target of the production choke valve opening and ESP intake pressure set-point control.

These recent research efforts have demonstrated the potential of MPC strategies in optimizing ESP operations by considering process constraints and achieving economic targets. However, such formulations tend to work well only around the

model linearization point, i.e., operating conditions. To overcome this limitation, some authors have proposed adaptive MPC structures. Delou et al. (2019) developed an adaptive MPC control law that broadens the ESP-lifted oil production operating range using step-response linear models. However, instead of tracking targets, the ESP power minimization was tracked by a conservative set-point, and the set of time-variant ESP operating envelope constraints was not incorporated into the control problem formulation. Delou et al. (2020) presented an adaptive constrained MPC based on a model scheduling strategy. The proposed scheduling strategy has equivalent performance compared to the successive linearization method. Additionally, a model scheduling Kalman filter coupled to the proposed MPC formulation addresses the losing measurements problem due to the aggressive subsea environment. Santana et al. (2021) extended the work of Fontes et al. (2020) by considering a linearization of a nonlinear phenomenological model of the system at each instant of sampling, which serves as the control model of the zone control IHMPC formulation. Using a fuzzy model approximation of the nonlinear system to a linear parameter-varying model, Matos et al. (2022) developed a fuzzy infinite horizon MPC (FIHMPC) strategy and applied it to an ESP-lifted oil well system in embedded hardware. Moreover, the ESP time-varying operation envelope is included as slacked terminal constraints and zone control scheme to ensure optimization feasibility.

In parallel, recent studies have suggested designing predictive controllers based on nonlinear models to capture the nonlinearities of the ESP system. Using a data-driven representation of the ESP system presented by Pavlov et al. (2014), Osnes (2020) developed a nonlinear MPC (NMPC) based on a recurrent network. Similarly, Hernes (2020) implemented an echo state network-based NMPC. However, both authors assumed that all variables are measured and did not consider operational envelope constraints. In contrast, Santana et al. (2022) proposed an implementable NMPC law based on a target zone scheme coupled with an extended Kalman filter estimator as a soft sensor while considering the downthrust and upthrust constraints.

Despite the notable progress made in controlling and optimizing ESP-lifted oil production, it is essential to highlight that the issue of MPC tuning has received limited attention thus far. Notably, there needs to be more research exploring MPC

tuning methods for enhancing ESP installations in terms of performance and economic considerations. Consequently, this thesis aims at addressing the economic requirements of oil wells lifted by ESP through the proposal of an auto-tuning strategy for Model Predictive Control with an economic focus.

2.2 An overview about model predictive control tuning methods

Tuning MPC parameters is especially challenging due to their non-intuitive interaction (Alhajeri & Soroush 2020). This section discusses this problem by conducting a systematic literature review of MPC tuning methods. Table 2.1 summarizes the main features of some tuning methods found in the literature from 2001 to 2022.

Table 2.1: Some tuning methods found in the literature from 2001 to 2022.

Ref.	MPC Formulation	Parameters	Tuning Criteria	Method and Implementation	
Al-Ghazzawi et al. (2001)	MPC-FIR MIMO	$\mathbf{Q_y}$ and $\mathbf{R}$	PV response	Tunnel/ Quadratic Optimization	Online
Ali (2001)	MPC-FIR MIMO	$\mathbf{Q_y}$, $\mathbf{R}$ and p	PV response	Tunnel/ Fuzzy Inference System	Online
Li & Du (2002)	GPC(AS) SISO	$\mathbf{R}$	PV response	Fuzzy decision sets	Online
Wojsznis et al. (2003)	DMC(AS) SISO	$\mathbf{R}$	Robustness	Mismatch/ analytical Expressions	Offline
Han et al. (2006)	DMC(AS) MIMO	$\mathbf{R}$, p and m	PV and MV response / Robustness	Min-Max optimization/-Mismatch	Offline
van der Lee et al. (2008)	DMC(AS) MIMO	$\mathbf{R}$, p and m	PV response	Multi-objetive fuzzy decision making optimization	Offline
Fan & Stewart (2009)	MPC(AS) MIMO	$\mathbf{Q_y}$, $\mathbf{Q}_u$, $\mathbf{R}$	Robustness	Frequency Analysis/ Max-Min optimization	Online
Francisco et al. (2010)	IHMPC-SS SISO	$\mathbf{R}$	Robustness	Frequency domain/ Min-max optimization	Offline
Exadaktylos & Taylor (2010)	MPC-SS MIMO	$\mathbf{Q_y}$ and $\mathbf{R}$	PV response	Multi-objective Goal-attainment Optimization	Offline
Cairano & Bemporad (2010)	DMC/MPC-SS(AS) SISO	$\mathbf{Q}_x$ and $\mathbf{R}$	Equivalence with linear controller	Inverse Matching	Offline
Shah & Engell (2011)	GPC(AS) MIMO	$\mathbf{Q_y}$ and $\mathbf{R}$	PV response	Frequency domain/ Semi-Definite Programming Problem Optimization	Offline
(AS) - Analytical Solution of Unconstrained MPC			SS - State Space Model		A - Adaptive

9

Ref.	MPC Formulation	Parameters	Tuning Criteria	Method and Implementation	
Waschl et al. (2012)	MPC-SS(AS) MIMO	$\mathbf{Q_y}$ and $\mathbf{R}$	PV and MV response	Quadratic Optimization	Offline
Suzuki et al. (2012)	MPC-SS MIMO	$\mathbf{Q_y}$ and $\mathbf{R}$	PV response	Particle Swarm Optimization	Offline
Tran et al. (2014)	MPC-SS MIMO	$\mathbf{R}$	Optimal bandwith	Extremum Seeking/ Quadratic Optimization	Offline
Ho et al. (2014)	AGPC(AS) SISO	$\mathbf{R}$	Robustness	Conditional number/ analytical Expressions(Shridhar & Cooper 1997)	Online
Nery et al. (2014)	MPC-SS MIMO	$\mathbf{Q_y}$, $\mathbf{R}$, p and m	PV and MV response/ Robustness	Worst-Case Optimization	Offline
Yamashita et al. (2016)	MPC-SS MIMO	$\mathbf{Q_y}$ and $\mathbf{R}$	PV response	Multi-objective Optimization	Offline
Short (2016)	DMC / AGPC(AS) SISO	$\mathbf{R}$	Robustness	Well-Conditioned/ analytical Expressions	Offline/ Online
Abrashov et al. (2017)	GPC(AS) MISO	$\mathbf{Q}$ and $\mathbf{R}$	Robustness	Frequency domain/ Optimization	Offline
Weber dos Santos et al. (2017)	MPC MIMO	$\mathbf{Q}$, $\mathbf{R}$ and S_y	PV response / Robust Performance Number (RPN)	Optimization	Offline
Klopot et al. (2018)	DMC(AS) SISO	T_s, m, p, N, $\mathbf{R}$	Embedded	analytical Expressions	Offline
Ira et al. (2018)	MPC-SS MIMO	$\mathbf{Q}$, e $\mathbf{R}$	PV response	Machine learning / Gradient-free Optmization	Offline
Jabbour & Mademlis (2018)	AMPC-SS(AS) SISO	$\mathbf{R}$	PV response	Fuzzy Inference System	Online
Weber dos Santos et al. (2019)	MPC MIMO	$\mathbf{Q}$, $\mathbf{R}$ and S_y	Pv response / relative RPN	Optimization / Diferent operacional points	Offline
De Carvalho & Alvarez (2020)	IHMPC MIMO	$\mathbf{Q}$, $\mathbf{R}$	Simultaneous process design and control	Optimization	Offline
De Schutter et al. (2020)	MPC MIMO	SP trajectories, steady states, and cost matrices	Economic NMPC equivalency	Optimization	Offline
Elsisi et al. (2021)	NMPC	T_s, m, p, $\mathbf{Q}$, and $\mathbf{R}$	PV response	Neural Network	Offline

(AS) - Analytical Solution of Unconstrained MPC	SS - State Space Model	A - Adaptive

Ref.	MPC Formulation	Parameters	Tuning Criteria	Method and Implementation	
Nebeluk & Ławryńczuk (2021)	DMC MIMO	$\mathbf{Q}$	PV response	Optimization	Offline
Giraldo et al. (2022)	MPC MIMO	m, p, $\mathbf{Q}$, and $\mathbf{R}$	PV and MV response	Hybrid Optimization	Offline
Yu et al. (2022)	NMPC	$\mathbf{Q}$, and $\mathbf{R}$	PV and MV response	Optimization Genetic Algorithm	Online
(AS) - Analytical Solution of Unconstrained MPC			SS - State Space Model		A - Adaptive

Like other controllers, MPC performance is related to its tuning parameters: the weighting matrices of the controlled, manipulated and state variables ($\mathbf{Q_y}$, $\mathbf{Q_u}$, and, $\mathbf{Q_x}$); manipulated variation weights ($\mathbf{R}$) and slack variables weighting ($\mathbf{S}$); prediction, model and control horizons (p,N,m); reference trajectory filters. Due to the flexibility of the MPC algorithm, different MPC formulations with different characteristics are found. Therefore, the MPC tuning problem is considered a non-trivial task and, for this reason, different methods of parameter adjustment are found in the literature (Rani & Unbehauen 1997, Garriga & Soroush 2010, Alhajeri & Soroush 2020).

Several of these MPC tuning methods are based on heuristic techniques (methods based on guidelines), as seen in Rani & Unbehauen (1997), Garriga & Soroush (2010) and Alhajeri & Soroush (2020). In general, such methods present a list of instructions and simple algebraic expressions to meet predetermined requirements. In contrast, Garriga & Soroush (2010) present methods described as auto-tuning or self-tuning. Unlike the guidelines-based methods, auto-tuning methods are based on optimization that offers the advantage of not requiring much knowledge about the system, however, they have the disadvantage of high computational cost, since there are two simultaneous optimization problems: the tuning one and the MPC itself (Garriga & Soroush 2010).

Regardless of the method types, as for implementation, they can be offline, like most heuristic or auto-tuning methods, or online, such as some methods based on heuristic rules or auto-tuning with simplifications of the optimization problems (Table 2.1). The limitation of the offline methods lies in the fact that their designs must be repeated to ensure good performance of the control system either to unforeseen

changes, namely operating condition changes and unmeasured disturbance, or even in scenarios of performance criteria changes. On the other hand, the implementation of online strategies attempts to circumvent these drawbacks as they correct the system parameters in a real-time mode to meet specifications designed from a nonconformity detected.

Most of the tuning methods are specific to conventional controllers, such as Dynamic Matrix Control (DMC) (Wojsznis et al. 2003, Han et al. 2006, van der Lee et al. 2008, Cairano & Bemporad 2010, Short 2016, Klopot et al. 2018, Nebeluk & Ławryńczuk 2021), Generalized Predictive Control (GPC) (Li & Du 2002, Short 2016, Ho et al. 2014, Abrashov et al. 2017) or MPC based on the state space model (MPC-SS) (Exadaktylos & Taylor 2010, Cairano & Bemporad 2010, Waschl et al. 2012, Suzuki et al. 2012, Tran et al. 2014, Nery et al. 2014, Yamashita et al. 2016, Jabbour & Mademlis 2018) (Table 2.1). The specificities of these methods are usually tied to the use of some properties of the controllers, such as: analytical solution (Li & Du 2002, Wojsznis et al. 2003, Han et al. 2006, van der Lee et al. 2008, Fan & Stewart 2009, Cairano & Bemporad 2010, Shah & Engell 2011, Waschl et al. 2012, Ho et al. 2014, Short 2016, Abrashov et al. 2017, Klopot et al. 2018, Jabbour & Mademlis 2018) and objective function (Francisco et al. 2010); or process type, such as: Single Input Single Output (SISO) Li & Du (2002), Francisco et al. (2010), Cairano & Bemporad (2010), Ho et al. (2014), Short (2016), Klopot et al. (2018), Jabbour & Mademlis (2018). Due to the specificities of the methods, the applications in other controller formulations require the restructuring of equations, guidelines, or optimization problems in order to adapt it to new controllers or process dynamics. For example, Ali (2001) presents an online tuning method of Finite Impulse Response MPC (MPC-FIR) using a Fuzzy Inference System (FIS), based on heuristic knowledge to meet controlled variables performance requirements. This FIS is modified for different applications, such as the work of Ali & Al-Ghazzawi (2008), who use the same MPC-FIR but applied in another system, and Ali (2003) and Zarkogianni et al. (2011), who apply it in a Nonlinear MPC (NMPC) with different systems.

In this case, the present work contributes to a method based on an online closed-loop simulation in the presence of model-plant mismatch, which can be designed from

the MPC and plant model desired, enabling flexibility and easy implementation in different cases.

Another important point for tuning methods is the performance/robustness requirements. It is known that heuristic methods have pre-set adjustment criteria, while auto-tuning methods are based on the desired response information. However, most auto-tuning methods are designed to meet either the robustness or performance criteria, highlighting some research (Table 2.1) that explicitly considers the robustness requirement in the tuning method through min-max optimization formulations. For instance, Han et al. (2006) and Francisco et al. (2010) deal with frequency domain based formulations, whereas Nery et al. (2014), Weber dos Santos et al. (2017) and Weber dos Santos et al. (2019) use robustness criteria based on time-domain model analysis. The solution of these cases can be more complex, with most methods implemented offline, apart from the online methods proposed by Fan & Stewart (2009), Ho et al. (2014) and Short (2016). These last papers present some simplifications on the optimization problem, derived from specific MPC analytical solutions, in order to decrease the computational cost and enable online implementations.

In the performance criteria case, the requirements are mostly represented by indices describing the behavior of the controlled variables in the time domain and the parameters are then adjusted from the comparison of the closed-loop simulation to the desired response, using optimization or heuristic rules (Al-Ghazzawi et al. 2001, Ali 2001, Li & Du 2002, van der Lee et al. 2008, Shah & Engell 2011, Suzuki et al. 2012, Yamashita et al. 2016, Weber dos Santos et al. 2017, Ira et al. 2018, Jabbour & Mademlis 2018, Weber dos Santos et al. 2019). The parameters evaluated to achieve performance criteria indexed based on the response of controlled variables (PV) only may result in a more aggressive control action since there is a tendency to value the PV response to the detriment of manipulated variables (MV). Thus, some works explicitly show the combination of the variables' response (Han et al. 2006, Waschl et al. 2012, Nery et al. 2014, Elsisi et al. 2021, Giraldo et al. 2022, Yu et al. 2022) and others are based on multi-objective formulations, which may allow the implementation of requirements for the PVs and MVs (van der Lee et al. 2008, Exadaktylos & Taylor 2010, Yamashita et al. 2016, Ira et al. 2018).

It is crucial to highlight that a few studies have investigated the association between economic requirements and MPC tuning methods (De Carvalho & Alvarez 2020, De Schutter et al. 2020). Due to the trade-off between performance and economic criteria, optimal economic solutions are hardly associated with a well-behaved system response, as a better system response can only provide implicit economic improvements.

In addition, in presenting a flexible structure for the different MPC strategies, this work proposes an auto-tuning method based on a receding horizon optimization problem with an objective trade-off function designed to encompass performance (including MV response) and explicit economic requirement. The closed-loop simulation in the presence of model-plant mismatch coupled with this optimization framework contributes to robustness issues and more flexible performance criteria.

In terms of implementation, online methods are designed for simplifications in closed-loop simulation (Al-Ghazzawi et al. 2001, Ali 2001, 2003, Ali & Al-Ghazzawi 2008), MPC analytical solution (Li & Du 2002, Fan & Stewart 2009, Jabbour & Mademlis 2018) or updating of the prediction model (Adaptive MPC) followed by the application of guidelines corresponding to the controller formulation and model structure (Ho et al. 2014, Short 2016), resulting in limited applications.

Therefore, the optimization framework proposed in this work also includes decision variables called tuning actions. These tuning actions are comparable to the MPC control actions and are evaluated for a defined horizon, and only the first value is implemented, contributing to the online implementation.

In summary, in the current context, a range of MPC tuning methods is mainly dedicated to specific controller strategies, performance/robustness criteria, and implementation. In addition, online implementation methods are based on simple mathematical expressions, heuristic rules, or simplifications of the optimization problem, and economic tuning requirements are not implemented in an explicit online form.

Consequently, there needs to be more research concerning MPC auto-tuning methods that prioritize economic objectives while remaining adaptable to various control formulations. In light of this gap, this study introduces the development of an online auto-tuning approach that offers flexibility for different MPC formulations,

14

performance criteria, and economic targets.

Chapter 3

Tracking MPC performance goals by an auto-tuning framework

The auto-tuning method proposed in this chapter is a layer of receding horizon optimization problem whose objective function is able to consider the performance/robustness through a trade-off representation combining the responses of the process variables and the control actions. The tuning parameters are evaluated based on a closed-loop simulation in the presence of model-plant mismatch, which is compared to the desired tunnel response in the time domain. The method is tested for two types of model predictive control, and its flexibility and suitability for different scenarios of fit criteria are presented. The results point to the feasibility of the applications of the method, keeping the system close to the ideal setting and highlighting the importance of evaluating the behavior of control actions in the tuning problem.

The text included here is part of the published paper in the Industrial & Engineering Chemistry Research

- FONTES, R. M.; MARTINS, M. A. F.; ODLOAK, D. An Automatic Tuning Method for Model Predictive Control Strategies. Industrial & Engineering Chemistry Research, vol. 58, no. 47, p. 21602–21613, 27 Nov. 2019. DOI 10.1021/acs.iecr.9b03502.

3.1   Proposed MPC auto-tuning framework

MPC auto-tuning methods have the disadvantage of high computational cost due to the formulation being based on two simultaneous optimization problems, parameter

adjustments and the MPC itself (Garriga & Soroush 2010). As a result, some authors propose the use of auto-tuning methods in an offline way or the use of MPC algorithm simplifications for online applications, as seen in Chapter 2 (Table 2.1).

This section presents a method based on optimization with the capacity for online applications which is flexible for different MPC and without any simplification of the MPC algorithms. The main feature is in the formulation of a receding optimization problem responsible for the tuning of the MPC parameters.

The idea behind the proposed method follows the philosophy of the MPC scheme itself. In MPC, the following elements can be highlighted: the model, used to predict the open-loop plant behavior; control actions, decision variables of the optimization problem representing the manipulated variable increments; prediction horizon, which determines the time instants of model predictions; control horizon, which determines the size of sequence of control actions; constraints, limits for the evaluation of control actions; optimizer, responsible for evaluating the optimal control actions sequence from the prediction model, horizons and constraints.

Like MPC, the proposed automatic tuning formulation is based on a receding horizon optimization scheme, whose decision variables (tuning parameters) are evaluated from the prediction of the closed-loop system behavior. Compared to MPC, the following elements of the proposed method are highlighted: Closed-Loop Simulation (CLS), used to predict the closed-loop process behavior ($\hat{\mathbf{y}}, \hat{\mathbf{u}}$); tuning actions, which are the decision variables of the optimization problem that represent relative parameter increments ($\boldsymbol{\Delta\theta}$); simulation horizon, which determines the time instants of closed-loop prediction; tuning horizon, which determines the size of tuning actions sequence; constraints, limitations for the evaluation of the tuning actions; optimizer, which is responsible for evaluating the optimal tuning actions sequence, given the closed-loop simulation, horizons and constraints. Table 3.1 summarizes the elements and their respective functions.

Within this paradigm, we propose an auto-tuning method capable of receiving plant measurements ($\mathbf{y}, \mathbf{u}$), reference signals ($\mathbf{y}_{\text{sp}}$), performance criterion to optimally adjust the tuning parameters ($\boldsymbol{\theta}$) of an existing MPC in order to meet specified requirements. From the multilevel control structure point of view, this proposed layer integrates with the lower MPC layer, and its execution is split into two steps,

Table 3.1: Comparison between elements and functions of the MPC with the proposed auto-tuning method

Function	MPC Element	Proposed Tuning Element
System prediction	Open-loop Model	Closed-loop Simulation
Decision variables	Manipulated Variables Increments	Tuning Parameters Increments
Time instants of predictions	Prediction Horizon	Simulation Horizon
Size of Sequence Increments	Control Horizon	Tuning Horizon

as can be seen in Figure 3.1.

(a)

(b)
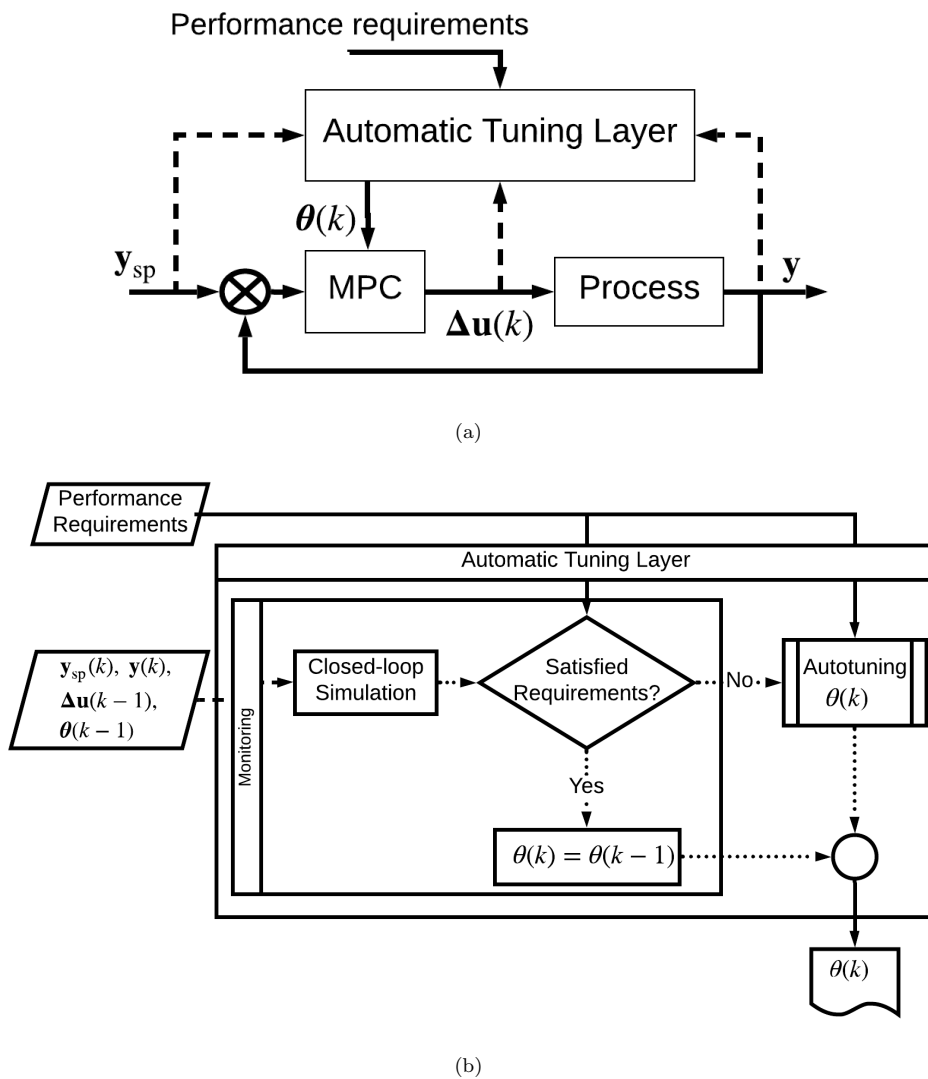
Figure 3.1: Representation of the MPC online automatic tuning layer.

First step - Monitoring: The first step is to monitor the process through the

simulation of the closed-loop system, which is responsible for providing the simulated values of the controlled ($\hat{\mathbf{y}}(k)$) and manipulated variables ($\hat{\mathbf{u}}(k)$), using a set of MPC tuning parameters ($\boldsymbol{\theta}(k-1)$). If the predicted values of the closed-loop system simulation do not meet the predefined criteria the second step is activated so as to compute new tuning parameters.

Second step - Tuning: The second step evaluates the new parameters in order to meet the desired performance criteria when they are violated through the closed-loop system simulation.

The implementation structure helps to adjust only at the desired moment, i.e., the optimization problem is only activated when it is detected that the control system will not remain within the expected criteria, which avoids unnecessary computing, contributing to the feasibility of online implementation. For the implementation of the proposed method, it is important to highlight some points:

Note 1: For better numerical conditioning of the optimization problem, it is recommended normalizing all variables.

Note 2: Simulation and tuning horizons (h_{sim}, h_T) can be configured on the basis of the desired closed-loop trajectory. These specifications can be made based on the prior knowledge of the designer or with the aid of a rigorous offline simulation. In order to comply computational issues, the following guideline can be used:

- $h_{\text{sim}} \leq$ highest settling time
- $h_T \leq h_{\text{sim}}/2$

Note 3: The set of parameter constraints must be defined in order to avoid unwanted scenarios, such as open-loop and higher control effort (importance and suppression matrix are zeroed).

Note 4: The constraints applied to tuning actions ($\Delta\boldsymbol{\theta}_{\text{min}}, \Delta\boldsymbol{\theta}_{\text{max}}$) play a significant role in determining the behavior of the proposed automatic tuning approach. These constraints directly influence how the system adjusts its parameters in

response to changing conditions. It is worth noting that the magnitude of these constraints directly impacts the characteristics of the tuning actions.

When small values are assigned to the constraints, the adjustment actions become smoother and more gradual, which can be beneficial in scenarios where stability and gradual convergence toward optimal performance are desired. The smaller constraints limit the magnitude of parameter changes, preventing sudden and drastic adjustments that could destabilize the system.

On the other hand, when large constraint values are employed, the tuning actions can become more aggressive and pronounced, which means that the auto-tuning framework has the freedom to make larger parameter adjustments in a shorter period. While aggressive actions can lead to faster convergence toward optimal performance, they also introduce a higher risk of instability. Therefore, it is crucial to carefully consider the potential trade-off between rapid convergence and system stability when selecting larger constraint values.

<u>Note 5:</u> The simulated results were evaluated on a computer with an octa-core processor with 3.2 GHz and 16 Gb of RAM, with MAC operational system.

As for the optimization algorithms used, the controllers were implemented in quadratic programming, while the tuning problem was solved through the Active-sets algorithm, using *quadprog* and *fmincon* of the MATLAB software (version 2021b)

The ordinary differential equations system was solved by a variable-steps and variable-orders method based on numerical differentiation formulas of orders 1 to 5.

It is important to emphasize that the choice of the numerical method can degrade the solution's quality and computational time. In this regard, attention to this point is recommended before implementation in a real-time system.

3.2 Presenting the main elements

To help illustrate the auto-tuning framework design, details on each element, function, and the implementation of the proposed tuning technique will be presented in

the following subsections.

3.2.1 Closed-Loop Simulation (CLS)

The closed-loop simulation is performed to forecast the system's future behavior based on current conditions, in which the time interval considered in these predictions is called the simulation horizon (h_{sim}). As can be seen in Figure 3.2, the same formulation of MPC implemented in the plant (G_P), including the same constraints, is considered together with a representation of the plant model (G_M) in the Closed-Loop Simulation. To obtain an offset-free CLS, a bias term ($\mathbf{e}(k|k)$), defined by the difference between the current measured value ($\mathbf{y}(k)$) and the simulated value of the closed-loop $\hat{\mathbf{y}}(k|k)$, is added at each simulation time step to provide the CLS prediction $\hat{\mathbf{y}}_k = [\hat{\mathbf{y}}(k+1|k), \ldots, \hat{\mathbf{y}}(k+h_{\text{sim}}|k)]^{\top}$.

Under these circumstances, from the current measurement ($\mathbf{y}(k)$, $\mathbf{u}(k-1)$), the closed-loop simulation generates controlled and manipulated variables values in order to accommodate a more realistic scenario of practical implementation purposes, i.e., the plant-model mismatch case. In this case, the parameters are evaluated under the model uncertainty scenarios, which contributes to the proposed method robustness feature. Figure 3.2 shows the schematic representation of the proposed method. It is important to highlight in Figure 3.2 that the state estimator is only applied if the MPC formulation requires state feedback. In these cases, the bias term is not necessary.

To simplify the representation, Eq. (3.1) provides the mathematical representation of the concept Closed Loop Simulation (CLS) as a function of the tuning actions, reference values and current measurements.

$$[\hat{\mathbf{y}}_k, \Delta\hat{\mathbf{u}}_k] = \text{CLS}\left(\boldsymbol{\theta}(k-1), \Delta\boldsymbol{\theta}_k, \mathbf{y}_{\text{sp}_k}, \mathbf{y}(k), \mathbf{u}(k-1)\right) \qquad (3.1)$$

in which, $\hat{\mathbf{y}}_k = [\hat{\mathbf{y}}(k+1|k), \ldots, \hat{\mathbf{y}}(k+h_{\text{sim}}|k)]^{\top}$, $\Delta\hat{\mathbf{u}}_k = [\Delta\hat{\mathbf{u}}(k|k), \ldots, \Delta\hat{\mathbf{u}}(k+h_{\text{sim}}-1|k)]^{\top}$, are the simulated values of the controlled and manipulated variables, respectively; $\mathbf{y}_{\text{sp}_k} = [\mathbf{y}_{\text{sp}}(k+1|k), \ldots, \mathbf{y}_{\text{sp}}(k+h_{\text{sim}}|k)]^{\top}$ are the references values along the simulation horizon, $\mathbf{y}(k)$ and $\mathbf{u}(k-1)$ are the current measurements and $\Delta\boldsymbol{\theta}_k = [\Delta\boldsymbol{\theta}(k|k), \ldots, \Delta\boldsymbol{\theta}(k+h_{\text{sim}}-1|k)]^{\top}$ are the sequence of tuning actions; $\boldsymbol{\theta}(k-1)$ are current MPC parameters.
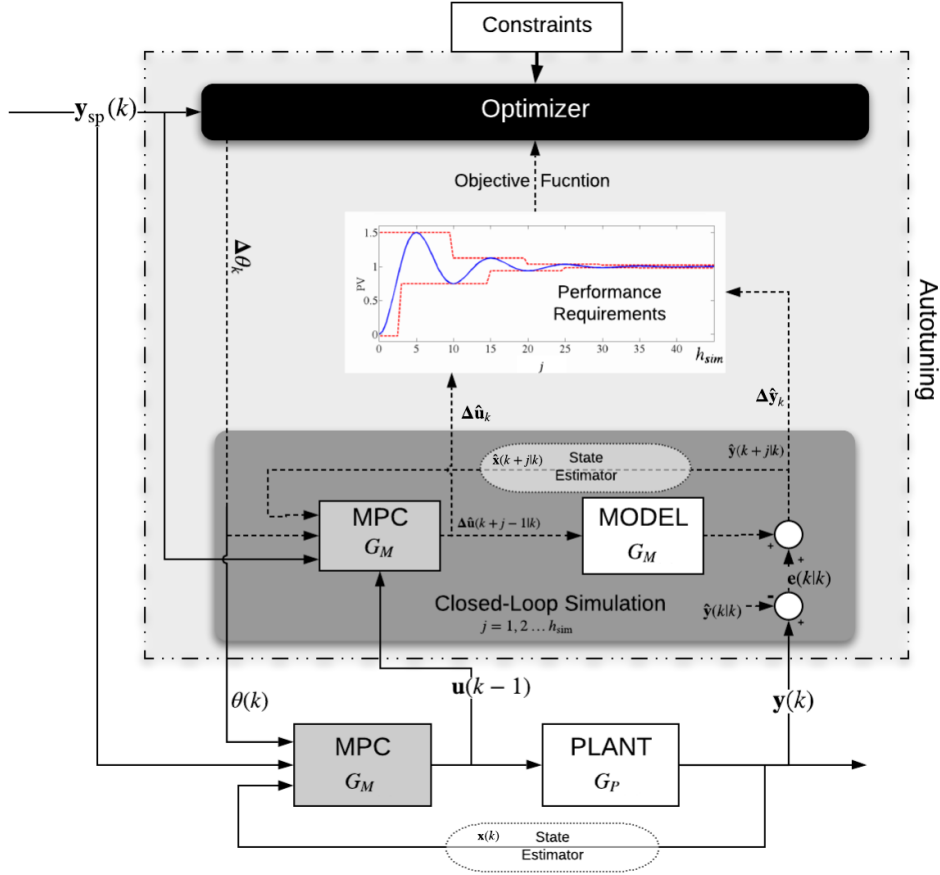
Figure 3.2: The proposed performance tracker auto-tuning layer.

This CLS construction allows the engineer to choose the MPC + Model combination that best represents the goals to be achieved by the tuning method. The proposed system therefore facilitates the use of different MPC formulations and adjustment objectives.

3.2.2   Tuning Action ($\Delta\boldsymbol{\theta}$)

As seen previously (Figure 3.2), the Closed-Loop Simulation configuration allows the inclusion of different MPC structures. As well as this, the structure called tuning actions is proposed, where $\boldsymbol{\theta}$ represents the set of tunable parameters.

Since the parameters are evaluated from an optimization problem as main characteristic of auto-tuning approach (Garriga & Soroush 2010), in this work, we propose

updating tuning parameters in a similar way to the MPC scheme. The proposed algorithm estimates a sequence of relative parameter increments, denoted here as tuning actions,

$$\boldsymbol{\Delta\theta}_k = [\boldsymbol{\Delta\theta}(k|k), \ldots, \boldsymbol{\Delta\theta}(k + h_{\text{sim}} - 1|k)]^\top. \tag{3.2}$$

Like in MPC, in which the control horizon limits the size of the control action sequence, the tuning horizon (h_T) defines the size of the tuning action sequence in the proposed method. As a result, $\boldsymbol{\Delta\theta}(k + h_T) = \boldsymbol{\Delta\theta}(k + h_T + 1) = \ldots = \boldsymbol{\Delta\theta}(k + h_{\text{sim}} - 1) = 0$ reducing the size of the tuning actions to

$$\boldsymbol{\Delta\theta}_k = [\boldsymbol{\Delta\theta}(k|k), \ldots, \boldsymbol{\Delta\theta}(k + h_T - 1|k)]^\top. \tag{3.3}$$

Although the optimal sequence of the tuning actions is computed, only the first relative increment is used to obtain the current set of tuning parameters according to the following expression:

$$\boldsymbol{\theta}(k) = [1 + \boldsymbol{\Delta\theta}(k|k)] \cdot \boldsymbol{\theta}(k - 1). \tag{3.4}$$

Eq. (3.4) facilitates comprehending the tuning action constraints, since they are relative values, and improves the numerical behavior. However, this constraint introduces a significant nonlinearity to the problem, as described as follows.

The constraints defined for the parameters delimit the search region and avoid values that can cause damage to the control system, such as when the importance matrix or suppression matrix are zeroed. As a result, because the parameters should be limited over the simulation horizon,

$$\underbrace{\begin{bmatrix} \boldsymbol{\theta}_{\min}(k) \\ \boldsymbol{\theta}_{\min}(k+1) \\ \vdots \\ \boldsymbol{\theta}_{\min}(k + h_{\text{sim}} - 1) \end{bmatrix}}_{\boldsymbol{\theta}_{\min}} \leq \underbrace{\begin{bmatrix} \boldsymbol{\theta}(k|k) \\ \boldsymbol{\theta}(k+1|k) \\ \vdots \\ \boldsymbol{\theta}(k + h_{\text{sim}} - 1|k) \end{bmatrix}}_{\boldsymbol{\theta}_k} \leq \underbrace{\begin{bmatrix} \boldsymbol{\theta}_{\max}(k) \\ \boldsymbol{\theta}_{\max}(k+1) \\ \vdots \\ \boldsymbol{\theta}_{\max}(k + h_{\text{sim}} - 1) \end{bmatrix}}_{\boldsymbol{\theta}_{\max}}. \tag{3.5}$$

Expanding Eq. (3.4)

$$\boldsymbol{\theta}(k|k) = (1 + \boldsymbol{\Delta\theta}(k|k)) \cdot \boldsymbol{\theta}(k - 1)$$

$$\boldsymbol{\theta}(k + 1|k) = (1 + \boldsymbol{\Delta\theta}(k + 1|k)) \cdot \boldsymbol{\theta}(k|k),$$

$$= (1 + \Delta\boldsymbol{\theta}(k+1|k)) \cdot (1 + \Delta\boldsymbol{\theta}(k|k)) \cdot \boldsymbol{\theta}(k-1)$$

$$\boldsymbol{\theta}(k+2|k) = (1 + \Delta\boldsymbol{\theta}(k+2|k)) \cdot \boldsymbol{\theta}(k+1|k)$$

$$= (1 + \Delta\boldsymbol{\theta}(k+2|k)) \cdot (1 + \Delta\boldsymbol{\theta}(k+1|k)) \cdot (1 + \Delta\boldsymbol{\theta}(k|k)) \cdot \boldsymbol{\theta}(k-1),$$

$$\boldsymbol{\theta}(k+h_{\mathrm{T}}-1|k) = \prod_{i=0}^{h_{\mathrm{T}}-1} (1 + \Delta\boldsymbol{\theta}(k+i|k)) \cdot \boldsymbol{\theta}(k-1)$$

$$\boldsymbol{\theta}(k+h_{\mathrm{T}}|k) = \boldsymbol{\theta}(k+h_{\mathrm{T}}+1|k) = \cdots = \boldsymbol{\theta}(k+h_{\mathrm{sim}}-1|k),$$

generalizing to an instant j, we have

$$\boldsymbol{\theta}(k+j|k) = \prod_{i=0}^{j} (1 + \Delta\boldsymbol{\theta}(k+i|k)) \cdot \boldsymbol{\theta}(k-1), \;\; j = 0, 1, \ldots, h_T - 1. \qquad (3.6)$$

Thus, the set of tunable parameters, $\boldsymbol{\theta}$, is subject to a set of constraints, $\boldsymbol{\Theta}$, defined as

$$\boldsymbol{\Theta} \equiv \begin{cases} \Delta\boldsymbol{\theta}_{\min} \leq \Delta\boldsymbol{\theta}_k \leq \Delta\boldsymbol{\theta}_{\max}, \\ \Delta\boldsymbol{\theta}(k+j|k) = 0, \; \forall j \geq h_T, \\ \boldsymbol{\theta}_{\min} \leq \displaystyle\prod_{i=0}^{j} (1 + \Delta\boldsymbol{\theta}(k+i|k)) \cdot \boldsymbol{\theta}(k-1) \leq \boldsymbol{\theta}_{\max}, \end{cases} \;\; , \; j = 0, 1, \ldots, h_{\mathrm{sim}} - 1$$

$$(3.7)$$

The use of the closed-loop simulation structure with the tuning actions, together with the simulation and tuning horizons, contribute to make it a flexible method for online implementation. These combined structures allow the construction of a receding horizon optimization problem, that is, at every instant, from the process measurements, a new simulation is evaluated, keeping the system closer to the realistic scenario and consequently, a new sequence of optimal parameters is computed.

3.2.3 Optimizer

The proposed auto-tuning consists of a Closed-Loop Simulation connected to an optimizer (Figure 3.2) responsible for calculating a sequence of optimal tuning relative parameter increments from the simulated values (Eq. (3.1)) and performance requirements.

Generally, there are different criteria that can be adopted to improve a control system, among them are overshoot, decay ratio, rise time, settling time, response

time, Integral of the Square Errors (ISE) and Integral of the Absolute Errors (IAE). In performance tracking, it is always interesting to accomplish a combination of criteria in an optimal sense. Here, the proposed tuning method is flexible in accommodating different criteria, particularly in a time domain tunnel form (Ali & Zafiriou 1993), as shown in Figure 3.3, which is a systematic method for a tuning formulation based on optimization problem.
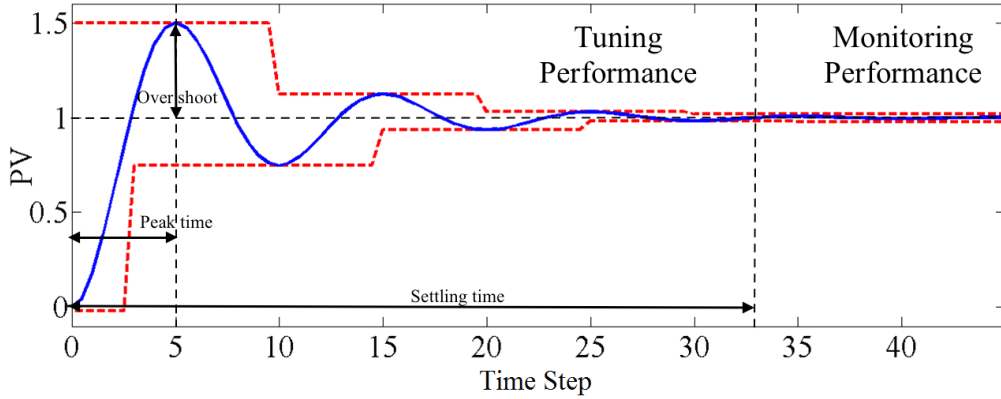
Figure 3.3: Example of tunnel performance for set-point tracking (dashed line) based on the desired closed-loop response (solid line).

For example, Figure 3.3 shows the construction of a performance tunnel from a desired closed-loop response in the tracking set-point case. It can be seen that the tunnel can contain information inherent to the desired response, such as overshoot, peak and settling time. The tunnel also has information about the steady state tolerance (Monitoring Performance) used for process monitoring. Thus, a performance tunnel can be built for each controlled variable. As the prediction is made under a moving horizon algorithm, the tunnels move to the right every time step until reaching the monitoring part. If any violation is detected, the tuning layer holds in the parameters adjusting stage. Otherwise, the system changes to the monitoring stage.

In the auto-tuning proposed in this work, the performance requirements tunnel is combined into an objective function form described by

$$\min_{\Delta\boldsymbol{\theta}_k} \sum_{j=1}^{h_{\text{sim}}} \|\hat{\mathbf{y}}(k+j|k) - \mathbf{y}_{\text{sp}}(k+j|k)\|_{\boldsymbol{\Gamma}}^2 + \sum_{j=0}^{h_{\text{sim}}-1} \|\boldsymbol{\Delta}\hat{\mathbf{u}}(k+j|k)\|_{\boldsymbol{\Omega}}^2 \qquad (3.8)$$

25

in which $\mathbf{\Gamma}$ represents a diagonal penalty matrix related to the performance tunnel limits, i.e. if the simulated CLS values exceed the tunnel limits, the objective function is penalized proportionally for the resulting violation; and $\mathbf{\Omega}$ is weighting matrix of the manipulated variables.

The main difference between the Al-Ghazzawi et al. (2001) proposal and Eq. (3.8) lies in the variations in the manipulated variables and the penalty matrix. In Al-Ghazzawi et al. (2001), in addition to using a simplified closed-loop simulation for a specific controller, only the highest tunnel violation, provided by the PV simulated values, is used. Furthermore, the MV simulated values are ignored in the objective function and consequently, in the evaluation of the controller parameters.

In Eq. (3.8), all the values of all the variables simulated by CLS are used to evaluate the objective function. In addition, the suggested penalty matrix can be constructed to fit the criteria desired by the specialist, providing more flexibility to implement the method. The diagonal elements ($\gamma_{i,i}$) of the weighting matrix $\mathbf{\Gamma}$ can be evaluated using the following expression:

$$\gamma_{i,i}(k+j) = \begin{cases} \dfrac{\hat{y}_i(k+j)}{y_{i,\max}(k+j)}, & \hat{y}_i(k+j) \geq y_{i,\max}(k+j) \\ \dfrac{2y_{i,\min}(k+j) - \hat{y}_i(k+j)}{y_{i,\min}(k+j)}, & \hat{y}_i(k+j) \leq y_{i,\min}(k+j) \\ \lambda, & \text{otherwise} \end{cases} \qquad (3.9)$$

in which, $i = 1, \ldots, n_y, j = 1, \ldots, h_{\text{sim}}$, n_y is the number of controlled variables, $\hat{y}_i(k+j)$ is the simulated value of the "i-th" controlled variable at instant $k+j$, $y_{i,\min}(k+j)$ and $y_{i,\max}(k+j)$ are the tunnel limits of the i-th controlled variable at instant $k+j$, and λ is a binary weighting, i. e., $\lambda \in \{0, 1\}$.

Although incorporating tunnel performance as a penalty matrix rather than a constraint simplifies the calculation of the optimizer solution, it also introduces a non-quadratic objective function. This can challenge the algorithm to converge effectively and potentially increase computation time.

The binary weighting λ defines two different criteria for the tuning parameters. The value should be chosen by the specialist based on the desired performance criteria. If $\lambda = 1$, this means that for the simulated CLS values within the tunnel boundaries, the resulting performance criterion is reduced to the target ISE. On the other hand, if the simulated values of CLS exceed the tunnel, ISE will be penalized,

26

resulting in the objective so-called Tunnel sum of the Squared Error (TISE). Consequently, the optimizer will converge to a closed-loop response with smaller tunnel violations and closer to the reference value.

If $\lambda = 0$, the simulated CLS values within the tunnel boundaries will not be considered in the objective function, which implies a response with fewer tunnel violations, with the MPC tracking the set-point. This requirement is referred to here as tunnel performance objective (T).

Furthermore, the behavior of the manipulated variables can be considered in the performance objectives of the proposed tuning method. The evaluation of tuning parameters based only on the response of the controlled variables can generate an increase in control effort, and consequently, a degradation in the final control element and even loss of system stability/robustness. In this work, the term added to incorporate the actions of the manipulated variables (MV) is denoted as the sum of Manipulated Variable Increments (IMVI) and the weighting matrix ($\boldsymbol{\Omega}$) represents the importance of the control actions according to the desired requirements by the engineers, as for example economic weights.

The distinct and full performance requirements desired for the control system, T+IMVI and TISE+IMVI, can be performed by the proposed tuning formula through the solution of

Problem 1:

$$\min_{\Delta\boldsymbol{\theta}_k} \sum_{j=1}^{h_{\text{sim}}} \|\hat{\mathbf{y}}(k+j|k) - \mathbf{y}_{\text{sp}}(k+j|k)\|_{\boldsymbol{\Gamma}}^2 + \sum_{j=0}^{h_{\text{sim}}-1} \|\boldsymbol{\Delta}\hat{\mathbf{u}}(k+j|k)\|_{\boldsymbol{\Omega}}^2$$

subject to:

$$\begin{cases} \Delta\boldsymbol{\theta}_{\min} \leq \Delta\boldsymbol{\theta}_k \leq \Delta\boldsymbol{\theta}_{\max}, \\ \Delta\boldsymbol{\theta}(k+j|k) = 0, \ \forall j \geq h_T, & j = 0, 1, \ldots, h_{\text{sim}} - 1 \\ \boldsymbol{\theta}_{\min} \leq \prod_{i=0}^{j} (1 + \Delta\boldsymbol{\theta}(k+i|k)) \cdot \boldsymbol{\theta}(k-1) \leq \boldsymbol{\theta}_{\max}, \end{cases}$$

$$[\hat{\mathbf{y}}_k, \boldsymbol{\Delta}\hat{\mathbf{u}}_k] = \text{CLS}\left(\boldsymbol{\Delta}\boldsymbol{\theta}_k, \mathbf{y}_{\text{sp}_k}, \mathbf{y}(k), \mathbf{u}(k-1)\right)$$

The proposed optimization problem results in a flexible tuning method for different performance and robustness criteria. Although it is a non-linear optimization problem (Problem 1), it can be characterized as a soft optimization, since the tunnel is not a constraint but a penalty. Thus, in addition to the sequence of parameter

27

increments, the tuning method has a degree of freedom to seek the solution provided by tuning actions to keep the system close to the desired criterion.

Finally, Figure 3.4 summarizes the steps to design the proposed method.
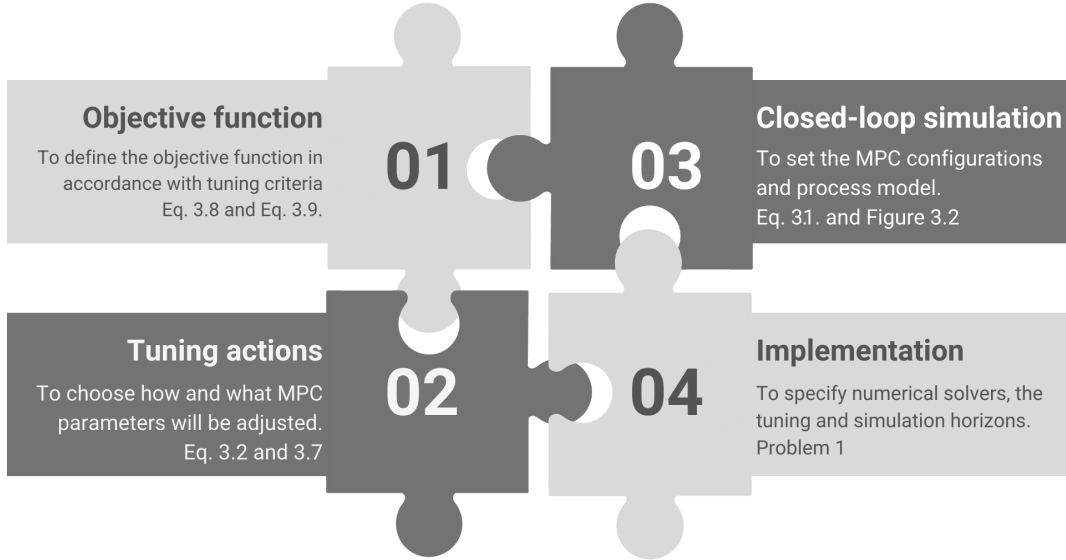
Figure 3.4: Summary of the steps to design the proposed method.

3.3 Applying the auto-tuning framework

The proposed auto-tuning method is a layer of receding horizon optimization problem whose objective function is able to tuning requirements through trade-off representation combining the responses of the process variables and the control actions. The tuning parameters are evaluated based on a closed-loop simulation in the presence of model-plant mismatch, which is compared to the desired tunnel response in the time domain. In this section, the method is tested for two types of model predictive control, and its flexibility and suitability for different scenarios of fit criteria are presented.

3.3.1 MPC formulations

This section presents the context of two distinct formulations of MPC controllers, Dynamic Matrix Controller (DMC) and Infinite Horizon MPC (IHMPC). In this work, the chosen formulations, DMC and IHMPC, evaluate the flexibility of the

method against two distinct forms of control laws, which represent the evolution of the predictive controllers, the classic DMC and a recent formulation of controllers with nominal stability guarantee.

The first one considered is the DMC (Dynamic Matrix Controller), described by the following control law:

Problem 2:

$$\min_{\Delta \mathbf{u}_k} \sum_{j=1}^{p} \|\mathbf{y}(k+j|k) - \mathbf{y}_{\text{sp}}\|_{\mathbf{Q_y}}^2 + \sum_{j=0}^{m-1} \|\Delta \mathbf{u}(k+j|k)\|_{\mathbf{R}}^2$$

subject to:

$$\begin{cases} \mathbf{u}_{\min} \leq \mathbf{u}(k-1) + \sum_{i=0}^{j} \Delta \mathbf{u}(k+i|k) \leq \mathbf{u}_{\max} \\ -\Delta \mathbf{u}_{\max} \leq \Delta \mathbf{u}(k+j|k) \leq \Delta \mathbf{u}_{\max} \qquad j = 0, \dots, m-1 \\ \Delta \mathbf{u}(k+j|k) = 0, \ \forall j \geq m, \end{cases} \tag{3.10}$$

$$y(k+j|k) = y(k+j-1) + \sum_{i}^{j} s_i \Delta \mathbf{u}(k+j-1|k) + d(k+j) \tag{3.11}$$

in which p and m are the prediction and control horizons, respectively; $\mathbf{Q_y}$ (weighting matrix) and $\mathbf{R}$ (suppression matrix) are diagonal positive definite; $\mathbf{y}_{\text{sp}}$ is the set-point vector; $\Delta \mathbf{u}(k) = \mathbf{u}(k) - \mathbf{u}(k-1)$ is the Manipulated Variable (MV) increment vector. $\mathbf{y}(k+j)$ is the prediction vector of the controlled variables based on the step response of the system; s_i is the coefficient of the step response; $d(k+j)$ is the constant bias along the prediction and it equals the difference between the measured output the model output; $\mathbf{u}_{\min}$ and $\mathbf{u}_{\max}$ are the bounds of the manipulated variables; $\Delta \mathbf{u}_{\min}$ and $\Delta \mathbf{u}_{\max}$ are the limits of the control actions;

The second formulation deals with an infinite horizon MPC (IHMPC) presented by Odloak (2004). This particular prediction model is based on the analytical expression of the step response of the system composed of distinct stable poles. The discrete-time state space model is described as follows:

$$\begin{cases} \begin{bmatrix} \mathbf{x}^s(k+1) \\ \mathbf{x}^d(k+1) \end{bmatrix} = \mathbf{A} \cdot \begin{bmatrix} \mathbf{x}^s(k) \\ \mathbf{x}^d(k) \end{bmatrix} + \mathbf{B} \cdot \Delta \mathbf{u}(k) \\ \\ \mathbf{y}(k) = \mathbf{C} \cdot \begin{bmatrix} \mathbf{x}^s(k) \\ \mathbf{x}^d(k) \end{bmatrix} \end{cases} \tag{3.12}$$

29

$\mathbf{x}^d$ and $\mathbf{x}^s$ are the system states, the first one stands for the stable modes of system while the second represents the artificial integrating states obtained from the incremental form of inputs and corresponds to the predicted output steady-state. Further details about the matrices $\mathbf{A}$, $\mathbf{B}$ and $\mathbf{C}$ are provided by Odloak (2004).

Considering the previous prediction model (Eq. (3.12)), the IHMPC control law is described by the optimization problem:

Problem 3:

$$\min_{\Delta \mathbf{u}_k, \boldsymbol{\delta}_{y,k}} \sum_{j=1}^{m} \|\mathbf{y}(k+j|k) - \mathbf{y}_{\mathrm{sp}} - \boldsymbol{\delta}_{y,k}\|_{\mathbf{Q_y}}^2$$

$$+ \sum_{j=0}^{m-1} \|\Delta \mathbf{u}(k+j|k)\|_{\mathbf{R}}^2 + \left\|\mathbf{x}^d(k+m|k)\right\|_{\bar{\mathbf{Q}}}^2 + \|\boldsymbol{\delta}_{y,k}\|_{\mathbf{S}_y}^2,$$

subject to Eq. (3.10), Eq. (3.12) and

$$\mathbf{x}^s(k+m|k) - \mathbf{y}_{sp} - \boldsymbol{\delta}_{y,k} = 0 \tag{3.13}$$

where $\boldsymbol{\delta}_{y,k}$ is a vector of slack variables, introduced in the control problem in order to enlarge the feasible region of the controller; $\mathbf{S}_y$ is assumed to be a diagonal positive definite weighting matrix associated with the slack vector; $\bar{\mathbf{Q}}$ is the terminal weighting matrix obtained for the solution of the Lyapunov equation of the system,

$$\mathbf{F}^\top \bar{\mathbf{Q}} \mathbf{F} = (\boldsymbol{\Psi} \mathbf{F})^\top \mathbf{Q} (\boldsymbol{\Psi} \mathbf{F}), \tag{3.14}$$

where the details about the matrices $\boldsymbol{\Psi}$ and $\mathbf{F}$ are described in Appendix A

Given the controller formulation, its use requires a state observer to estimate the artificial states of the prediction model. In this work, for the mismatch scenarios, the Kalman Filter (KF) is used with the covariance matrices associated with measurement and process model noises tuned by simulation tests.

Considering the MPC formulations presented by Problems 2 and 3, the decision variables for the auto-tuning method (Problem 1) consist of relative increments on the matrix elements of output weights ($\mathbf{Q}$) and move suppression ($\mathbf{R}$). Thus, Eq. (3.3) and Eq. (3.4) can be rewritten as

$$\Delta \boldsymbol{\theta}_k = [\Delta q(k|k), \Delta r_1(k|k), \ldots, \Delta r_{nu}(k|k), \ldots, \Delta q(k+h_T-1|k),$$

$$\Delta r_1(k+h_T-1|k), \ldots, \Delta r_{nu}(k+h_T-1|k)]^\top \tag{3.15}$$

$$
\begin{cases}
q_i(k) = [1 + \Delta q(k|k)]\, q_i(k-1),\ i = 1, \ldots, ny \\
r_l(k) = [1 + \Delta r_l(k|k)]\, r_l(k-1),\ l = 1, \ldots, nu
\end{cases}
\tag{3.16}
$$

in which, n_y is the number of controlled variables, n_u is the number of manipulated variables, q_i is the "i-th" diagonal element of the weighting matrix ($\mathbf{Q_y}$) and r_l is the "l-th" diagonal element of the suppression matrix ($\mathbf{R}$).

The choice of these matrices, with emphasis on the suppression matrix, is because they represent the relationship between the variables, i.e. their manipulation and implementation are more intuitive, which is observed directly in the controller response. However, despite this, setting it manually will not guarantee the desired performance (Exadaktylos & Taylor 2010). In contrast, horizons represent time samples, integer variables, related to model prediction and control actions time samples. As a result, they interfere directly in the processing time of the MPC optimization, and therefore the majority of works has preferred the adjustments of them in offline method (Han et al. 2006, van der Lee et al. 2008, Nery et al. 2014, Klopot et al. 2018), with the exception of the work of Ali (2001).

In the case of the weighting matrix ($\mathbf{Q_y}$), the elements reflect the importance of the relationship existing among the controlled variables. In this sense, the increments evaluated by the tuning algorithm will vary only along the tuning horizon, thus maintaining the relationship required by the specialist, i.e. the importance among the controlled variables. On the other hand, the tuning actions corresponding to the suppression matrix can freely be varied along the tuning horizon and also the values among the manipulated variables.

3.3.2 Tuning DMC - Binary Column

The first case study is a binary distillation column (Wood & Berry 1973) represented by the following transfer function model in which the controlled variables are the top (y_1) and bottom (y_2) concentration, and the manipulated variables are the reflux (u_1) and steam (u_2) flow rates. To represent the model uncertainties, the gains are assumed at $\pm20\%$, time constants $\pm10\%$ and time delay ±10. Thus, there is a

constant plant-model phase mismatch, resulting in the following models

$$G_M(s) \equiv \begin{bmatrix} y_1(s) \\ y_2(s) \end{bmatrix} = \begin{bmatrix} \dfrac{12.8}{18.4s+1}e^{-1.1s} & \dfrac{-18.9}{18.9s+1}e^{-2.7s} \\ \dfrac{6.6}{9.81s+1}e^{-6.3s} & \dfrac{-19.4}{15.8s+1}e^{-3.3s} \end{bmatrix} \begin{bmatrix} u_1(s) \\ u_2(s) \end{bmatrix}, \qquad (3.17)$$

$$G_P(s) \equiv \begin{bmatrix} y_1(s) \\ y_2(s) \end{bmatrix} = \begin{bmatrix} \dfrac{15.4}{16.7s+1}e^{-1s} & \dfrac{-15.1}{21s+1}e^{-3s} \\ \dfrac{5.3}{10.9s+1}e^{-7s} & \dfrac{-23.3}{14.4s+1}e^{-3s} \end{bmatrix} \begin{bmatrix} u_1(s) \\ u_2(s) \end{bmatrix}. \qquad (3.18)$$

Based on Figure 3.2, Eq. (3.18) represents the Process (G_P) and Eq. (3.17) was applied as a model (G_M) in CLS and used to design the DMC controller, which dispenses the use of a state estimator.

As a performance criterion chosen for this control system, the method proposed by Shridhar & Cooper (1998) was adopted , in which the robustness of the system is prioritized through a smooth response. Table 3.2 presents the parameters evaluated by the heuristic tuning method proposed by Shridhar & Cooper (1998) and the remaining configurations for DMC.

Table 3.2: Table containing the settings used in the DMC controller.

Variables	Values	Variables	Values
$\mathbf{u}_{\max}$	[0.5; 0.05]	p	73
$\mathbf{u}_{\min}$	[-0.5; -0.5]	N	73
$\Delta\mathbf{u}_{\max}$	[0.3; 0.03]	m	17
$\mathbf{q}(0)$	[1;1]	T_s	1.5 min
$\mathbf{r}(0)$	[346;1157]	$\mathbf{\Omega}$	$\mathbf{I_2}$

N - Model horizon; T_s - Sample Time; $\mathbf{I_n}$ - n-by-n identity matrix

In this way, a desired closed-loop response can be performed from a nominal Closed-loop Simulation of this particular system. Thus, the performance tunnel, which would represent the desired dynamic behavior for the tuning parameters set (Table 3.2), evaluated by the heuristic adjustment method by Shridhar & Cooper (1998), can be designed as shown in Figure 3.5.

However, the application of these same parameters does not guarantee the same effectiveness when applied to the plant-model mismatch scenario (Figure 3.5). The-
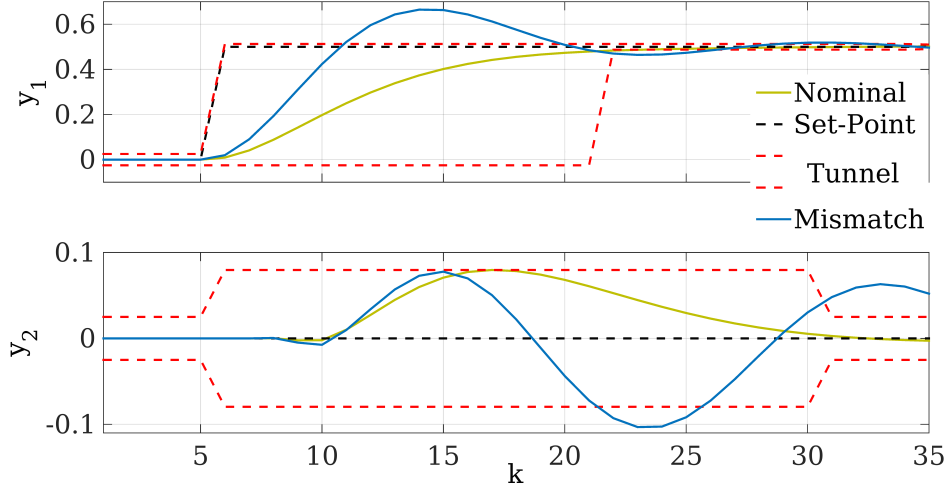
Figure 3.5: Behavior of the binary column for nominal and model-plant mismatch cases, with the tuning parameters obtained from Shridhar & Cooper (1998).

refore, the application of the proposed method aims to keep the plant as close as possible to the desired performance tunnel, by the nominal response.

To work around this, the setting adopted for the auto-tuning method is described in Table 3.3.

Table 3.3: Table containing the settings used in the performance tracking method.

Variables	Values	Variables	Values
h_T	3	h_{sim}	7
$\mathbf{q}_{\text{max}}$	$[\infty; \infty]$	$\mathbf{q}_{\text{min}}$	$[0.01; 0.01]$
$\Delta\mathbf{q}_{\text{max}}$	1	$\Delta\mathbf{q}_{\text{min}}$	-1
$\mathbf{r}_{\text{max}}$	$[\infty; \infty]$	$\mathbf{r}_{\text{min}}$	$[0.01; 0.01]$
$\Delta\mathbf{r}_{\text{max}}$	$[1; 1]$	$\Delta\mathbf{r}_{\text{min}}$	$[-1; -1]$

Based on the response of CLS for the nominal case (Figure 3.5), the simulation horizon was chosen as half of the settling time, and the tuning horizon as a quarter of the settling time.

Figures 3.6, 3.7 and 3.8 show the auto-tuning performance in a scenario of set-point tracking (from $k = 5$). Figures 3.6 and 3.7 show the closed-loop simulation of the process variables at the set-point changes ($k = 5$).

It can be observed (Figure 3.6) that the CLS dynamics obtained for the initial va-
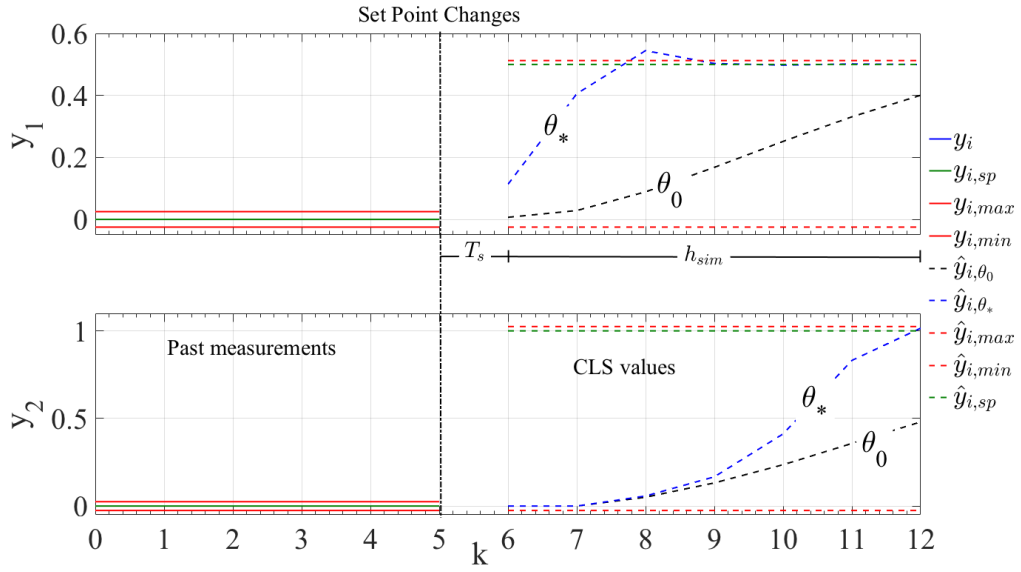
Figure 3.6: Performance of the auto-tuning layer for the case of set point tracking - simulated values for PV.
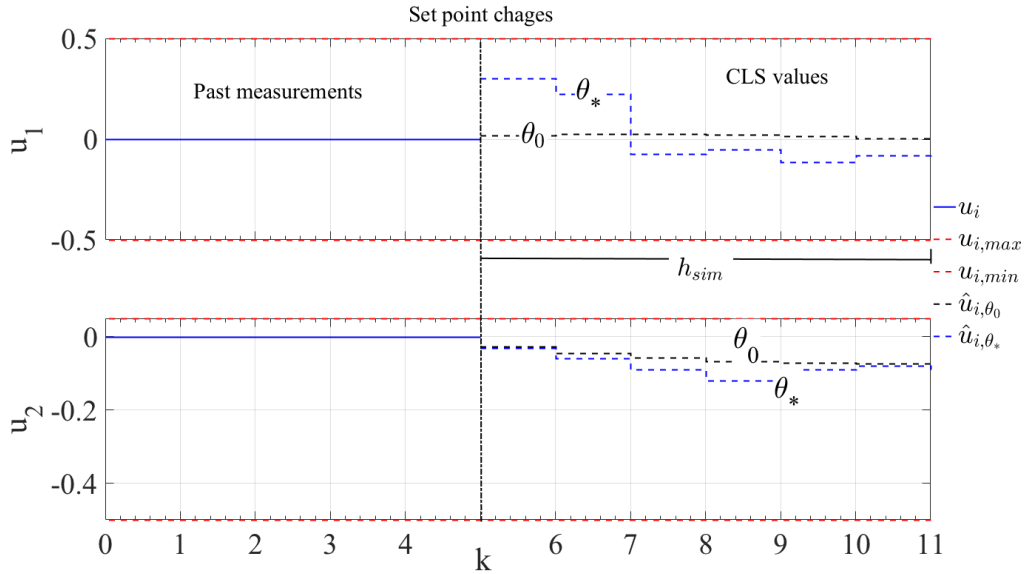
Figure 3.7: Performance of the auto-tuning layer for the case of set point tracking - simulated values for MV.

lues of the parameters, black dashed line - $\boldsymbol{\theta}_0 = \boldsymbol{\theta}(k-1) = \boldsymbol{\theta}(4) = [\mathbf{q}(4), r_1(4), r_2(4)]^\top$, have a greater error than the CLS dynamics obtained by optimal parameters, dashed blue line - $\boldsymbol{\theta}_* = \boldsymbol{\theta}(k) = \boldsymbol{\theta}(5) = [\mathbf{q}(5), r_1(5), r_2(5)]^\top$.

If the initial parameters were maintained, i.e. the optimal relative increments $\boldsymbol{\Delta\theta}_{5,*} = [\Delta q, \Delta r_1, \Delta r_2] = [0, 0, 0]$, it would result in a slower response and conse-

34

quently a higher value of the objective function (TISE+IMVI). The tuning action predominantly increases the PV weighting matrix and reduces the MV suppression matrix, as shown in Figure 3.8, Eq. (3.19) and Eq. (3.20).

$$\boldsymbol{\Delta\theta}_{5,*} = [\Delta q(5|5), \Delta r_1(5|5), \Delta r_2(5|5), \Delta q(6|5), \Delta r_1(6|5), \Delta r_2(6|5)$$

$$\Delta q(7|5), \Delta r_1(7|5), \Delta r_2(7|5)]^\top \tag{3.19}$$

$$\boldsymbol{\Delta\theta}_{5,*} = [1, -1, -0.4967, 1, 0.776, -0.785, 0.5584, -0.3295, -0.4516]. \tag{3.20}$$
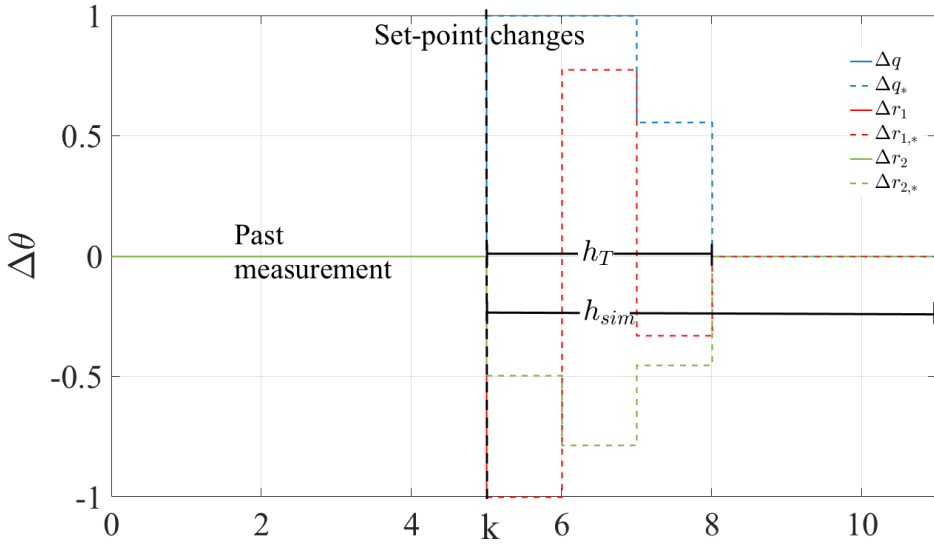
Figure 3.8: Performance of the auto-tuning layer for the case of set point tracking - tuning actions

From Eq. (3.16), the optimal values $q_1(5) = 2$, $q_2(5) = 2$, $r_1(5) = 0.01$ and $r_2(5) = 582$ are implemented, and the steps are repeated from $k = 6$ until the simulation horizon finishes.

Figures 3.9 and 3.10 present the complete scenario of set-point tracking (from $k = 5$) and disturbance rejection (from $k = 40$. A systematic disturbance of -5% and 2.5% were added to u_1 and u_2, respectively). The performance tracking layer adjusts the parameters in order to obtain the minimum of the objective function (Problem 1) in each detection of non-compliance.

Figures 3.9 and 3.10 demonstrate how the choice of the objective function formulation affects the resulting dynamics.

Considering the objective T+IMVI, penalty matrix with $\lambda = 0$ (Eq. (3.9)), the variation in the manipulated variables becomes more important. Since the PVs
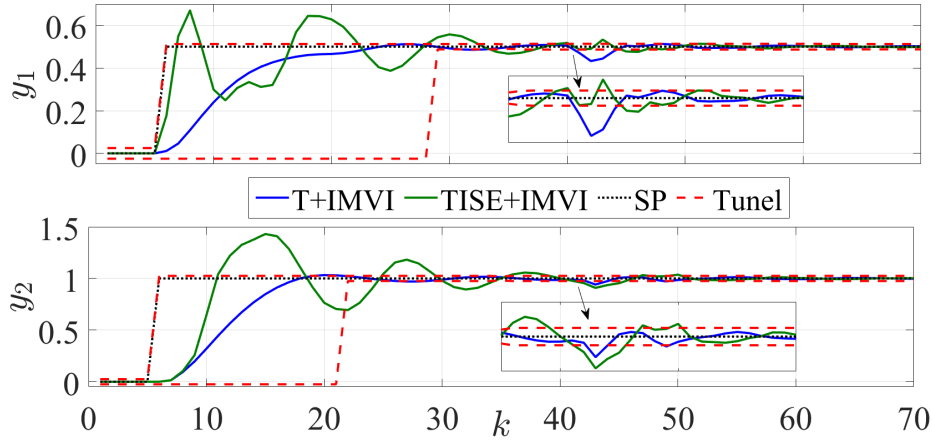
Figure 3.9: Outputs of the binary column system for different configurations of the performance tracking method with DMC.
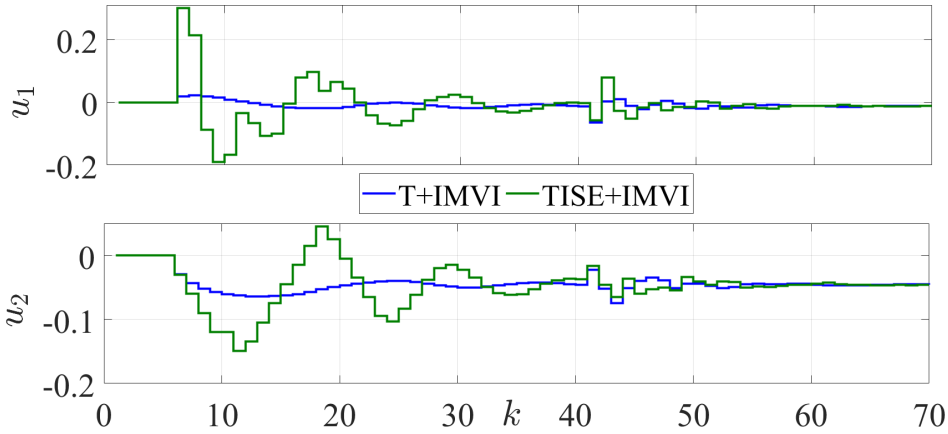
Figure 3.10: Inputs of the binary column system for different configurations of the performance tracking method with DMC.

simulation lies in the tunnel, the proposed algorithm attempts to keep the PVs closer to the tunnel, with the least control effort possible, resulting in a smoother response. On the other hand, when TISE+IMVI is considered (penalty matrix with $\lambda = 1$ in Eq. (3.9)), a different control performance is observed. The response obtained address to, not only approximate the simulated response to the tunnel, but also a smaller distance from the set point. Thus, even when the simulated values satisfy the tunnel limits, the method will provide new parameters considering the error between the PVs and their set-points and the MVs movements. The result is a more aggressive response to controlled variables, which proportionally increases

the control effort in comparison to the criterion T+IMVI.

Table 3.4 shows the traditional indexes of calculated performance, ISE and IMVI, for the presented scenario. In Table 3.4, it can be seen that there is a better global index when it is used TISE+IMVI objective function. However, it is noted an increase in the IMVI index due to the more aggressive response. This comparison shows that in this case, where a robust response is desired through smooth control actions and consequently a slower response as proposed by Shridhar & Cooper (1998), the choice of the T+IMVI objective function is the most adequate.

Table 3.4: Performance indexes evaluated for different configurations of the performance tracking method applied to the binary column with DMC.

Index	T+IMVI	TISE+IMVI
ISE(y_1)	0.8897	0.4982
ISE(y_2)	4.6054	4.6529
IMVI(u_1)	0.0093	0.2848
IMVI(u_2)	0.0042	0.0204
ISE + IMVI	5.5086	5.4563

A further point to highlight about the algorithms is the behavior of the parameters, as shown in Figures 3.11 and 3.12.
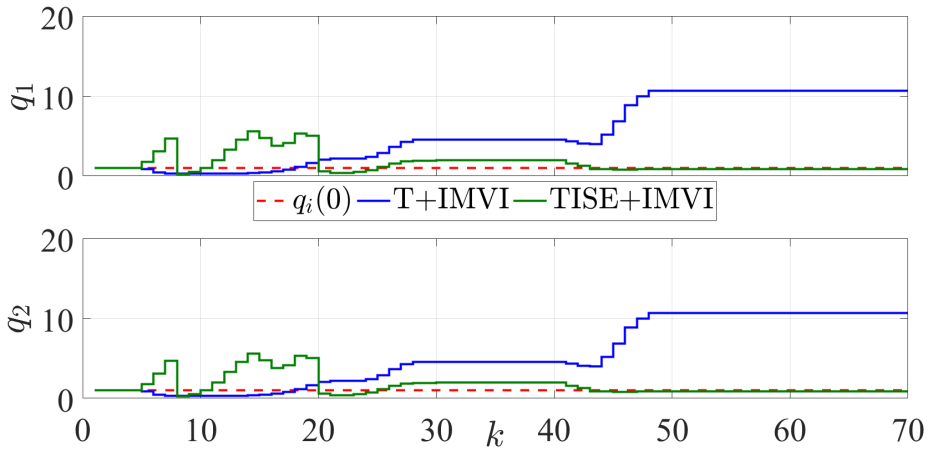
Figure 3.11: Responses of the weighting elements $\mathbf{Q_y}$ of DMC for different configurations of the performance tracking method, applied to the binary column system.
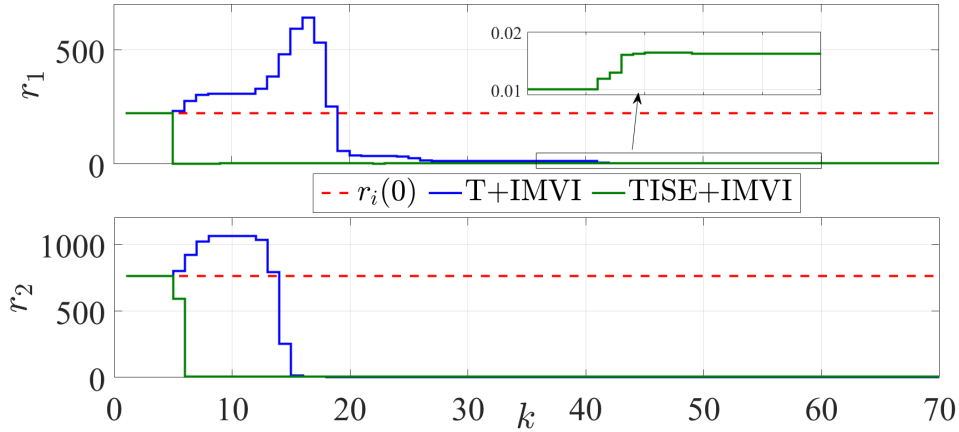
Figure 3.12: Responses of the weighting elements **R** of DMC for different configurations of the performance tracking method, applied to the binary column system.

In Figure 3.11 it can be seen that the proportionality among the weights of the controlled variables (tuning action for each q_i) is maintained. Furthermore, in Figures 3.11 and 3.12 it can be seen that for the TISE+IMVI index, the elements q_i are rapidly increased, while the elements r_i are abruptly reduced as soon as the change in the set-point is detected, when compared to the parameters evaluated by the T+IMVI approach. This occurs because, in this case, the sum of ISEs contributes more to the objective function, which implies that using TISE+IMVI provides tuning actions that prioritize the PV performance improvement. However, after the disturbance, the values q_i are reduced as the controlled outputs are already close to the reference values, thus prioritizing the control effort through a slight increase in the move suppression matrix elements. In contrast, the T+IMVI approach firstly reduces the elements q_i and increases the elements r_i by virtue of the performance criterion adopted.

From the results shown, it can be affirmed that the most suitable criterion for the auto-tuning implementation in this system is T+IMVI, because the desired requirement, obtained by Shridhar & Cooper (1998), imposes a more conservative behavior of the system. The use of the T+IMVI is able to approximate the curve of the system to the tunnel, keeping a smooth response for both controlled and manipulated variables.

The online practicability of the proposed auto-tuning framework in an online setting is evaluated by examining the ratio between the computational time and

auto-tuning sample time, as illustrated in Figures 3.13 and 3.14. The computational time is determined when the method is initiated and includes the duration of the monitoring step, the optimization solver, and the updating of MPC parameters.
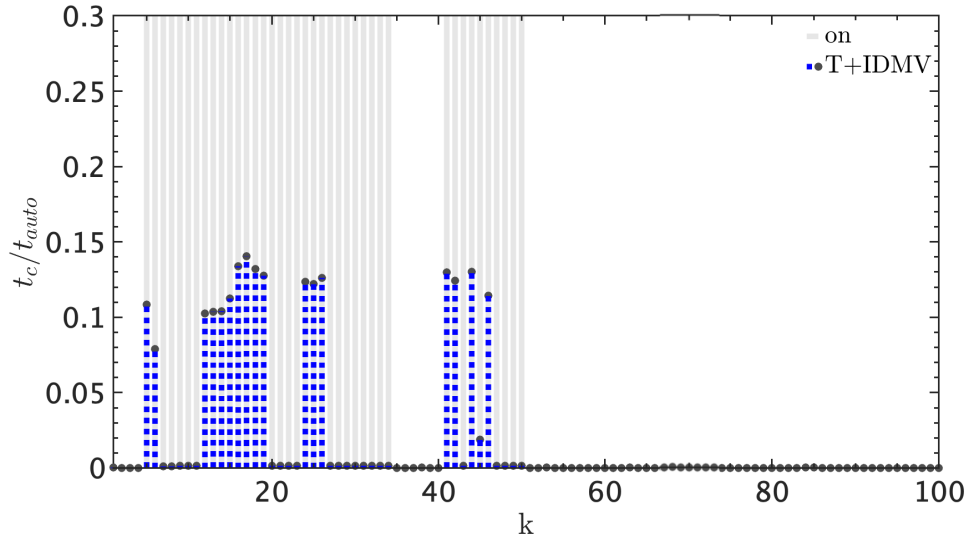
Figure 3.13: Ratio of the computational and auto-tuning sample time for T+IMVI computed when the framework is triggered (On - gray zone), in which $t_{auto} = T_s$.
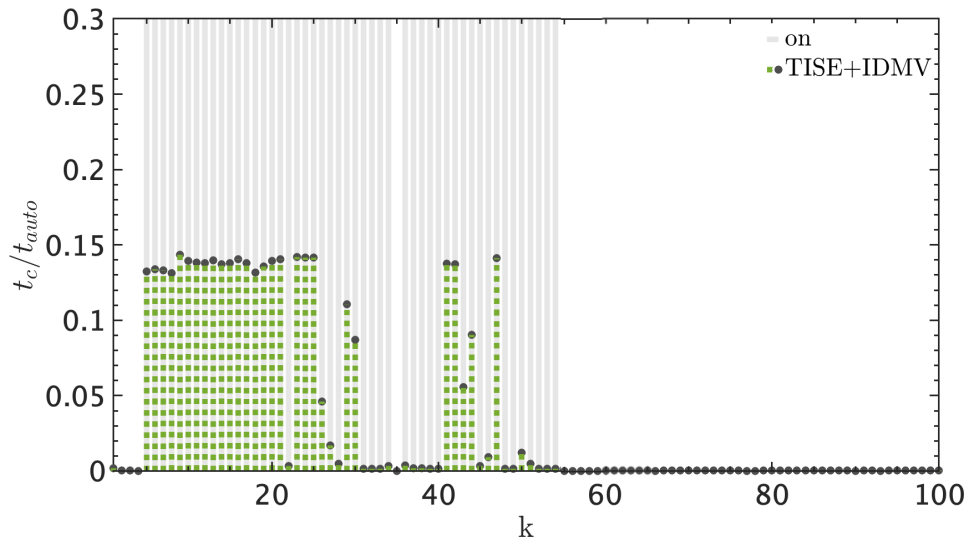
Figure 3.14: Ratio of the computational and auto-tuning sample time for TISE+IMVI computed when the framework is triggered (On - gray zone), in which $t_{auto} = T_s$.

Figures 3.13 and 3.14 reveal that the maximum ratio value is approximately 15% of the sample time, which serves as a validation for the successful online implemen-

tation of the proposed framework. These figures also highlight the occurrences of auto-tuning triggers, indicated by the gray rectangles. It is noteworthy that the auto-tuning is only triggered when deemed necessary.

To investigate the sensitivity of the auto-tuning system to its hyperparameters, Figures 3.15, 3.16, 3.17 and 3.18 show the behavior of the process for different tuning horizon values based on the objective described by TISE+IMVI. Note that
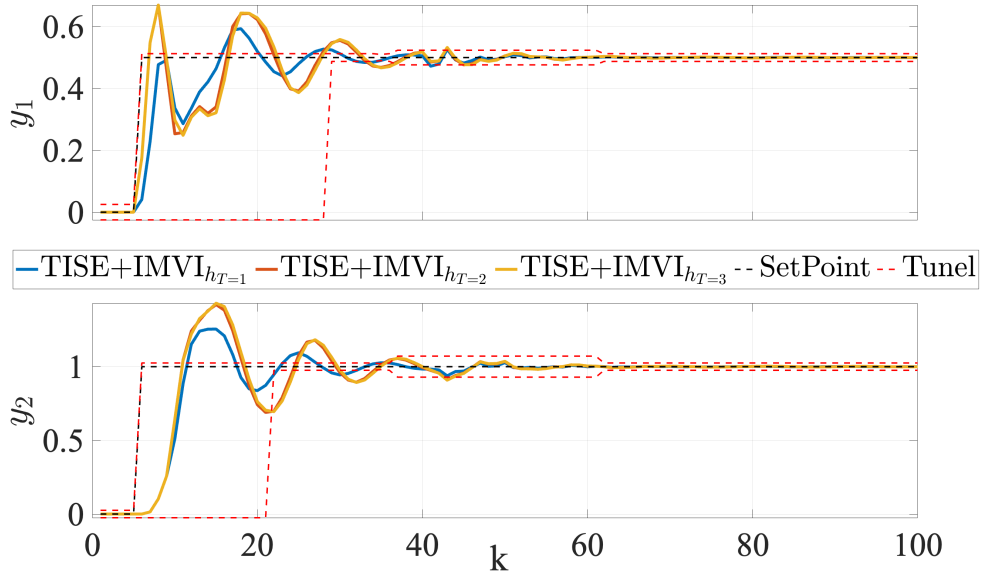
Figure 3.15: Behavior of PV for different tuning horizons.

the response obtained for the tuning horizon equal to 1 stands out compared to the others, remaining viable even with a reduced horizon.

3.3.3 Tuning IHMPC - Continuous Stirred Tank Reactor (CSTR)

The second case study deals with a CSTR (Continuous Stirred Tank Reactor), which assumes a constant level. The reagent concentration (C_A) and reactor temperature (T) are controlled by IHMPC (Odloak (2004)), considering the inlet flow rate (F_{in}) and the cooler temperature (T_c) as manipulated variables. The plant is represented by the following set of nonlinear ordinary differential equations (Martins et al.
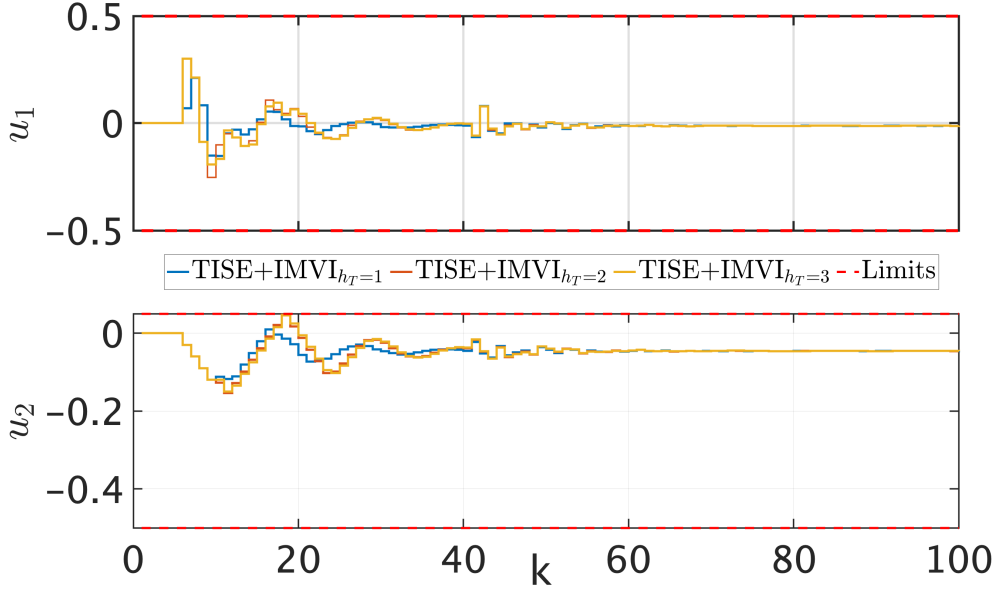
Figure 3.16: Behavior of MV for different tuning horizons.
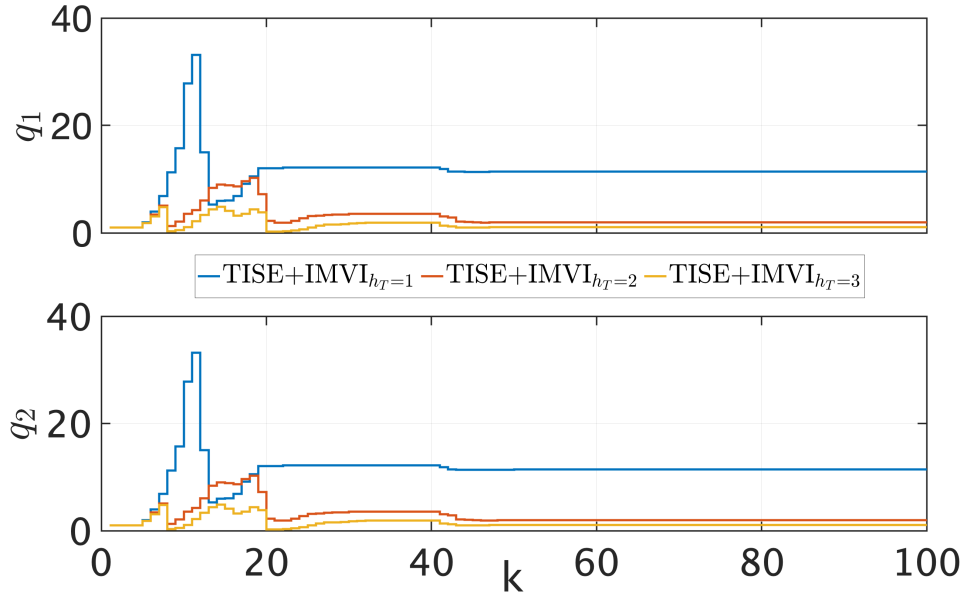
Figure 3.17: Behavior of Q for different tuning horizons.

(2013)):

$$
\begin{cases}
\dfrac{dc_A(t)}{dt} &= \dfrac{[c_{A,in} - c_A(t)]\, F_{in}(t)}{\pi r^2 h} - k_0 c_A(t) \exp\left[-\dfrac{E}{RT(t)}\right], \\[2ex]
\dfrac{dT(t)}{dt} &= \dfrac{[T_{in} - T(t)]\, F_{in}(t)}{\pi r^2 h} - k_0 c_A(t) \exp\left[-\dfrac{E}{RT(t)}\right]\dfrac{\Delta H}{\rho C_p} + \dfrac{2U}{\rho r C_p}\left[T_c(t) - T(t)\right]
\end{cases}
$$

$$(3.21)$$

41
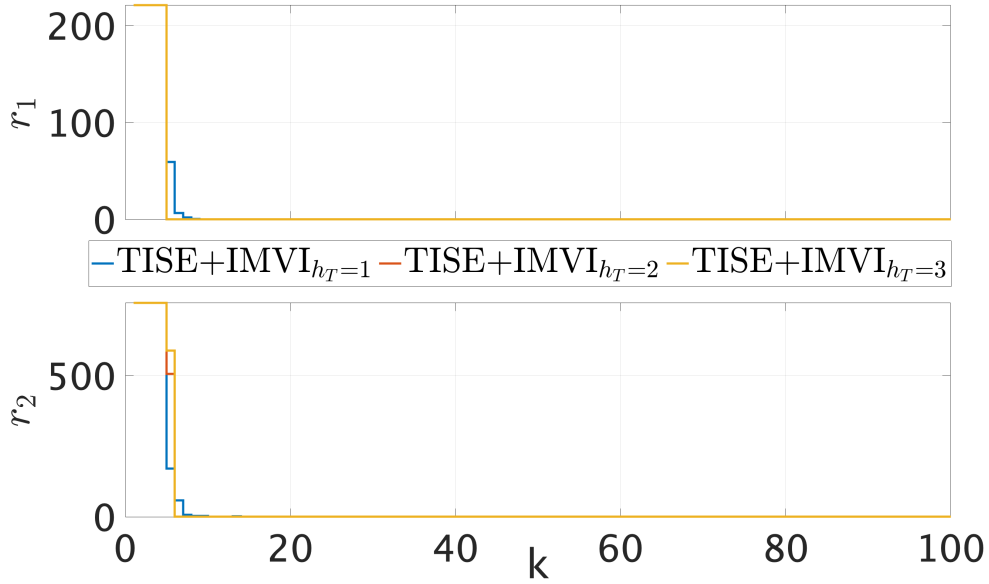
Figure 3.18: Behavior of R for different tuning horizons.

in which the steady-state values are $C_A = 0.9267$ kmol/m^3, $T = 317.92$ K, $F_{in} = 0.05$ m^3/min and $T_c = 295$ K. The constant values used in Eq. (3.21) and the controller settings are summarized in Table 3.5.

Table 3.5: Constant values and IHMPC parameters applied to CSTR.

Variables	Description	Values
$C_{A,in}$	Reactant concentration in feed system	1.0 kmol/m^3
k_0	Pre-exponetial factor	7.2×10^{10} min^{-1}
T_{in}	Temperature in feed stream	350 K
h	Liquid level in the reactor	0.327 m
r	Radius of the reactor	0.197 m
C_p	Heat capacity of the reaction mixture	239 J/(kg K)
ρ	Density of the reaction mixture	1000 kg/m^3
U	Overral heat transfer coefficient	915.6 W/(m^2 K)
E/R	Activation energy/universal gas constant	8750 K
ΔH	Enthalpy of reaction	-5×10^7 J/kmol
$T_{c,\max}$	Maximum cooler temperature	442.5 K
$T_{c,\min}$	Minimum cooler temperature	277.3 K

Continuation of Table 4.1

Variables	Description	Values
$\Delta T_{c,\max}$	Maximum increment of cooler temperature	147.5 K
$F_{in,\max}$	Maximum inlet flow rate	0.10 m^3/min
$F_{in,\min}$	Minimum inlet flow rate	0 m^3/min
$\Delta F_{in,\max}$	Maximum increment of inlet flow rate	0.025 m^3/min
Ts	Sample time	30s
$\mathbf{q}(0)$	Initial weighting values	$[0.02; 1]$
$\mathbf{r}(0)$	Initial suppression values	$[0.01; 1]$
$\mathbf{W}$	Measurement covariance	$0.5 \cdot \mathbf{I}_{10}$
$\mathbf{V}$	Process model covariance	$0.05 \cdot \mathbf{I}_2$

For this controller, a state estimator is required as mentioned in Section 3.3.1. In this work, it was implemented a Kalman filter, whose measurement covariance, $\mathbf{V}$, and process model covariance, $\mathbf{W}$, obtained by simulation tests, are presented in Table 3.5. Based on Figure 3.2, the Process ($G_P(k)$) is represented by the nonlinear system of ordinary differential equations (Eq. (3.21)), the Model ($G_M(k)$) is the respective discrete space-state (Eq. (3.12)) linearized at a steady-state (Appendix A).

The performance tunnel for the set-point tracking is assumed by the prior knowledge of the process specialist as a step response for a second-order transfer function with time peak equal to 5 minutes and overshoot equal to 40% and 5% for the reactor concentration and temperature, respectively. With regard to the disturbance rejection case, the equivalent impulse response is adopted. Other configurations of the proposed method can be found in Table 3.6.

Two scenarios are tested and compared in order to present the flexibility of the proposed method in choosing the performance criteria and their impact on the tuned parameters. The first scenario considers the total performance objective TISE+IMVI, while in the second scenario the objective is to consider only the performance of controlled variables (TISE).

Figure 3.19 demonstrates that tracking the objective TISE results in a better performance of the controlled variables by quickly stabilizing them within the spe-

Table 3.6: Setting of the performance tracking method for the CSTR system.

Variables	Values	Variables	Values
h_T	8	h_{sim}	33
$\mathbf{q}_{max}$	$[\infty; \infty]$	$\mathbf{q}_{min}$	$[0.002; 0.1]$
$\Delta\mathbf{q}_{max}$	1	$\Delta\mathbf{q}_{min}$	-1
$\mathbf{r}_{max}$	$[\infty; \infty]$	$\mathbf{r}_{min}$	$[0; 0]$
$\Delta\mathbf{r}_{max}$	$[1; 1]$	$\Delta\mathbf{r}_{min}$	$[-1; -1]$

cified tunnel. Nevertheless, the manipulated variables F_{in} and T_c are subject to much more variation during the simulation period (cf. Figure 3.20). On the other hand, tracking the objective TISE+IMVI, which also considers the control effort in the evaluation of the tuning parameters, leads to smoother modifications, i.e. as expected, the method yields tuning actions in order to decrease variation in the manipulated variables.
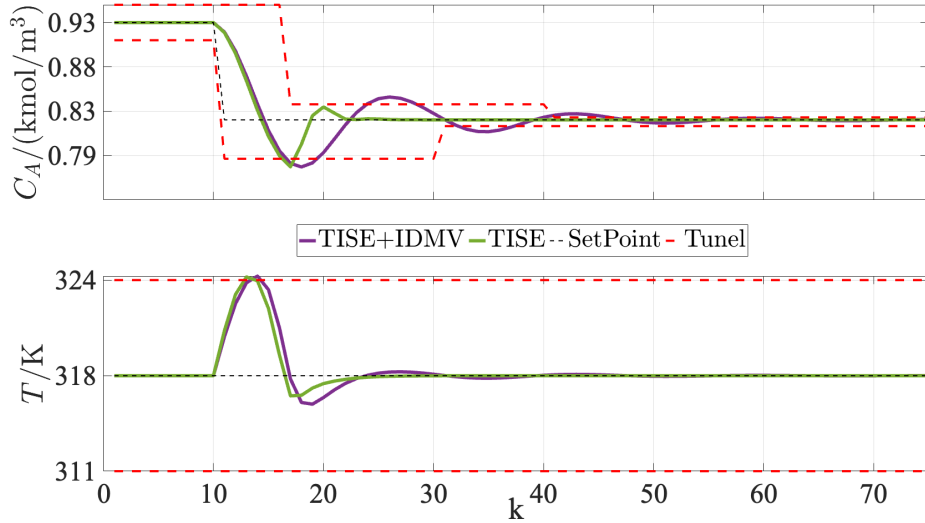
Figure 3.19: Outputs of the CSTR system for different configurations of the performance tracking method with IHMPC.

The behaviors addressed above can be quantitatively re-evaluated through control performance indices, as shown in Table 3.7.

By not explicitly considering the control effort in its formulation, the results reveal that the suppression matrix is almost zeroed (see Figure 3.21), which generates
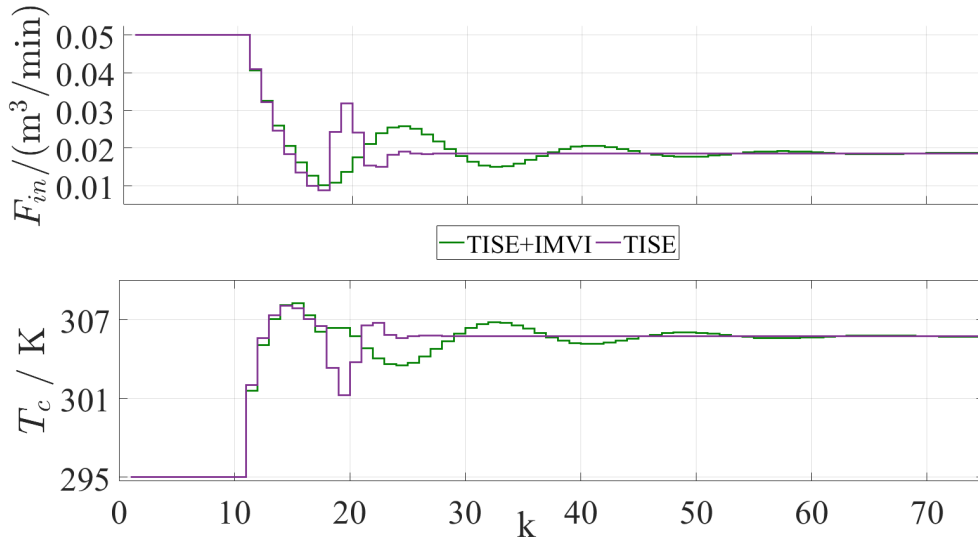
Figure 3.20: Inputs of the CSTR system for different configurations of the performance tracking method with IHMPC.

Table 3.7: Performance indices evaluated for different configurations of the performance tracking method applied to the CSTR system with IHMPC.

Index	TISE+IMVI	TISE
ISE(y_1)	0.0333	0.0232
ISE(y_2)	0.0016	0.0015
IMVI(u_1)	0.1334	0.2960
IMVI(u_2)	0.0007	0.0011
ISE + IMVI	0.1690	0.3218

a more aggressive response, worsening the overall performance. On the other hand, the tuning actions obtained from the objective TISE+IMVI resulted in a better overall performance, in particular a significant improvement in the inlet flow rate variations.

Another feature of adopting the objectives TISE and TISE+IMVI is shown in Figure 3.22. The TISE-based performance calculates the tuning actions to minimize only the objective TISE, which results in an increase in the importance matrix ($\mathbf{Q_y}$) and a decrease in the suppression matrix ($\mathbf{R}$). Although this tuning method configuration improves the performance of all the controlled variables, the system results in a worse global performance, caused by the increase in variation of both
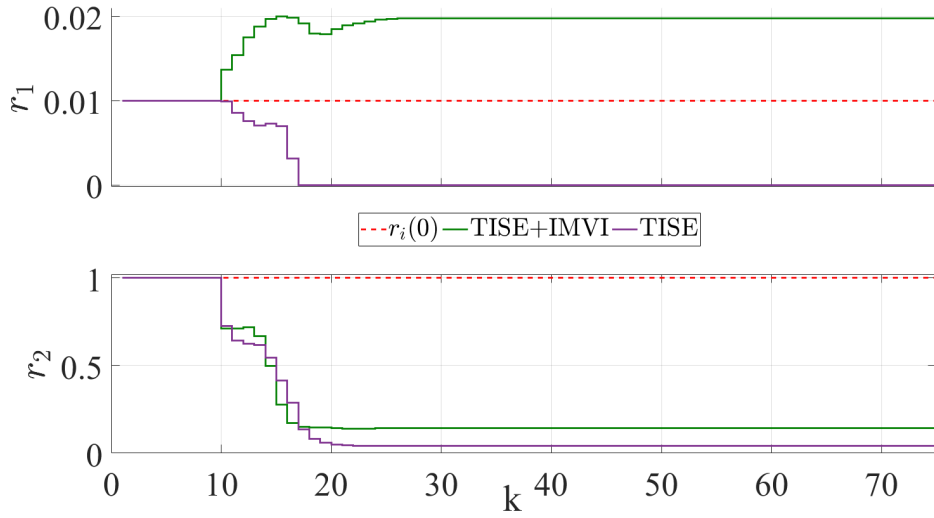
Figure 3.21: Responses of the weighting elements $\mathbf{R}$ of IHMPC for different configurations of the performance tracking method applied to the CSTR system.

manipulated variables. However, when considering the contribution of the control efforts (TISE+IMVI), a reduction in the values of q_i and r_2 combined with an increase in r_1 can be observed, which results in a better performance of the inlet flow rate, reagent concentration, and the process as a whole.
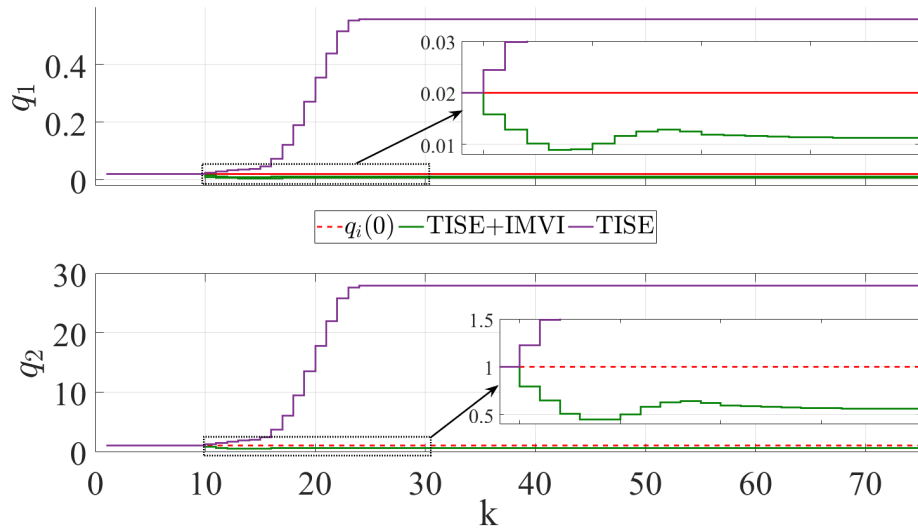
Figure 3.22: Responses of the weighting elements $\mathbf{Q}$ of IHMPC for different configurations of the performance tracking method applied to the CSTR system.

In this scenario, TISE+IMVI can be more appropriate for implementing auto-

tuning if a smooth response is desired. The process remains close to the tunnel established by the specialist with less control effort, contributing to the overall process improvement. On the other hand, if a fast response is required, TISE results in a quicker dynamic behavior within the performance tunnel but with a higher control effort, resulting in worse overall performance.

Regarding online practicability, the ratio between the computational time and the auto-tuning sample time is depicted in Figures 3.23 and 3.24. It is observed that the maximum ratio value is close to five times greater than the sample time, making the online implementation of the proposed framework challenging.
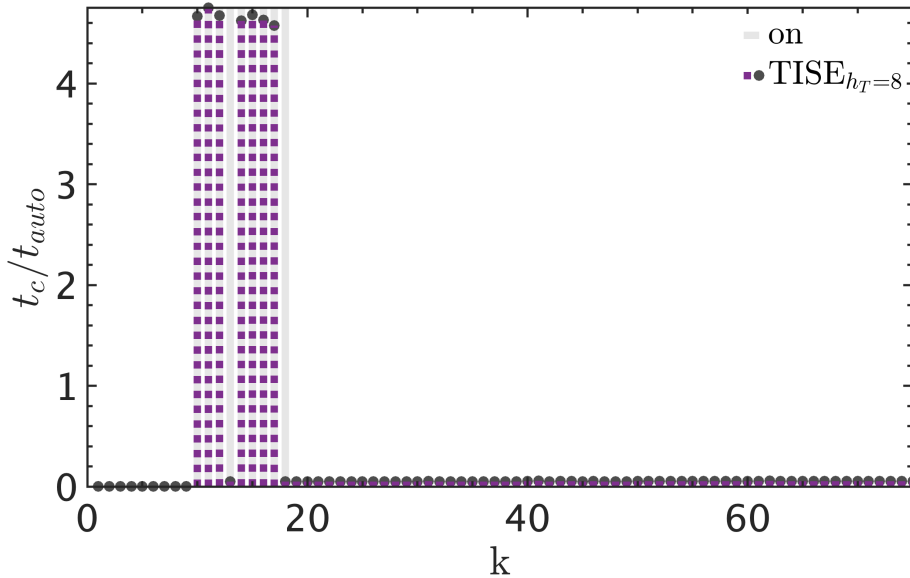
Figure 3.23: Ratio of the computational and auto-tuning sample time for TISE computed when the framework is triggered (On - gray zone), in which $t_{auto} = T_s$.

To address this issue, it is essential to investigate features such as the ODE and optimization solvers, script improvements, or revise auto-tuning horizons. In this way, Figures 3.25, 3.26, 3.27 and 3.28 present the impact of the tuning horizon on the system dynamic and the computational time, using the TISE+IMVI as the objective function. Note that the responses obtained are very similar for all tuning horizons tested, with differences only in the computational time and sample time ratio (Figures 3.29 and 3.30). $h_T = 1$ can provide a similar dynamic response with $tc/t_{auto} \leq 0.5$, making the online implementation viable.

47
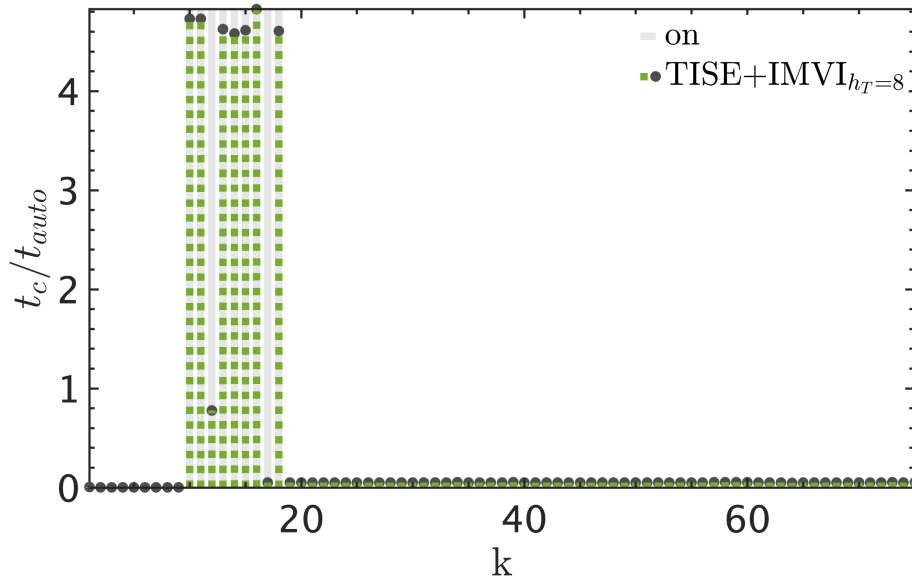
Figure 3.24: Ratio of the computational and auto-tuning sample time for TISE+IMVI computed when the framework is triggered (On - gray zone), in which $t_{auto} = T_s$.
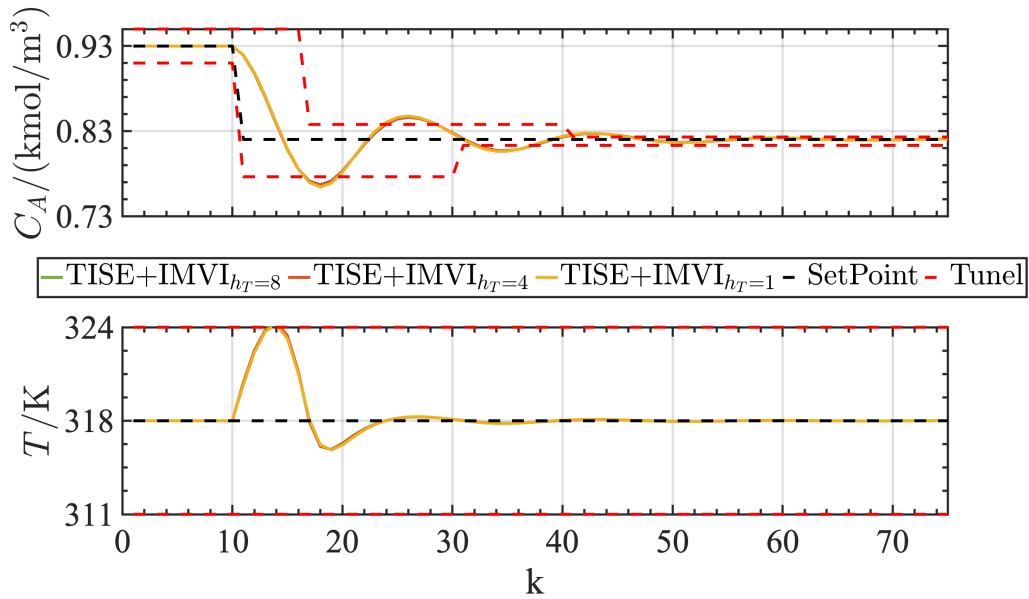
Figure 3.25: Behavior of CSTR process variables for different tuning horizons.

3.4   Partial conclusions

The method proposed in this work presented the combination of three main elements: closed-loop simulation in the presence of model-plant mismatch, tuning actions sequence and receding horizon optimization. Together, these elements provide
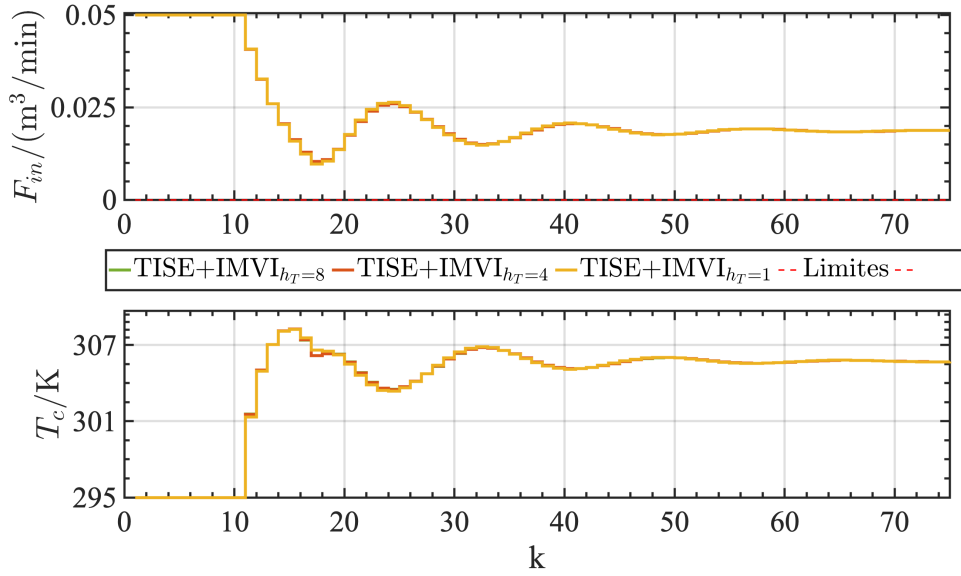
Figure 3.26: Behavior of CSTR manipulated variables for different tuning horizons.
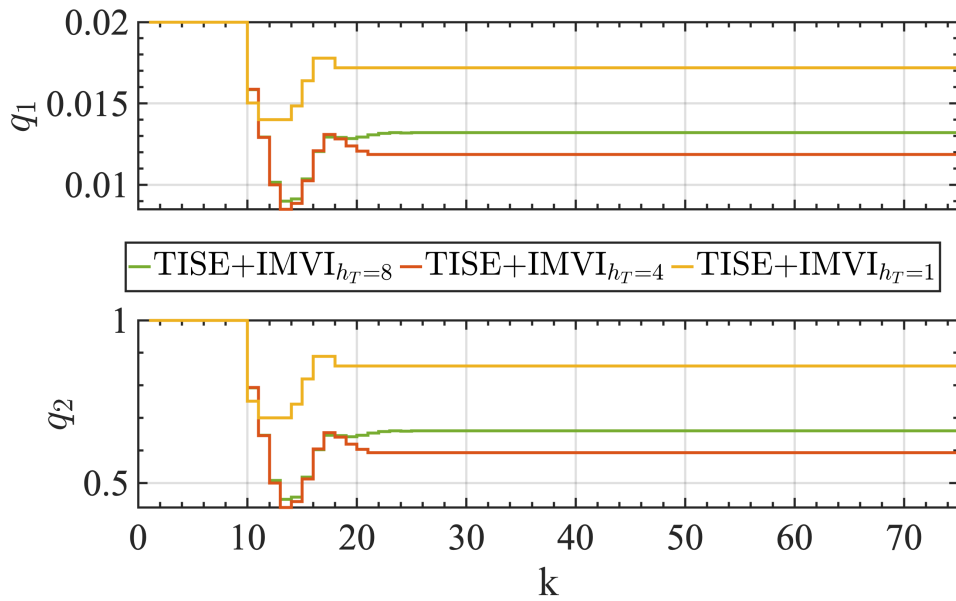
Figure 3.27: Behavior of Q for different tuning horizons in CSTR case.

greater flexibility for applications, regarding MPC type, process type, performance requirements (represented by time-domain tunnels and objective function) and robustness requirements (represented by the closed-loop simulation in the presence of mismatch with receding horizon optimization and Integral of Manipulated Variables Increments associated with time-domain tunnels). In addition, they enable

49
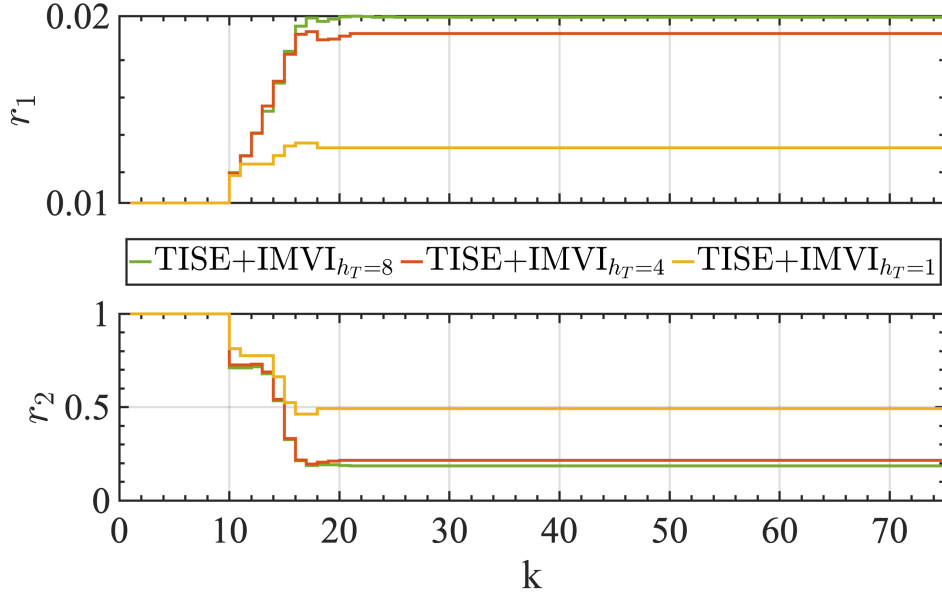
Figure 3.28: Behavior of R for different tuning horizons in CSTR case.
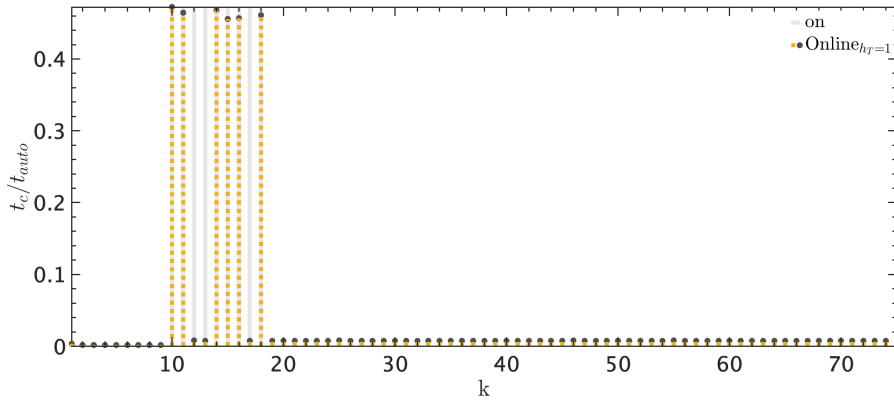
Figure 3.29: Behavior of tc/t_{auto} for $h_T = 1$ in CSTR case with $t_{auto} = T_s$.

online implementation, given that they allow a degree of freedom and update the optimization problem at each instant.

The results show that the closed-loop simulation in the presence of model-plant mismatch structure accepts different processes and MPC, which is demonstrated and justified by the tests in a DMC and an IHMPC. Moreover, the insertion of the penalty matrix in the performance tunnel has been demonstrated to promotes a better adaptation to the criteria desired by the expert and the addition of the MV increments lead to a smoother tuning, improving performance of the the system with less control effort.
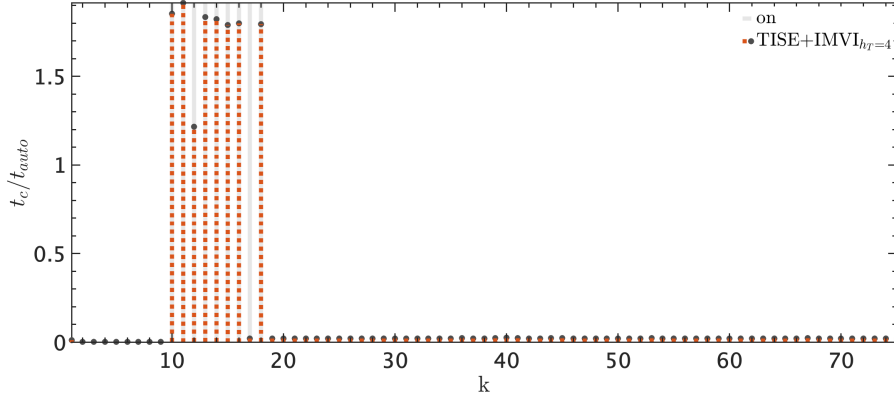
Figure 3.30: Behavior of tc/t_{auto} for $h_T = 4$ in CSTR case with $t_{auto} = T_s$.

The sensitivity analysis of the tuning horizon indicated that the optimization problem stayed practicable, even for small values, which may result from the proposed structure for the optimizer. Since the tunnel performance is inserted as a penalty matrix and not as constraints, the calculation of the solution was facilitated. However, this same penalty matrix creates a non-quadratic objective function, making it difficult for the algorithm to converge and may increase the computation time.

In this scenario, the next chapter presents modifications to auto-tuning problems to provide a smoother optimization problem, improving its feasibility and online implementation—additionally, a new perspective on MPC tuning problems. The optimal parameter values are computed to reach economic goals, highlighting the trade-off between performance and economic criteria.

Chapter 4

Tracking economic goals of an ESP-lifted oil well by an auto-tuning method

This chapter proposes a novel economic requirements-oriented online tuning strategy for MPC, the design of which encompasses the well-known operational particularities of oil production wells with ESP installations, e.g. operational envelope, maximization of oil production, minimization of power consumption, and profit maximization. The proposed tuning strategy is based on an online receding horizon optimization framework that can interact with RTO layers and different MPC techniques in a computation time appropriate for real- time implementations. The benefits of the proposed method are demonstrated by a case study that investigates different tuning requirements applied to provide an optimal ESP-lifted operation. It shows that using economic goals for MPC tuning problems is an effective way to achieve improved ESP-lifted oil operation.

The text included here is part of the published paper in the Journal of Petroleum Science and Engineering:

- FONTES, R. M.; SANTANA, D. D.; MARTINS, M. A. F. An MPC auto-tuning framework for tracking economic goals of an ESP-lifted oil well. Journal of Petroleum Science and Engineering, vol. 217, no. July, p. 110867, 2022. DOI 10.1016/j.petrol.2022.110867.

4.1 An implementable zone MPC approach

Several works present ESP validated and reliable models applicable to conceive controllers and optimizers structures (Mohammadzaheri et al. 2020, Costa et al. 2021). Costa et al. (2021) present a review of first principles-based ESP modeling methods, which are obtained from mass and momentum balances considering single-phase flow. Furthermore, Costa et al. (2021) developed a single-phase dynamic phenomenological model that accurately describes an ESP-lifted oil well pilot plant. The model parameters are estimated by Bayesian inference and validated with experimental data collected from an ESP apparatus installed at the CTAI Laboratory located at the Federal University of Bahia. On the other hand, some oil reservoirs present some gas concentration, characterizing a, at least, two-phase flow (Mohammadzaheri et al. 2020). Mohammadzaheri et al. (2020) present a review of multi-phase ESP empirical modeling, whose use is justified when the gas-oil ratio becomes significant to change the flow dynamics and consequently the ESP operation. The same authors also contribute to this modeling issue, developing an artificial neural network-based two-phase flow-type model validated with experimental data borrowed from literature.

Since the single-phase models can represent ESP-lifted oil well dynamics with appropriate accuracy, even with low gas concentration, the model presented by Costa et al. (2021) is used in this paper. The ordinary differential equation system (ODES) considers an ESP with 15 stages and a mineral lubricant equivalent to API 10 oil in the liquid phase. Accordingly, ODES is described from mass and momentum balances as follows

$$
\begin{cases}
\dfrac{dL_a(t)}{dt} = \dfrac{K_r\sqrt{p_r(t) - p_{bh}(t)} - q_m(t)}{A}, \\
\dfrac{dp_{wh}(t)}{dt} = \dfrac{\beta_2 \cdot \left(q_m(t) - K_c \cdot z_c(t) \cdot \sqrt{p_{wh}(t) - p_m}\right)}{V_2}, \\
\dfrac{dq_m(t)}{dt} = \dfrac{\bar{A} \cdot (p_{pbh}(t) - p_{wh}(t) + \Delta p_p(t) - \Delta p_h - \Delta p_f(t))}{\rho \cdot \bar{L}},
\end{cases}
\tag{4.1}
$$

where $L_a(t)$ is the oil level in the annulus in m; $z_c(t)$ is the choke valve opening; $p_{wh}(t)$, $p_r(t)$, $p_{bh}(t)$ and $p_m(t)$ are the wellhead, reservoir, bottom and manifold pressures in Pa, respectively; $q_m(t)$ is the average flow rate in the production column in m^3/s; $\Delta p_p(t)$ is the differential pressure in Pa; $\Delta p_f(t)$ is the friction factor in Pa;

Δp_h is hydrostatic pressure in Pa; $\bar{L} = \dfrac{L_1 + L_2}{2}$ is the average well length.

The friction factor, Δp_f, hydrostatic pressure, Δp_h, and differential pressure (Pa), $\Delta p_p(t)$, are described by (Costa et al. 2021):

$$\Delta p_f(t) = \pi \cdot \sum_{i=1}^{2} \frac{f_i(t)\rho q_m(t)}{2\pi r_i^3} \tag{4.2}$$

$$\Delta p_h = g \cdot \sum_{i=1}^{2} \rho \cdot h_i \tag{4.3}$$

$$f_i(t) = \begin{cases} \dfrac{64}{\text{Re}(q_m(t))}, & \text{if } \text{Re}(q_m(t)) < 4000 \\[2ex] 0.3164\text{Re}(q_m(t))^{-0.25}, & \text{otherwise} \end{cases} \tag{4.4}$$

$$\Delta p_p(t) = H(t)g\rho \tag{4.5}$$

$$H(t) = \frac{f(t)}{f_0} \sum_{i=0}^{2} \alpha_i q_m^i(t) \tag{4.6}$$

where f_i is the friction factor; Re is the Reynolds number; $H(t)$ is the pump head which depends on the rotational frequency, $f(t)$, in Hz, and the average flow rate, $q_m(t)$ More details about the constant values of the ESP structure can be consulted in Table 4.1.

Table 4.1: ESP parameters obtained from Costa et al. (2021)

Parameter	Description	Value
h_2	Height from the reservoir to choke	32.0 m
h_1	Height from the pump intake to choke	22.7 m
L_1	length from the reservoir to choke	9.3 m
L_2	Length from the pump intake to choke	22.7 m
r_1	Pipe radius below ESP	0.11 m
r_2	Pipe radius above ESP	0.038 m
A	Cross-section area of the annulus	0.034 m^2
$\bar{A}$	Average cross-section area	0.011 m^2
$\bar{L}$	Average length	16.0 m
V_2	Pipe volume above ESP	0.10 m^3
g	Gravity constant	9.81 m/s^2
μ	Fluid viscosity	0.01 Pa.s

Parameter	Description	Value
ρ	Fluid density	855.0 kg/m^3
β_2	Bulk modulus	1.8×10^9 Pa
f_0	ESP characteristics ref. freq.	60.0 Hz
K_c	Choke valve constant	3.8×10^{-6} m^3/(sPa$^{0.5}$)
K_r	Reservoir valve constant	3.2×10^{-6} m^3/(sPa$^{0.5}$)
α_0	Head's polynomial coefficient	180.79 m
α_1	Head's polynomial coefficient	7.90 s/m^2
α_2	Head's polynomial coefficient	-75.40 s^2/m^5

Furthermore, regarding the control of an ESP-lifted oil well, MPC strategies have been adopted due to their optimal control law and the way that they can efficiently incorporate process constraints. However, some MPC strategies can yield unfeasible solutions due to conflict among the system constraints, terminal equality constraints and process disturbances (Fontes et al. 2020). Consequently, MPC-based solutions with guaranteed feasibility have been presented as a viable alternative to mitigate issues in ESP-lifted oil well control, as suggested by Fontes et al. (2020) and Santana et al. (2021). So, an infinite horizon-based stabilizing MPC (IHMPC), proposed by Fontes et al. (2020), is applied to an ESP-lifted oil pilot plant, simulated by Eq. (4.1) and Eq. (4.2), where $\mathbf{y} \equiv [L_a,\ H]^\top$ are the controlled variables, $\mathbf{u} \equiv [f,\ z_c]^\top$ are manipulated variables. Problem 4 describes the control law of the proposed IHMPC.

Problem 4:

$$\min_{\Delta\mathbf{u}_k,\mathbf{y}_{\mathrm{sp}},\boldsymbol{\delta}_\mathbf{y},\boldsymbol{\delta}_\mathbf{u}} F_k = \sum_{j=0}^{\infty} \|\mathbf{y}(k+j|k) - \mathbf{y}_{\mathrm{sp}} - \boldsymbol{\delta}_\mathbf{y}\|_{\mathbf{Q}_\mathbf{y}}^2 + \sum_{j=0}^{m-1} \|\Delta\mathbf{u}(k+j|k)\|_{\mathbf{R}_\mathbf{u}}^2$$

$$+ \sum_{j=0}^{\infty} \|\mathbf{u}(k+j|k) - \mathbf{u}_{tg} - \boldsymbol{\delta}_\mathbf{u}\|_{\mathbf{Q}_\mathbf{u}}^2 + \|\boldsymbol{\delta}_\mathbf{y}\|_{\mathbf{S}_\mathbf{y}}^2 + \|\boldsymbol{\delta}_\mathbf{u}\|_{\mathbf{S}_\mathbf{u}}^2,$$

subject to:

$$\begin{cases} \mathbf{u}_{\min} \leq \mathbf{u}(k-1) + \sum_{i=0}^{j} \Delta\mathbf{u}(k+i|k) \leq \mathbf{u}_{\max}, \\ -\Delta\mathbf{u}_{\max} \leq \Delta\mathbf{u}(k+j|k) \leq \Delta\mathbf{u}_{\max} \qquad j = 0,\ldots,m-1, \\ \Delta\mathbf{u}(k+j|k) = 0,\ \forall j \geq m, \end{cases} \qquad (4.7)$$

$$\begin{cases} \mathbf{x}(k+j|k) = \mathbf{A} \cdot \mathbf{x}(k+j-1|k) + \mathbf{B} \cdot \Delta\mathbf{u}(k+j-1|k), \\ \mathbf{y}(k+j|k) = \mathbf{C} \cdot \mathbf{x}(k+j|k), \end{cases} \tag{4.8}$$

$$\mathbf{x}^{\mathrm{s}}(k+m|k) - \mathbf{y}_{\mathrm{sp}} - \boldsymbol{\delta}_{\mathbf{y}} = 0, \tag{4.9}$$

$$\mathbf{u}(k+m-1|k) - \mathbf{u}_{tg} - \boldsymbol{\delta}_{\mathbf{u}} = 0, \tag{4.10}$$

$$\underbrace{\begin{bmatrix} La_{\min}(k) \\ \hat{H}_{\min}(k|k) \end{bmatrix}}_{\mathbf{y}_{\min}} \leq \underbrace{\begin{bmatrix} La_{\mathrm{sp}} \\ H_{\mathrm{sp}} \end{bmatrix}}_{\mathbf{y}_{\mathrm{sp}}} \leq \underbrace{\begin{bmatrix} La_{\max}(k) \\ \hat{H}_{\max}(k|k) \end{bmatrix}}_{\mathbf{y}_{\max}}, \tag{4.11}$$

where m is the control horizon, $\mathbf{y}(k+j|k)$ is the output vector at time step $k+j$ evaluated with information at time step k, $\mathbf{y}_{\mathrm{sp}}$ is the optimal set-point output estimated by the IHMPC, $\mathbf{y}_{\min}$ and $\mathbf{y}_{\max}$ are the output bounds where $La_{\min}(k|k)$ and $La_{\max}(k|k)$ are the specified oil level limits, $\hat{H}_{\min}(k|k)$ and $\hat{H}_{\max}(k|k)$ are computed based on the average flow estimate obtained by an Extended Kalman Filter (EKF). $\mathbf{x}(k+j|k)$ is the state vector, $\mathbf{x}^{\mathrm{s}}(k+j)$ is the integrating states produced by the incremental form of inputs in the state space, $\mathbf{u}(k+j|k)$ is the input vector with the respective constraints $\mathbf{u}_{\min}$ and $\mathbf{u}_{\max}$, $\Delta\mathbf{u}(k+j)$ is the input increment constrained by $\Delta\mathbf{u}_{\min}$ and $\Delta\mathbf{u}_{\max}$, $\mathbf{u}_{tg}$ is the input target defined by an RTO layer, and $\boldsymbol{\delta}_{\mathbf{y}}$, $\boldsymbol{\delta}_{\mathbf{u}}$ are slack variables to soften the terminal equality constraints. $\mathbf{S}_{\mathbf{u}}$, $\mathbf{S}_{\mathbf{y}}$, $\mathbf{Q}_{\mathbf{u}}$, $\mathbf{Q}_{\mathbf{y}}$, and $\mathbf{R}$ are weighting matrices. The detailed description of the state-space design and matrices $\mathbf{A}$, $\mathbf{B}$, $\mathbf{C}$ and the numeric values are shown in Appendix A.

Figure 4.1 illustrates the installations of ESP-lifted oil pilot plant with the proposed advanced control structure used in this work and its possible integration with an RTO layer.

Note that, Figure 4.1 highlights, in gray, the operational envelope for the upthrust to avoid violations caused by an external disturbance. The minimum head $\left(\hat{H}_{\min}(k|k)\right)$ is evaluated based on the upper limit of the gray zone called the safe limit. These operational limits $\left(\hat{H}_{\max}(k|k), \hat{H}_{\min}(k|k)\right)$ are computed by the average flow rate estimate $(\hat{q}(k|k))$ obtained by an EKF, which uses the measured variables $\left(\mathbf{y} \equiv [L_a, H]^\top \text{ and } \mathbf{u} \equiv [f, z_c]^\top\right)$ to estimate the non-measured states. Additionally, an RTO layer or a specialist can also provide a choke valve opening target $\left(z_{c_{tg}}\right)$ based on the process measurements. The benefit of using this MPC strategy for the ESP operation is incorporating the operational envelope explicitly into the control problem Eq. (4.11) and tracking the optimal targets $\left(z_{c_{tg}}\right)$, allowing to reach
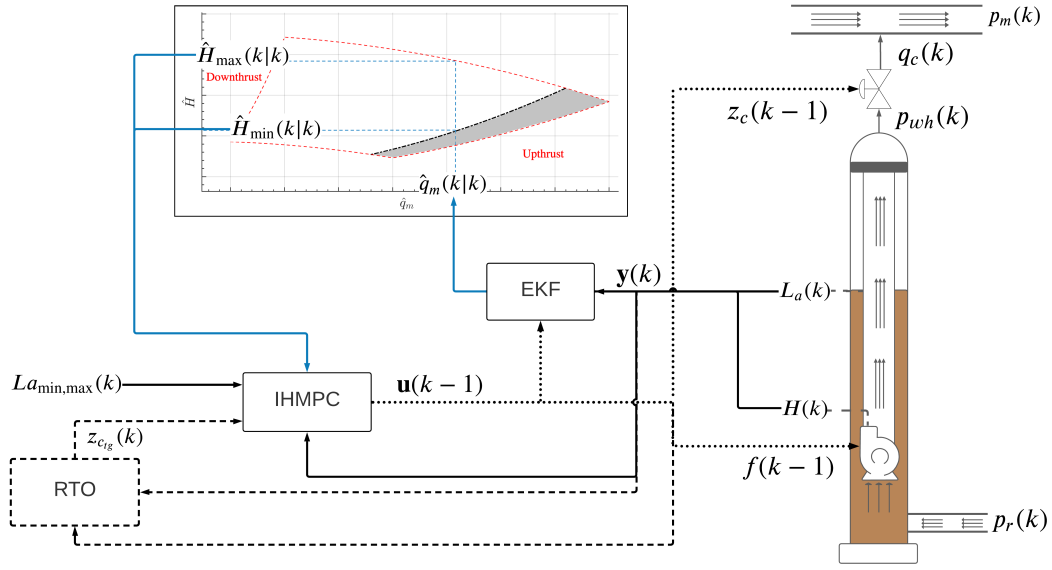
Figure 4.1: Representation of the ESP-lifted pilot plant with the proposed control structure and a suggested interaction with an RTO layer.

specified economic requirements while maintaining the process within the operation zone with a more straightforward numerical optimization problem solution since it is designed with soft constraints and offers an implementable MPC approach in practice.

The benefit of using this MPC strategy for the ESP operation is incorporating the operational envelope explicitly into the control problem Eq. (4.11) and tracking the optimal targets $\left(z_{c_{tg}}\right)$. This approach allows for reaching specified economic requirements while maintaining the process within the operation zone. It offers a more straightforward numerical optimization problem solution since it is designed with soft constraints and provides an implementable MPC approach.

Furthermore, ESP-lifted control system should be flexible to track economic gains, such as minimum pump energy consumption, maximum oil production, or maximum profit. In order to achieve these requirements and keep the oil production process at its most efficient point, one is required to choose the appropriate MPC parameters. However, MPC tuning is an uphill task, and even if the MPC is offline-tuned, keeping a fixed set of parameters does not ensure the desired goal due to unmeasured disturbances and process changes (Garriga & Soroush 2010, Fontes et al. 2019, Alhajeri & Soroush 2020). Therefore, the following section presents

57

the major contribution of this work: an MPC auto-tuning framework capable of encompassing economic and performance criteria.

4.2 The proposed economic tracking MPC auto-tuning formulation.

MPC performance is associated with its tuning parameters, however, tuning such parameters is laborious, given the non-intuitive interaction between them (Fontes et al. 2019, Alhajeri & Soroush 2020).

To address this issue, this thesis contributes with an MPC auto-tuning formulation based on a receding horizon optimization scheme whose MPC parameters ($\boldsymbol{\theta}$) are evaluated from a nonlinear closed-loop system simulation. Within this paradigm, the proposed auto-tuning framework can receive plant measurements ($\mathbf{y}$,$\mathbf{u}$), reference signals, and different tuning criteria to optimally adjust the tuning parameters of an existing MPC to meet specified economic requirements and keep the process inside the control zone for as long as possible. Based on this paradigm, Figure 4.2 illustrates the implementation of the proposed framework applied to the ESP-lifted oil case.

When the IHMPC (Problem 4) is implemented on the ESP-lifted oil pilot plant model, the chosen tunable parameters are the elements of the weighting matrices, $\mathbf{Q_y}, \mathbf{R}$ and $\mathbf{Q_u}$. The control horizon, m, is not online-tuned because it corresponds to the number of control actions, impacting the IHMPC computational time. Consequently, it is not recommended to change its value at each sample time. Furthermore, targets are solely set for the opening choke valve $\left(z_{c_{tg}}\right)$ in this work, so the set of tunable parameters is defined as

$$\boldsymbol{\theta}(k|k) = [q_{y_1}(k|k), q_{y_2}(k|k), r_{u_1}(k|k), r_{u_2}(k|k), q_{u_2}(k|k)]^\top. \tag{4.12}$$

The following subsections describe the main elements shown in Figure 4.2 in more detail, for the proposed MPC auto-tuning framework.
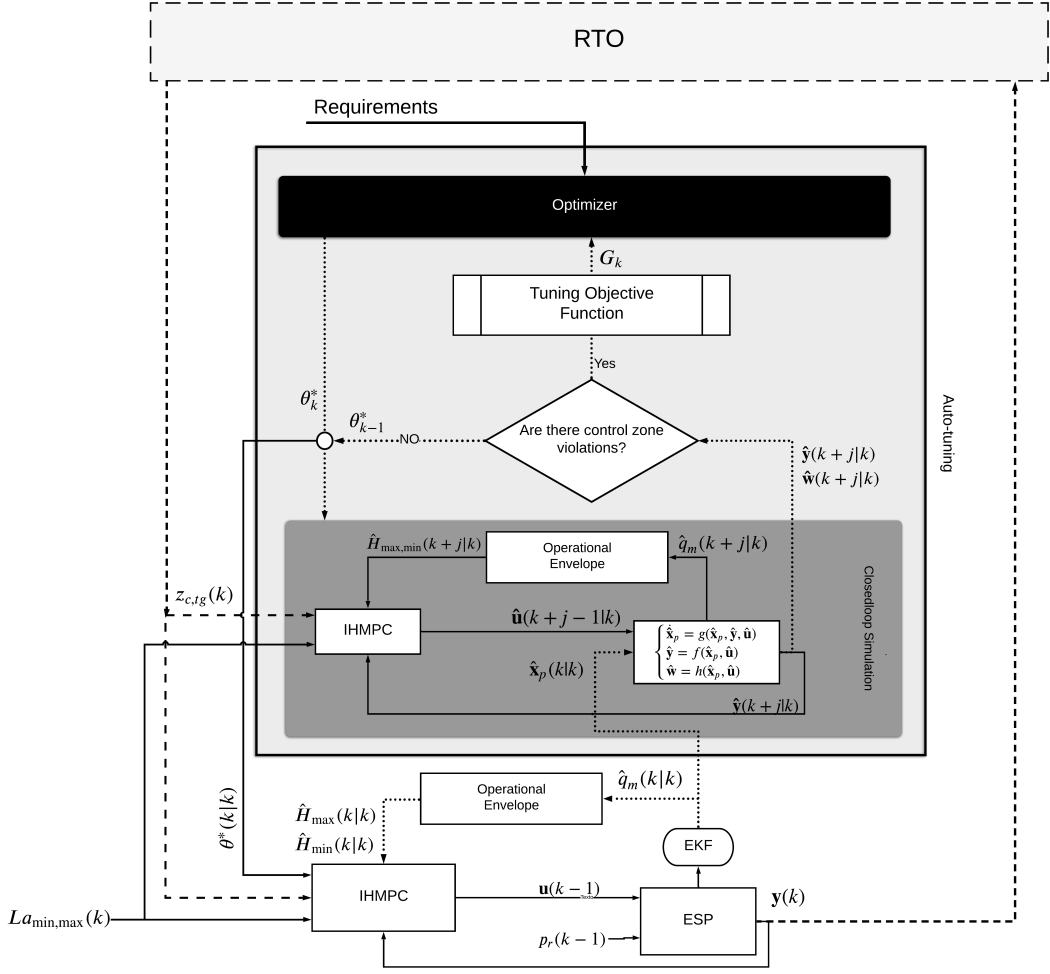
Figure 4.2: Implementation scheme for the proposed auto-tuning method to track the economic goals of the ESP-lifted oil well system with IHMPC controller.

4.2.1 Tuning actions

The proposed MPC auto-tuning framework computes the optimal parameter increments:

$$\Delta\boldsymbol{\theta}_k^* = [\Delta\boldsymbol{\theta}^*(k|k), \ldots, \Delta\boldsymbol{\theta}^*(k + h_{\mathrm{T}} - 1|k)]^\top, \qquad (4.13)$$

$$\boldsymbol{\theta}^*(k|k) = \boldsymbol{\theta}^*(k - 1) + \Delta\boldsymbol{\theta}^*(k|k), \qquad (4.14)$$

where $\Delta\boldsymbol{\theta}_k^*$ is the sequence of optimal parameter increments evaluated by the measurements at time step k; $\Delta\boldsymbol{\theta}^*(k|k)$ is the optimal parameter increment implemented at time step k; and h_{T} is denominated the tuning horizon. The first element of the optimal movement, $\Delta\boldsymbol{\theta}^*(k|k)$, is added to the current MPC parameters, $\boldsymbol{\theta}^*(k - 1)$, to provide the optimal MPC parameters $\boldsymbol{\theta}^*(k|k)$, as Eq. (4.14).

59

Since the tuning actions are the decision variables in this receding horizon optimization, the constraints associated with them are formulated by

$$\begin{cases} -\Delta\boldsymbol{\theta}_{\max} \leq \Delta\boldsymbol{\theta}_k \leq \Delta\boldsymbol{\theta}_{\max}, \\ \Delta\boldsymbol{\theta}\,(k+j|k) = 0, \ \forall j \geq h_T, \ j = 0, 1, \ldots, h_{\text{sim}} - 1 \quad , \\ \boldsymbol{\theta}_{\min} \leq \boldsymbol{\theta}(k-1) + \sum_{i=0}^{j} \Delta\boldsymbol{\theta}(k+i|k) \leq \boldsymbol{\theta}_{\max}, \end{cases} \quad (4.15)$$

where, $\boldsymbol{\theta}_{\min}$, $\boldsymbol{\theta}_{\max}$, and $\Delta\boldsymbol{\theta}_{\max}$ are the bounds related to tuning parameters. Compared to Eq. 3.7, Eq. 4.15 is simpler due to its linear structure, facilitating the implementation and solution of the optimizer.

Then, based on Eq. (4.12), the tuning actions are defined as

$$\Delta\boldsymbol{\theta}(k|k) = [\Delta q_{y_1}(k|k), \Delta q_{y_2}(k|k), \Delta r_{u_1}(k|k), \Delta r_{u_2}(k|k), \Delta q_{u_2}(k|k)]^{\top} . \quad (4.16)$$

4.2.2 Closed-Loop Simulation (CLS)

The framework uses a dynamic closed-loop simulation (CLS) to provide simulated values $(\hat{\mathbf{y}}_k, \hat{\mathbf{u}}_k, \hat{\mathbf{w}}_k)$ of the process for some time steps ahead, denoted as simulation horizon - h_{sim}. This CLS must provide reliable process responses and economic estimates. A nonlinear model is adopted in the auto-tuning CLS layer to provide a rigorous process simulation and enable efficient monitoring of the performance of the MPC in tracking the economic criteria.

It is fundamental to accentuate that this work used an ESP nonlinear model in the CLS auto-tuning layer because this is known and validated. However, a nonlinear model will not always be available in some systems. In these cases, other model structures such as linear, adaptive, and machine learning-based models can be used, given the flexible CLS structure. Whatever the model structure applied in the CLS scheme, the values should be updated at each auto-tuning sample time using an appropriate estimator, like a bias or a state estimator, to be equivalent to the real closed-loop. As this paper applies a nonlinear model in CLS, the extended Kalman filter (EKF) is implemented to update and correct the CLS values (Figure 4.2).

Note that (Figure 4.2), the CLS representation is similar to the process control structure in Figure 4.1. The controller used in the closed-loop simulation has the same design as the one implemented in the process (Figure 4.2), which in this case

is the IHMPC (Problem 4). Since the IHMPC is based on the linear state-space model Eq. (4.8) and the ESP is represented by a nonlinear model, Eq. (4.1) and Eq. (4.18), it is necessary to correct the mismatch effect. Consequently, a state estimator is implemented within the IHMPC structure to estimate the linear model internal states based on the measurement variables. This paper applies the well-known Kalman filter to handle this subject.

A closer inspection of Figure 4.2 shows that the same operational envelope bounds are also considered in the CLS and the reservoir pressure (p_r) as an unmeasured disturbance that excites the ESP oil lift system. To address this issue, the reservoir pressure is assumed to be a new state variable with the ordinary differential equation given by

$$\frac{dp_r(t)}{dt} = N(0,\sigma), \tag{4.17}$$

where $N(0,\sigma)$ is a Gaussian white noise with standard deviation σ. Then Eq. (4.17) is included in Eq. (4.1), given a new system of ordinary differential equation described as

$$\begin{cases} \dot{\hat{\mathbf{x}}}_p = g(\hat{\mathbf{x}}_p,\hat{\mathbf{y}},\hat{\mathbf{u}}) \\ \hat{\mathbf{y}} = f(\hat{\mathbf{x}}_p,\hat{\mathbf{u}}) \\ \hat{\mathbf{w}} = h(\hat{\mathbf{x}}_p,\hat{\mathbf{u}}). \end{cases} \tag{4.18}$$

where $\hat{\mathbf{x}}_p$ is the new set of state variables $\left[\hat{L}_a,\hat{p}_{wh},\hat{q}_m,\hat{p}_r\right]^\top$, and $\mathbf{w}$ is the output vector estimated from algebraic equations ($\hat{\mathbf{w}} = h(\hat{\mathbf{x}}_p,\hat{\mathbf{u}})$), e.g. pump power. These output variables can be applied to compose the economic objective functions, e.g. minimizing power consumption or maximizing profit, described in section 4.2.3.

The reservoir pressure is estimated by an Extended Kalman Filter (Figure 4.2), designed to take into account Eq. (4.18). In this case, the EKF provides all state estimates, including the reservoir pressure ($\hat{p}_r$), used as initial conditions ($\hat{\mathbf{x}}_p(k|k)$) to solve the ordinary differential equations Eq. (4.18). The EKF updates Eq. (4.18) at each time step, which keeps the CLS as similar as possible to the process closed-loop system.

The presented structure (Figure 4.2) is equivalent to a closed-loop mismatch simulation because the equations applied to represent the ESP process (Eq. (4.1)

and Eq. (4.2)) are different from Eq. (4.18), which is applied to the CLS in the auto-tuning layer. To simplify this, the following mathematical representation is used

$$[\hat{\mathbf{y}}_k, \hat{\mathbf{u}}_k, \hat{\mathbf{x}}_{p_k}, \hat{\mathbf{w}}_k] = \text{CLS}\left(\boldsymbol{\theta}_k, \mathbf{y}_{\min,\max}, \mathbf{u}_{tg}(k), \mathbf{y}(k), \hat{\mathbf{x}}_p(k|k), \mathbf{u}(k-1)\right) \qquad (4.19)$$

where, $\hat{\mathbf{y}}_k = [\hat{\mathbf{y}}(k+1|k), \dots, \hat{\mathbf{y}}(k+h_{sim}|k)]^\top$, $\hat{\mathbf{u}}_k = [\hat{\mathbf{u}}(k|k), \dots, \hat{\mathbf{u}}(k+h_{sim}-1|k)]^\top$, $\hat{\mathbf{x}}_{p_k} = [\hat{\mathbf{x}}_p(k+1|k), \dots, \hat{\mathbf{x}}_p(k+h_{sim}|k)]^\top$ and $\hat{\mathbf{w}}_k = [\hat{\mathbf{w}}(k+1|k), \dots, \hat{\mathbf{w}}(k+h_{sim}|k)]^\top$, are the estimated values of controlled, manipulated, state and output variables, respectively; $\mathbf{y}_{\min,\max}$ are set-point bounds; $\boldsymbol{\theta}_k$ is current tunable parameters sequence. $\mathbf{y}(k)$, $\mathbf{u}(k-1)$ are the current measurements of controlled and manipulated variables, respectively, and $\hat{\mathbf{x}}_p(k|k)$ are the state estimates at time step k.

4.2.3 Tuning objective function

In order to provide flexibility to the framework and a trade-off between better process variable response and economic requirements, the following objective function is applied:

$$G_k = f_{\text{eco}_k} + \|\boldsymbol{\delta}\|^2_{\mathbf{S}_\delta} + \sum_{j=1}^{h_{\text{sim}}} \|\hat{\mathbf{y}}(k+j|k) - \mathbf{y}_{\text{sp}}(k+j|k)\|^2 + \sum_{j=0}^{h_{\text{sim}}-1} \|\boldsymbol{\Delta}\hat{\mathbf{u}}(k+j|k)\|^2,$$
$$(4.20)$$

where f_{eco} represents the economic objective function; $\hat{\mathbf{y}}$ and $\hat{\mathbf{u}}$ is the simulated values of the controlled and manipulated variables; $\boldsymbol{\delta}$ and $\mathbf{S}_\delta$ are slack variables and their weighting matrix. The primary role of the slack variables is to guarantee the feasibility of the optimization problem even when the simulated values are not within the control zone. For this, the slack variables are incorporated into the constraints of the optimization problem:

$$\hat{\mathbf{y}}_{\min}(k+j|k) - \boldsymbol{\delta} \leq \hat{\mathbf{y}}(k+j|k) \leq \hat{\mathbf{y}}_{\max}(k+j|k) + \boldsymbol{\delta}, \qquad j = 1, \dots, h_{sim}, \quad (4.21)$$

where $\hat{\mathbf{y}}_{\max}(k+j|k)$ and $\hat{\mathbf{y}}_{\max}(k+j|k)$ delimits the control zone. When comparing Eq. 3.9 with Eq. 4.20 and 4.21, it becomes evident that the latter significantly enhances the feasibility of auto-tuning while still retaining the tunnel penalty and quadratic objective characteristics.

f_{eco} is connected to the same economic objective used in the RTO layer. In such a manner, the auto-tuning layer computes optimal parameters to correct a better dynamic trajectory between the RTO targets. In the case of ESP-lifted oil wells, these RTO economic goals include factors such as flow rate, oil price, the energy cost of booster pumps and ESP, and for multiphase flow cases, gas void ratio, water cut, and separation cost (Mohammadzaheri et al. 2016). Based on the single-phase lifting model Eq. (4.1) and the features of the ESP apparatus (Figure 4.1) used in this work, economic factors based on multiphase flows are not considered, and a comparison of a few economic objectives functions for tuning the MPC is assessed. The first one involves steady-state economic targets as follows

$$f_{\text{eco}_k} = J_k = \sum_{j=1}^{h_{\text{sim}}} \|\hat{\mathbf{u}}(k+j|k) - \mathbf{u}_{\text{tg}}(k+j|k)\|^2, \tag{4.22}$$

in which $\mathbf{u}_{\text{tg}}$ represents an economic target provided by an RTO layer or specialist.

In summary, Eq. (4.22), in association with Eq. (4.20), aims to achieve a better economic response by keeping the manipulated variables as close as possible to the desired target, smooth control effort while maintaining the system within the control zone.

Additionally, explicit economic goals such as maximizing oil production Eq. (4.23), minimizing power consumption Eq. (4.24), and maximizing profit Eq. (4.25) are considered.

$$f_{\text{eco}_k} = -\hat{V}_k = -\sum_{j=1}^{h_{\text{sim}}} \hat{q}_m(k+j|k) \tag{4.23}$$

$$f_{\text{eco}_k} = \hat{P}_k = \sum_{j=1}^{h_{\text{sim}}} \hat{p}(k+j|k) \tag{4.24}$$

$$f_{\text{eco}_k} = -\$_k = -\sum_{j=1}^{h_{\text{sim}}} c_q \cdot \hat{q}_m(k+j|k) - c_p \cdot \hat{p}(k+j|k), \tag{4.25}$$

where $\hat{P}_k$, $\hat{V}_k$ and $\$_k$ are the estimates of ESP power, oil production and profit, respectively, obtained by the CLS at time step k; $\hat{p}$ is the estimated instantaneous ESP power; c_q and c_p are oil price and energy cost, respectively.

4.2.4 Receding horizon optimization

Combining all the elements described in the previous subsections, the receding optimization problem is set as

Problem 5:

$$\min_{\boldsymbol{\Delta\theta}_k,\boldsymbol{\delta}} G_k = f_{eco_k} + \|\boldsymbol{\delta}\|^2_{\mathbf{S}_\delta} + \sum_{j=1}^{h_{\mathrm{sim}}} \|\hat{\mathbf{y}}(k+j|k) - \mathbf{y}_{\mathrm{sp}}(k+j|k)\|^2 + \sum_{j=0}^{h_{\mathrm{sim}}-1} \|\boldsymbol{\Delta}\hat{\mathbf{u}}(k+j|k)\|^2$$

subject to:

$$[\hat{\mathbf{y}}_k, \hat{\mathbf{u}}_k, \hat{\mathbf{x}}_{p_k}, \hat{\mathbf{w}}_k] = \mathrm{CLS}\left(\boldsymbol{\theta}_k, \mathbf{y}_{\mathrm{min,\,max}}, \mathbf{u}_{tg}(k), \mathbf{y}(k), \hat{\mathbf{x}}_p(k|k), \mathbf{u}(k-1)\right)$$

$$\begin{cases} -\boldsymbol{\Delta\theta}_{\mathrm{max}} \leq \boldsymbol{\Delta\theta}_k \leq \boldsymbol{\Delta\theta}_{\mathrm{max}}, \\[2mm] \boldsymbol{\Delta\theta}(k+j|k) = 0,\ \forall j \geq h_T, \qquad j = 0, 1, \ldots, h_{\mathrm{sim}}-1 \\[2mm] \boldsymbol{\theta}_{\mathrm{min}} \leq \boldsymbol{\theta}(k-1) + \displaystyle\sum_{i=0}^{j} \boldsymbol{\Delta\theta}(k+i|k) \leq \boldsymbol{\theta}_{\mathrm{max}}, \end{cases}$$

$$\hat{\mathbf{y}}_{\mathrm{min}}(k+j+1|k) - \boldsymbol{\delta} \leq \hat{\mathbf{y}}(k+j+1|k) \leq \hat{\mathbf{y}}_{\mathrm{max}}(k+j+1|k) + \boldsymbol{\delta}$$

Problem 5 offers a new perspective about tuning MPC problems as it introduces economic requirements directly into the cost function. Consequently, the tuning parameters are calculated to achieve a better economic performance for the process.

Furthermore, it is interesting to note that Problem 5 becomes infeasible only if the CLS cannot be solved. However, the IHMPC used in CLS guarantees the feasibility of the optimization problem. Thus the CLS can always be solved, and the proposed auto-tuning structure is also feasible.

The significant advantage of the proposed economic auto-tuning method for MPC controllers is that its elements (CLS, tuning actions, objective function, and the receding horizon optimization) provide a flexible approach suitable for different MPC strategies and economic goals, i.e., they can be adapted for various cases.

4.2.5 Implementation

From the multi-level control hierarchy point of view, the proposed framework consists of a layer integrated with the MPC (Figure 4.2) which is executed in two steps:

First step - Monitoring: The first step monitors the process through the CLS, which provides the simulated values of the controlled, manipulated, state and

output variables $(\hat{\mathbf{y}}_k, \hat{\mathbf{u}}_k, \hat{\mathbf{x}}_{pk}, \hat{\mathbf{w}}_k)$ using the previous set of MPC tuning parameters $(\boldsymbol{\theta}(k-1))$. If the simulated values violate the control zone, the second step is activated to compute the optimal MPC parameters.

Second step - Auto-tuning: The second step evaluates the optimal MPC parameters to meet the desired tuning criteria by solving the non-linear receding horizon optimization, Problem 5.

With this two step implementation structure, Problem 5 is activated if the monitoring step detects that the control zone will be violated some time steps ahead. Consequently, the optimization is performed only when necessary, contributing to the feasibility of online implementation. Figure 4.3 depicts a trigger point in case of set-point change. The monitoring step detects a zone control violation using the current measurements and MPC parameters. After that, the auto-tuning step computes an optimal MPC parameter to keep the response in the control zone.
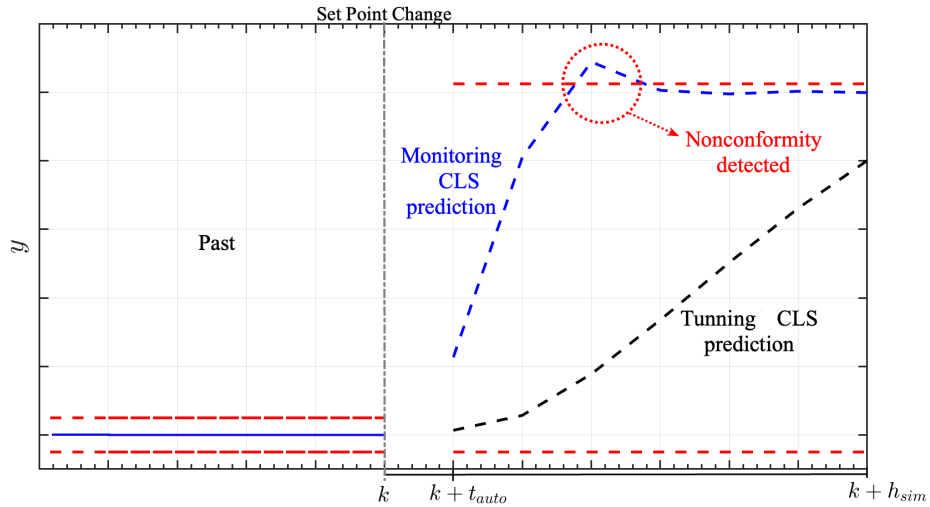
Figure 4.3: Illustration of the nonconformity detected by the prediction of the monitoring step and the optimal solution obtained by auto-tuning step.

For the implementation of the proposed method, it is essential to highlight some points:

<u>**Note 1:**</u> Normalizing the variables is crucial for better numerical conditioning. Further, the normalization balances each objective function term in this work, bringing all the variables to the same scale.

Regardless, it is essential to highlight that the objective function design addresses the desired tuning requirements. Thus, each objective function term can be weighted to emphasize its importance, aiming to represent the desired tuning criteria if required.

Note 2: The set of parameter constraints must be defined based on the prior knowledge of the specialist or with the aid of a rigorous offline simulation.

Note 3: The values of the slack weighting matrix elements must be higher than the elements of the other matrices ($\mathbf{S_y}, \mathbf{S_u} \geq \mathbf{Q_y}, \mathbf{Q_u}, \mathbf{R}_u$).

Note 4: The auto-tuning sample time (t_{auto}) should be higher or equal to the MPC sample time (t_{mpc}) and lower or equal to the RTO sample time (t_{rto}) (Figure 4.4).
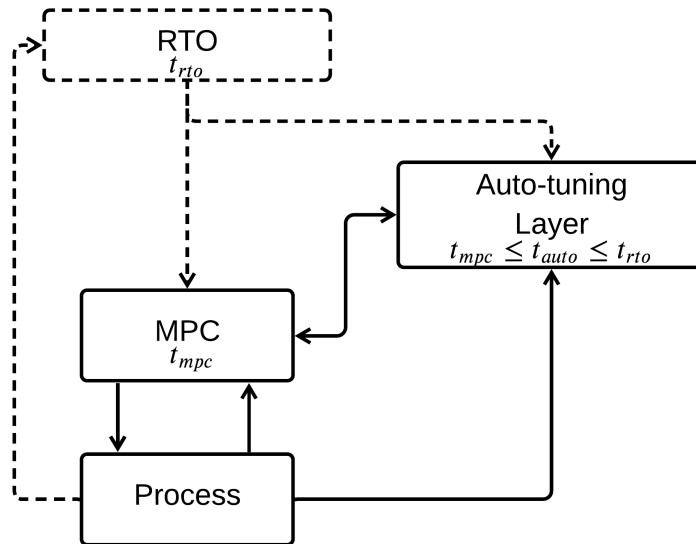
Figure 4.4: Illustration of a suggested implementation of the proposed auto-tuning framework.

Note that, Figure 4.2 presents a new hierarchy control structure inputting the proposed auto-tuning layer between the RTO and MPC layers. This structure allows the auto-tuning to dynamically evaluate optimal MPC parameters to lead the system into a better trajectory between the executions of the RTO layer.

Additionally, the auto-tuning layer is designed based on the same MPC strategy. Thus, t_{auto} should be defined according to the prediction model of the

MPC. Moreover, t_{rto} encompasses the solver computation time, when the process achieves a steady-state, which, this last one, is not required for the auto-tuning layer, allowing this layer to work in parallel or in series with the RTO layer to tune the MPC during process dynamic transitions. In summary, t_{auto} must be large enough to encompass the computation time of the optimization problem (Problem 5) but avoid the aliasing of the model predictions.

<u>**Note 5:**</u> The simulated results were evaluated on a computer system equipped with an octa-core processor running at 3.2 GHz and accompanied by 16 GB of RAM, operating on the macOS operating system.

Regarding the optimization algorithms employed, the controllers were implemented using the quadprog, and the problem was addressed using the Active-sets algorithm (fmincon)—both optimization subroutines of MATLAB version 2021b.

The system of ordinary differential equations was solved using a variable-steps and variable-orders method, employing numerical differentiation formulas ranging from orders 1 to 5.

It is crucial to emphasize that the choice of the numerical method can impact both the quality of the solution and the computational time required. Therefore, it is advisable to carefully consider this aspect before implementing the solution in a real-time system.

The next section presents results of the proposed MPC auto-tuning framework. It is capable of driving the ESP-lifted oil well to its desired operating point regarding the economic performance criteria.

4.3 Economic tracking results from an ESP-lifted oil well

As mentioned, the proposed auto-tuning method computes a sequence of optimal MPC parameters increments if nonconformities are detected. Violations of the control zone are therefore defined as a nonconformity criterion in this case study.

The discretized model of the IHMPC was formulated based on the linearization of Eq. (4.1) and Eq. (4.2) at the steady-state point ($z_c = 0.25$ and $f = 50$Hz), and the sample time (t_{mpc}) of 30 s. The assumed controlled variables are the level ($y_1 = L_a$) and the pump head ($y_2 = H$), and the manipulated variables are defined as the rotational frequency ($u_1 = f$) and the choke opening ($u_2 = z_c$). In terms of control zone, the minimum and maximum values of oil level ($L_{a_{min}}, L_{a_{max}}$) and the estimates of (up and down)-thrust $\left(\hat{H}_{min}, \hat{H}_{max} \right)$ were adopted. The other settings of the IHMPC and the auto-tuning layer are summarized in Table 4.2.

Table 4.2: Parameters of the IHMPC and the auto-tuning layer

Parameters	Values	Parameters	Values
m	3	h_T	1
t_{mpc}	30s	h_{sim}	5
c_q	10 R\$/l	c_p	45 R\$/kWh
$\mathbf{u}_{max}$	$[60\text{Hz},0.5]^\top$	$z_{c_{tg}}$	0.4
$\mathbf{u}_{min}$	$[30\text{Hz},0.1]^\top$	t_{auto}	60s
$\mathbf{Q}_y(0)$	$[1,1]^\top$	$\boldsymbol{\theta}_{min}$	$[0.01,0.01,0,0,0.01]^\top$
$\mathbf{R}_u(0)$	$[1,1]^\top$	$\Delta\boldsymbol{\theta}_{max}$	$[2,2,2,2,2]^\top$
$\mathbf{Q}_u(0)$	$[0,1]^\top$	$\boldsymbol{\theta}_{max}$	$[\infty,\infty,\infty,\infty,\infty]^\top$
$\Delta\mathbf{u}_{max}$	$[0.5\text{Hz/s},0.003/s]^\top$		

Note that the initial parameters ($\mathbf{Q}_y(0), \mathbf{R}_u(0), \mathbf{Q}_u(0)$) in Table 4.2 consider that all process variables have the same importance, except for the rotational frequency target, which is zero for all simulations ($q_{u_1} = 0$) since there is no target for this variable. The q_{y_1}, q_{y_2} and q_{u_2} elements are limited to a minimum equal to 0.01 to avoid an open-loop system, and all parameter increments ($\Delta\boldsymbol{\theta}_{max}$) are bound by two to avoid sudden parameter variations.

Regarding the economic target ($\mathbf{u}_{tg}$), the process specialist provided a fixed value for the choke valve opening ($z_{c_{tg}}$). The value was specified as equal to 0.4 to keep the ESP operation as close as possible to the safety limit.

Finally, as the solution time of the auto-tuning can be longer than the MPC solution time, the framework is designed based on a sample time (t_{auto}) equal to 60

s, i.e., the discretized model of the CLS IHMPC and the ODE integration is based
on this time.

Then, the process variable responses obtained by the economic objectives ($\min_J$
Eq. (4.22)), maximizing the oil production ($\max_V$ Eq. (4.23)), minimizing pump
energy ($\min_P$ Eq. (4.24)), and maximizing profit ($\max_\$$ Eq. (4.25)) are compared
in a scenario with changes in the operational zones, and external disturbances. All
the results of the system using the auto-tuning method with the different economic
objectives are compared with the system without the auto-tuning layer (Off). Figu-
res 4.5, 4.6, 4.7, 4.8, 4.9, and 4.10 present the controlled variables response in such
conditions.

Figure 4.5: $L_a(t)$ response for the different economic objective functions chosen.

Figures 4.6, 4.7, 4.8, 4.9, and 4.10 make it clear that the operational envelop
has a time-varying behavior when used as zone control (Eq. 4.11). Note that for
each simulation, different control zones are calculated as a result of the variation in
$q_m(t)$, which is estimated by an extended Kalman filter. Additionally, Figures 4.11
and 4.12 present the manipulated variables response for all simulated scenarios.

Note that (Figure 4.12) $\max_V$ and $\max_\$$ keep a higher rotational frequency and
lower oil level for as long as possible, highlighting the instant 20 min where it is ex-
plicit that the oil level slowly returns to the control zone maximizing the production
and consequently profit. This effect is more clear in Figures 4.13 and 4.14.
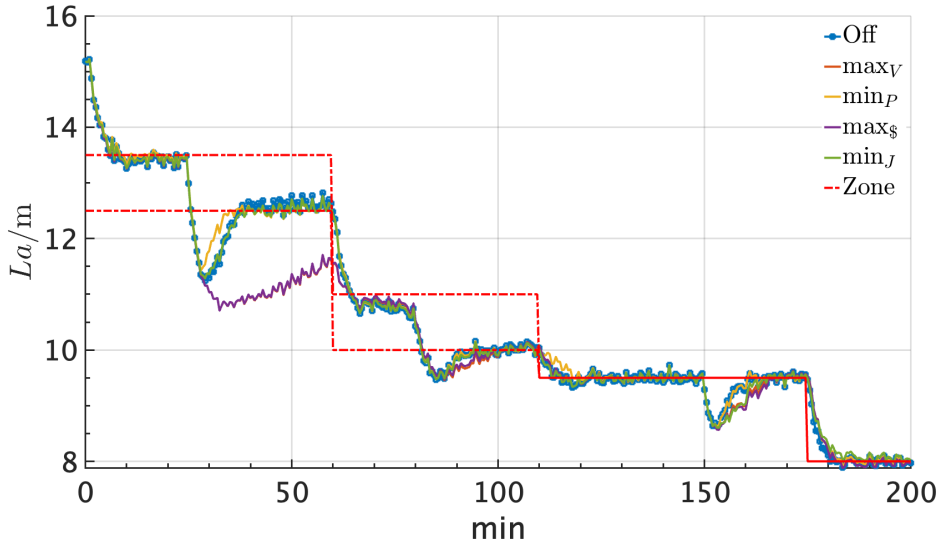
Figures 4.13 and 4.14 show a gradual reduction in average flow and profit rates
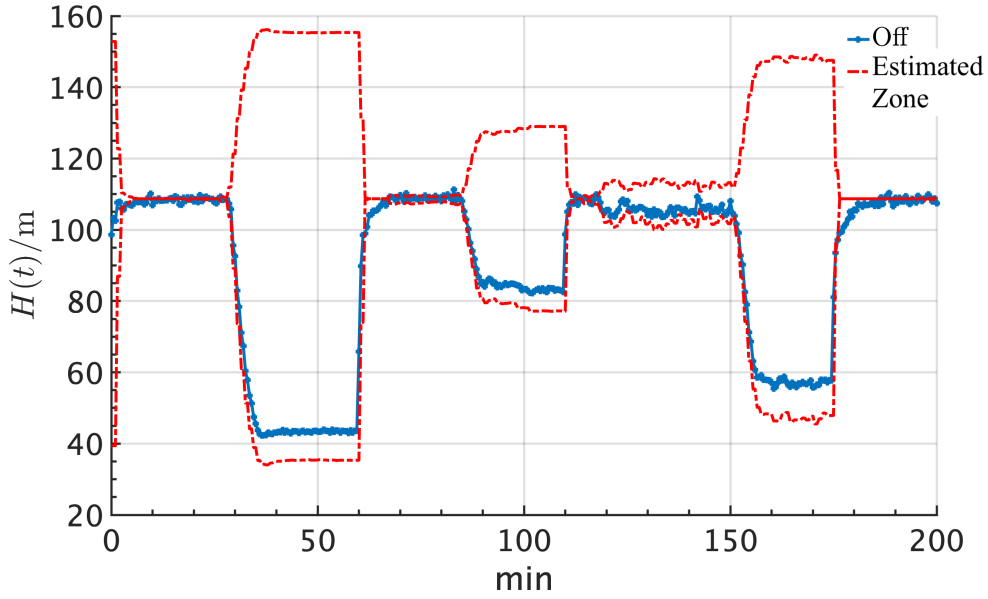
Figure 4.6: $H(t)$ response without the auto-tuning method.
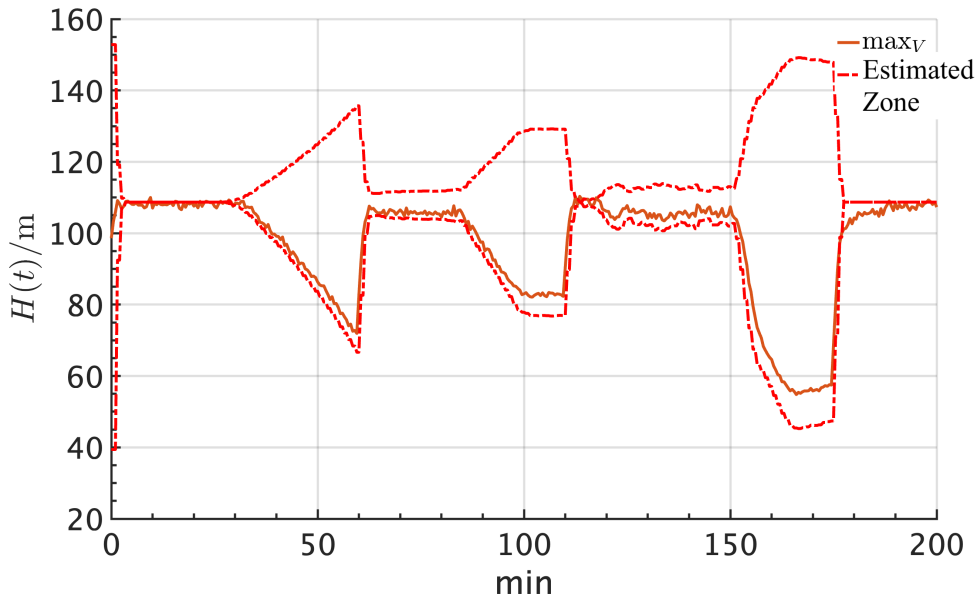
Figure 4.7: $H(t)$ response for the $\max_V$ objective function.

caused by the rotational frequency response. The auto-tuning layer computes MPC parameters to suppress the rotational increments and reduce the oil level priority, aiming for lower oil level and higher frequency for as long as possible, which favors maximizing the profit and oil production.

In contrast, $\min_P$ drives the simulation scenario towards lower values of rota-
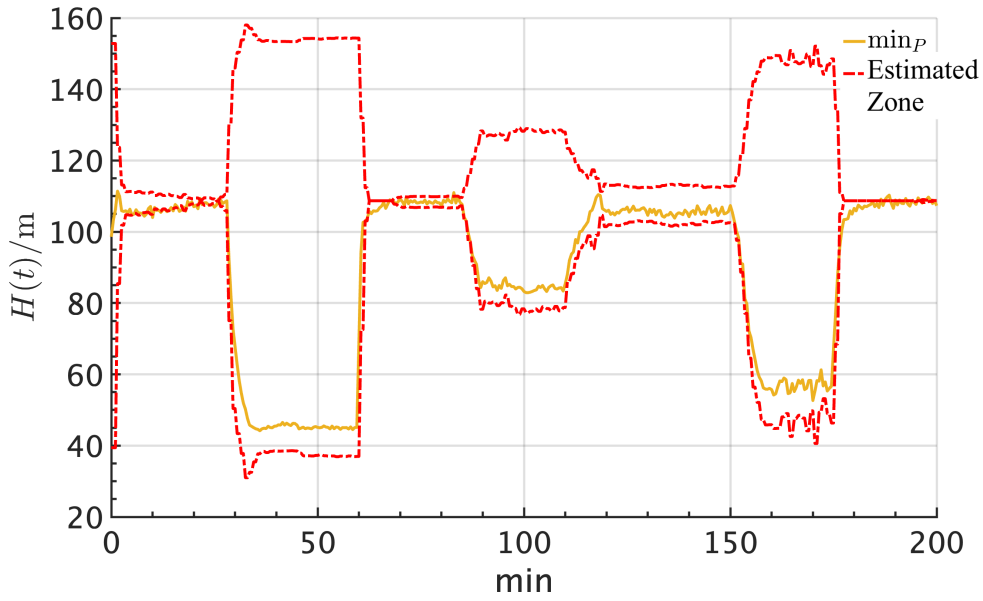
Figure 4.8: $H(t)$ response for the $\min_P$ objective function.
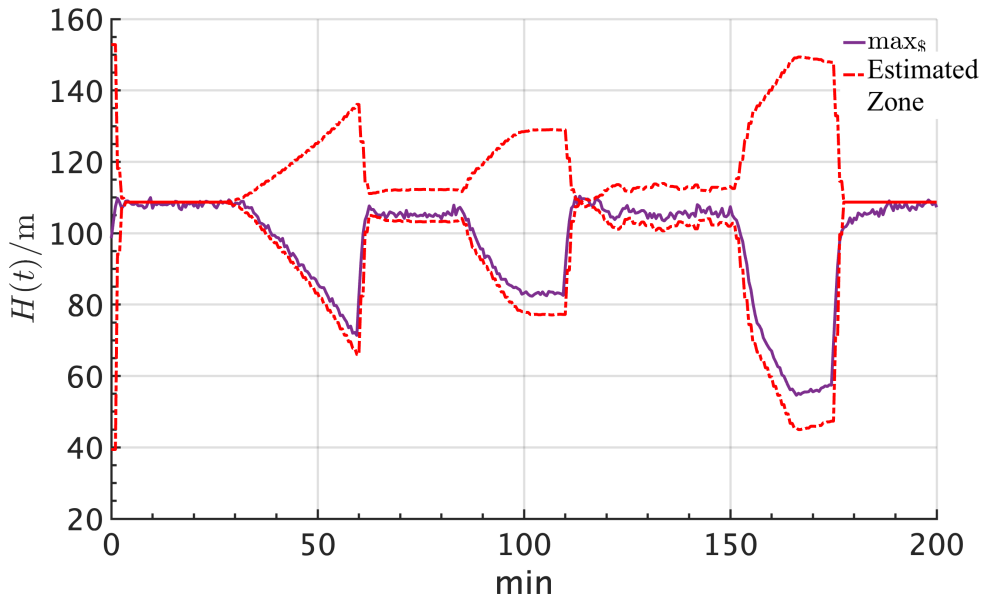
Figure 4.9: $H(t)$ response for the $\max_\$$ objective function.

tional frequency (Figure 4.12), favoring lower values of pump power (Figure 4.15). From 110 min, $L_a(t)$ zone is collapsed to simulate a case of set-point tracking which becomes a more complex control problem. Figure 4.12 shows a slightly more pronounced oscillation in the $f(t)$, between 160 and 180 minutes, propagating to the pump power response (Figure 4.15).

71

Figure 4.10: $H(t)$ response for the $\min_J$ objective function.

This effect is caused since the auto-tuning computes a set of parameters to decrease the rotational frequency suppression, r_{u_2} close to zero (see Figure 4.19), keeping the process at the desired point and rejecting process noise and disturbance.

Regarding the external disturbance, the reservoir pressure drops at the instants 20 min, 80 min, and 150 min (Figures 4.5, 4.12 and 4.11). Even though an EKF was used to estimate this variable, the auto-tuning framework calculated the MPC parameters to drive the ESP back to the control zones respecting each objective and keeping z_c closer to $z_{c_{tg}} = 0.4$ (Figure 4.11). Even in the presence of unmeasured disturbances, the state estimate provided by the EKF could sync both layers, IHMPC, and autotuning, bringing the process back to the desired operating point in all scenarios (Figures 4.5 and 4.11).

Figures 4.16, 4.17, 4.18, 4.19, and 4.20 depict the response of the tuning parameters for the scenario presented. Some constant values of the MPC parameters can be seen for some periods. These intervals correspond to the periods when the proposed auto-tuning is not activated, so the parameters are maintained constant until nonconformities are detected. In this way, the framework increases or decreases the importance of the process variables according to the desired objective. Based

Figure 4.11: $z_c(t)$ response for the different objective functions chosen.

on these findings, it can be highlighted:

- q_{y_2} (Figure 4.17) increases to minimize the operational envelope violations for all objectives

- The lower values of r_{u_1} and r_{u_2} (Figures 4.18 and 4.19) obtained from the $\min_P$ objective enables the IHMPC to use more z_c and decrease f faster, when necessary.

- The higher values of r_{u_2} and q_{u_2} (Figures 4.19 and 4.20) obtained from the scenario using $\max_V$ and $\max_\$$ objectives aim to reduce z_c variations and keep the value of z_c closer to its target for longer.
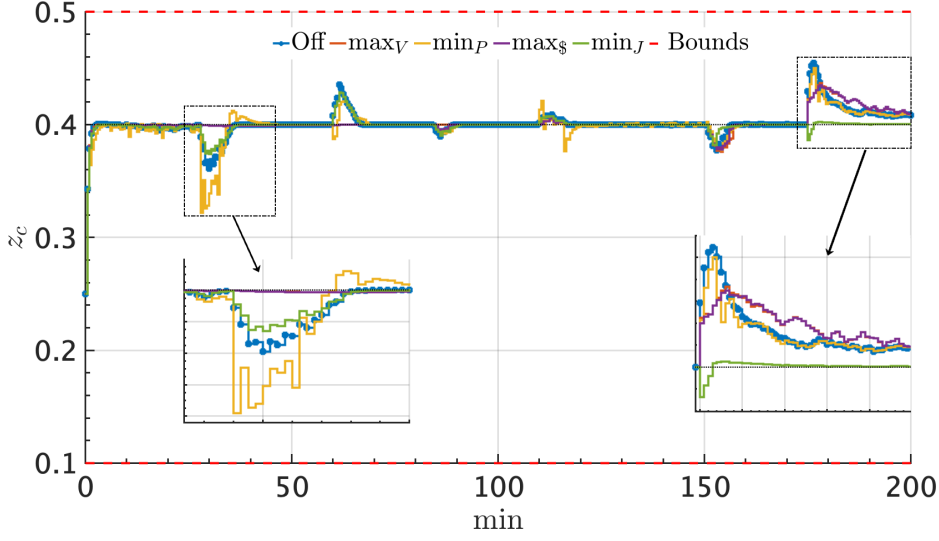
- The higher values of r_{u_1} (Fig. 4.18) obtained from the scenario using $\max_V$ and $\max_\$$ provide a smooth $f(t)$ response and keep it in higher values for longer

- The intermediate values of the all parameters obtained by $\min_J$ objective aim for an equilibrium between lower control effort and tracking the set-point and economic target.

To summarize these results, some indices are calculated to present the efficiency of the proposed framework. The values are presented in Table 4.3.

73

Figure 4.12: $f(t)$ response for the different objective functions chosen.

Figure 4.13: $\hat{q}_m(t)$ response for the different objective functions chosen.

The *Production*, *Power*, and *Profit* indexes are computed based on the average flow rate and pump power estimates, and the global performance (GP) index is calculated as the sum of the square of the tuning actions and the square error of the set-point and economic target, as follows:

$$ISE_{\mathbf{y}} = \sum_{j=1}^{400} \|\hat{\mathbf{y}}(k+j) - \mathbf{y}_{\text{sp}}(k+j)\|^2 \tag{4.26}$$

74

Figure 4.14: Profit rate 4.14 response for the different objective functions chosen.

Table 4.3: Indexes evaluated for all the tuning objectives and without the tuning framework.

Cases	$ISE_{\mathbf{y}}$	$ISE_{\Delta\mathbf{u}}$	$ISE_{\mathbf{u}}$	GP	Production (m^3)	Power (kWh)	Profit (kR\$)
Off	1.29	0.51	0.73	2.54	10.5	9.4	104.8
max$_V$	1.98	0.27	0.49	2.74	11.1	10.4	110.8
min$_P$	1.41	0.66	1.05	3.12	10.4	9.2	103.9
max$_\$$	1.96	0.27	0.47	2.72	11.1	10.4	110.8
min$_J$	1.31	0.46	0.24	2.01	10.5	9.4	104.8
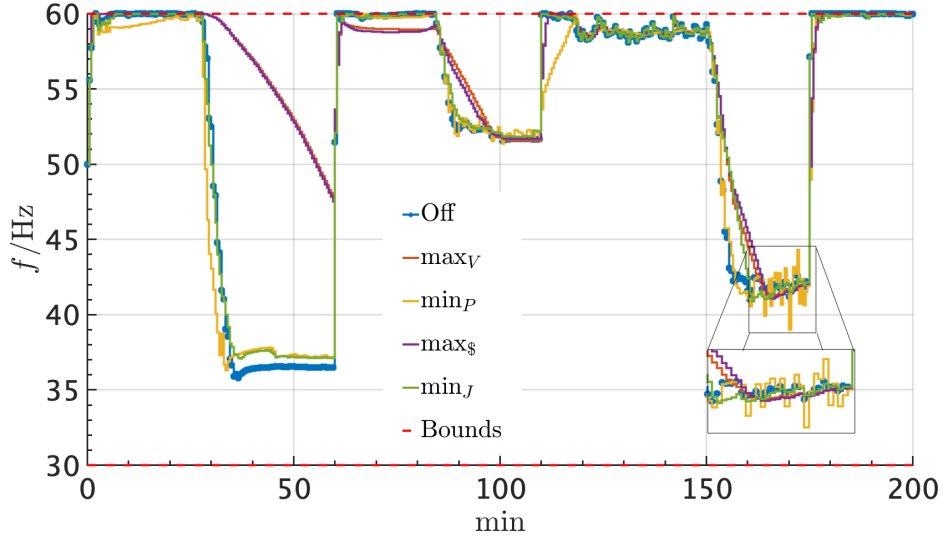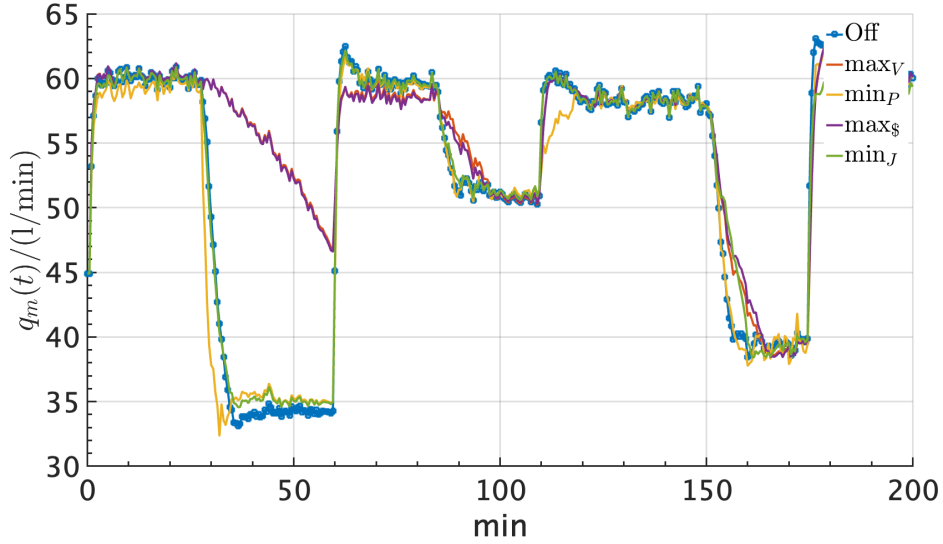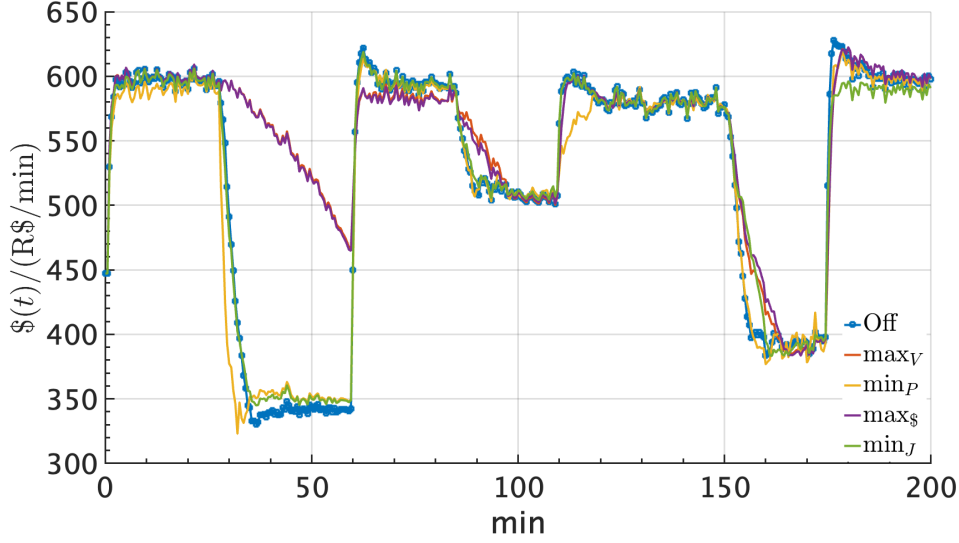
$$ISE_{\Delta\mathbf{u}} = \sum_{j=1}^{400} \|\mathbf{\Delta}\hat{\mathbf{u}}(k+j-1)\|^2 \tag{4.27}$$

$$ISE_{\mathbf{u}} = \sum_{j=1}^{400} \|\hat{\mathbf{u}}(k+j) - \mathbf{u}_{tg}(k+j)\|^2 \tag{4.28}$$

$$GP = ISE_{\mathbf{y}} + ISE_{\Delta\mathbf{u}} + ISE_{\mathbf{u}}. \tag{4.29}$$

Compared to the system without the auto-tuning layer, the simulation using max$_V$ and max$_\$$ economic objectives increases the power consumption by 10.6 %, which is compensated by the 5.7 % increase in oil production, increasing profit by 5.7 %. On the other hand, the min$_P$ objective results in 2.1 % less power than the system without the auto-tuning layer but provides worse production and profit percentages.

Figure 4.15: Pump power response for the different objective functions chosen.

Figure 4.16: Comparison between the q_{y_1} responses obtained by the system without the auto-tuning layer (Off) and the different economic goals.

As shown in Table 4.3, these results indicate the $\max_V$ and $\max_\$$ objectives providing similar responses of the process variables, corroborating with the behavior observed in process variable responses (Figures 4.5, 4.12, 4.11, and 4.21). This similarity is explained by the low energy cost and the increase in production associated with greater power consumption without compromising profit.
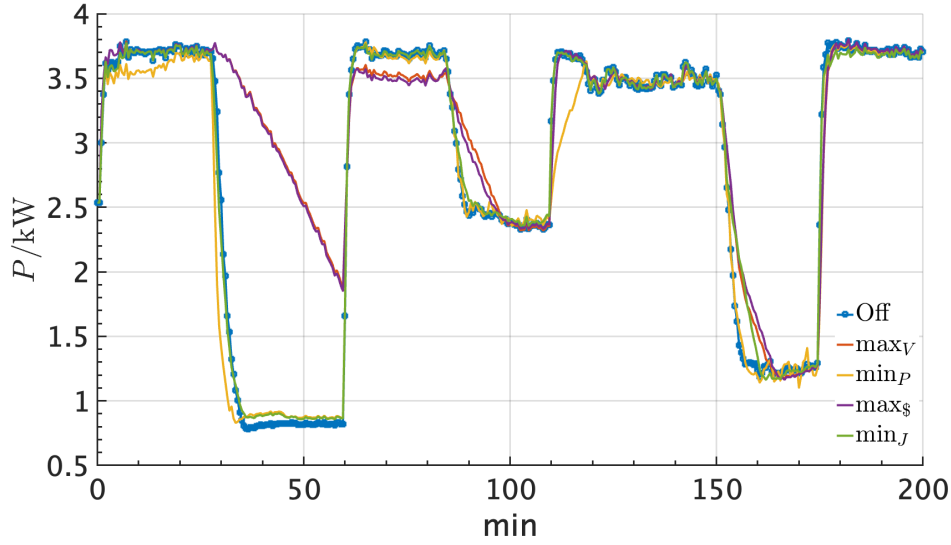
Moreover, the maximization of production or profit increases 8 % in the global performance index compared to the system without the auto-tuning framework (Ta-
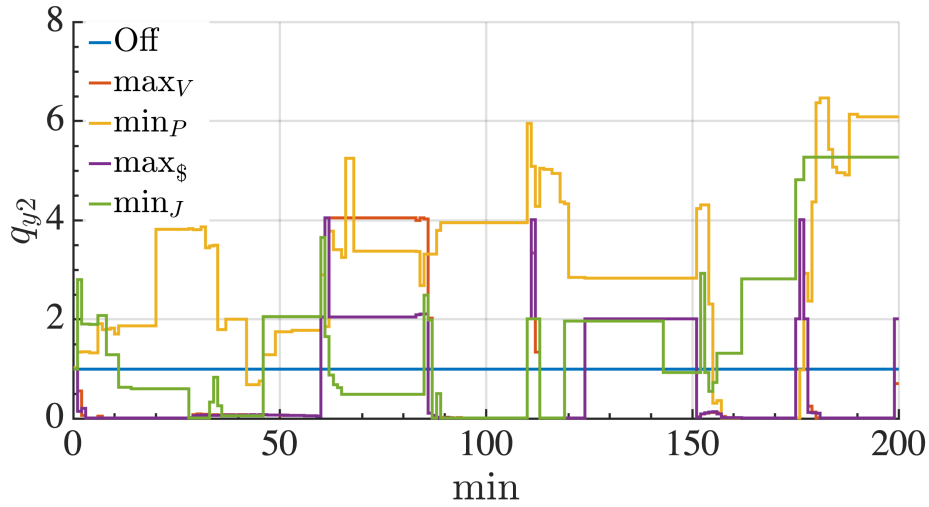
Figure 4.17: Comparison between the q_{y_2} responses obtained by the system without the auto-tuning layer (Off) and the different economic goals.
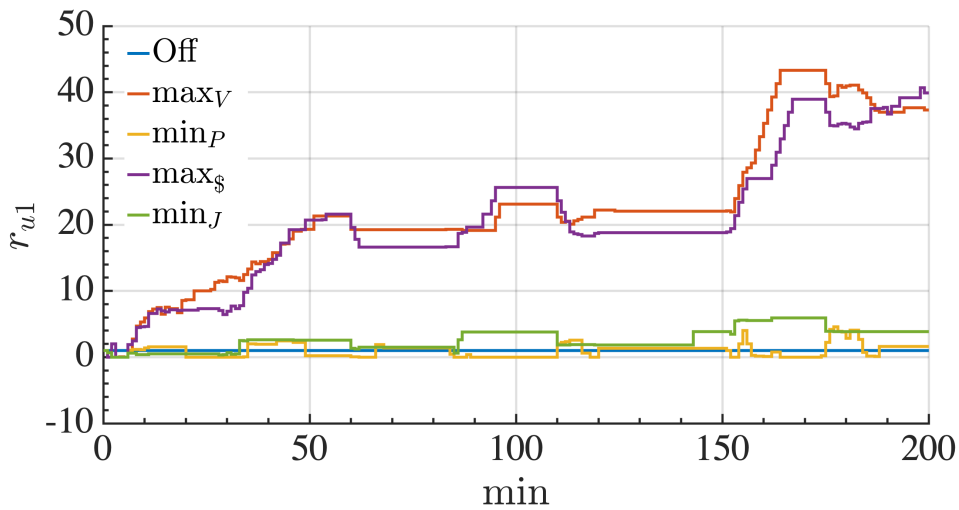
Figure 4.18: Comparison between the r_{u_1} responses obtained by the system without the auto-tuning layer (Off) and the different economic goals.

ble 4.3). In contrast, an increase of 24 % in the same indicator is observed when power is minimized (Table 4.3). This is made clear by the slower return of the oil level to the control zone, resulting in the highest $ISE_\mathbf{y}$ (Figure 4.5), compensated by the lower values of $ISE_{\Delta\mathbf{u}}$ and $ISE_\mathbf{u}$, which represent smooth control actions and lower economic target error (Figures 4.12 and 4.11). On the other hand, minimizing power provides more significant manipulated variable variations and economic target error, indicated by the highest values of $ISE_{\Delta\mathbf{u}}$ and $ISE_\mathbf{u}$, resulting in the

77
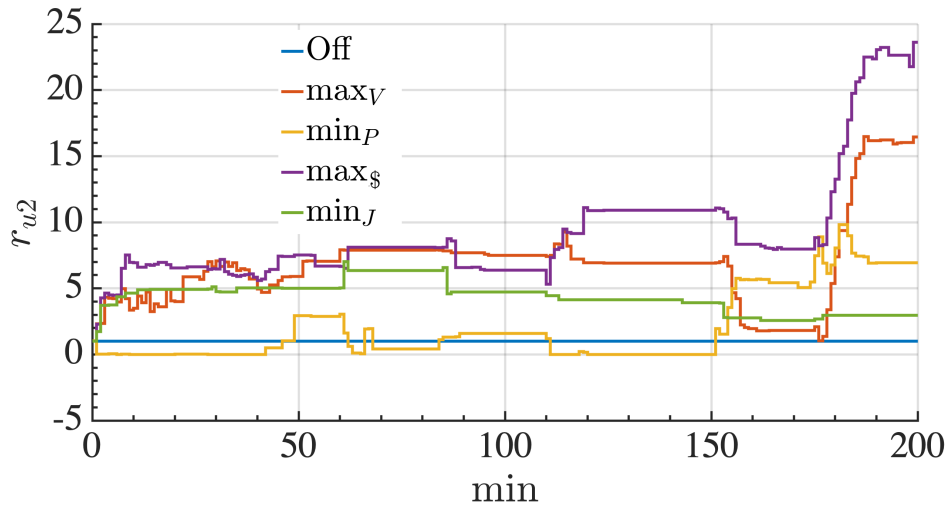
Figure 4.19: Comparison between the r_{u_2} responses obtained by the system without the auto-tuning layer (Off) and the different economic goals.
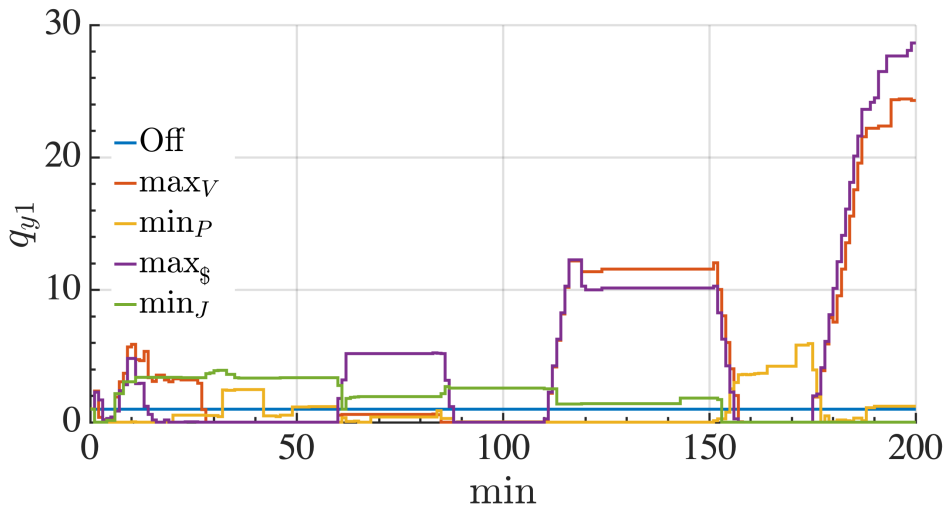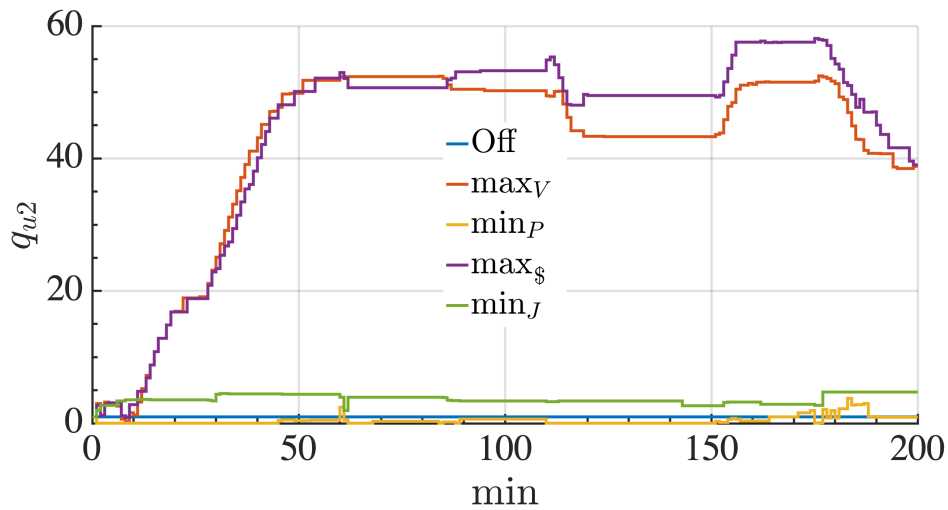

Figure 4.20: Comparison between the q_{u_2} responses obtained by the system without the auto-tuning layer (Off) and the different economic goals.

worst case for global performance.

In contrast, $\min_J$ objective significantly reduces 25% in the global performance indices, keeping the economic goals equal to the system without the auto-tuning framework. Since this objective prioritizes the minimum error of the process variables, a significant reduction of 67% and 9.8% in the $ISE_{\mathbf{u}}$ and $ISE_{\Delta\mathbf{u}}$ indexes is obtained, which can be interpreted as an improvement in the useful life of the final control elements, providing lower control effort and maintaining the system closer to
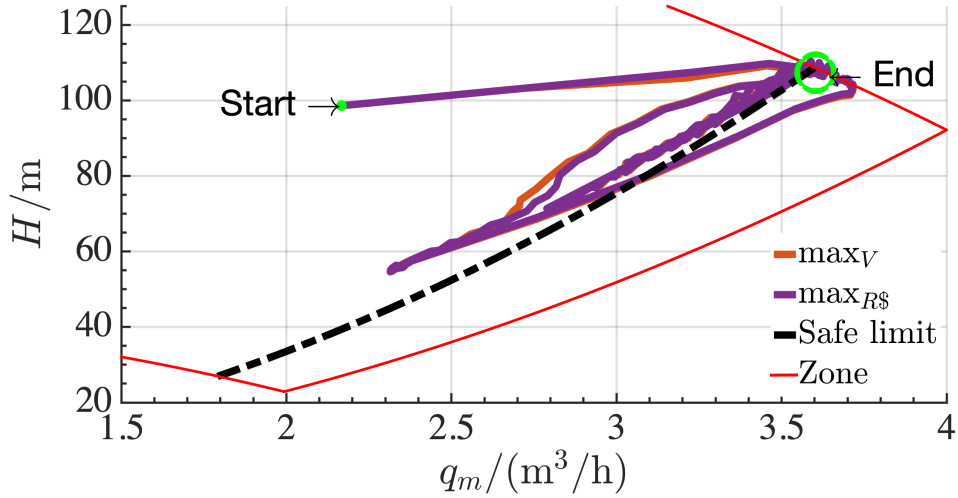
Figure 4.21: Comparison between the $H(t)$ responses obtained by the different economic goals, $\max_V$ and $\max_\$$.

the safety limit defined by the target, when compared with the other scenarios. Figure 4.11 highlights the differences between $z_c(t)$ responses, which are more evident between 20 to 50 minutes and 180 to 200 minutes.

Compared to the other objectives, $\min_J$ achieves better profit only when compared to $\min_P$, increasing by 0.8 % and decreasing 5.4 % compared to the other objectives. Figure 4.22 depicts the operational envelope obtained by these two economic objectives, where the best response is performed by $\min_J$ and the worst by $\min_P$.

Concerning the operational envelope (Figures 4.21 and 4.22), the auto-tuning framework can bring the process back to the operational zone, especially in the presence of external disturbances. Since the auto-tuning is triggered and the objective functions are penalized when the process violates the bounds, the proposed framework computes MPC parameters to force the head to go back to the specified zone.

These results explain the trade-off between performance (better process variable responses) and economic tuning requirements. It is apparent that $\min_J$ aims to minimize control effort and tracks the set point and target, resulting in intermediate parameter values to provide a smooth response with less error and, consequently. In contrast, the other objectives prioritize the economic indicator directly, updating

Figure 4.22: Comparison between the $H(t)$ responses obtained by the different economic goals, $\min_J$ and $\min_P$.

the parameters to provide better economic outcomes and then improving variable behavior.

The online feasibility of the proposed auto-tuning framework is evaluated by the ratio between the computational and auto-tuning sample time shown in Figures 4.23, 4.24, 4.25, and 4.26. The computational time is assessed when the method is triggered, and it is composed of the time spent by monitoring step, the optimization solver, and updating the MPC parameters.

Figure 4.23: Ratio of the computational and auto-tuning sample time for $\max_V$ computed when the framework is triggered (On - gray zone).

Figure 4.24: Ratio of the computational and auto-tuning sample time for $\min_P$ computed when the framework is triggered (On - gray zone).

What is striking about Figures 4.23, 4.24, 4.25, and 4.26 is that the worst ratio value is close to 30 % of the auto-tuning sample time, which means that the worst computational time was approximately equal to 18 s, validating the online implementation of the proposed framework. Another interesting observation about these figures is the periods where the auto-tuning is triggered (gray rectangles), highlighting the scenarios using $\max_V$ and $\max_\$$. In these cases, the auto-tuning remained triggered for the initial 60 min approximately, which resulted in the slow response of the oil level and rotational frequency (Figures 4.5 and 4.12) to reach the desired objective, in particular, increasing the oil production, and consequently profit.

Additionally, Figures 4.27, and 4.28 corroborate the online implementation feasibility of the auto-tuning framework showing the behavior of the slack variables associated with the proposed auto-tuning framework. Note that the slack variables increase when necessary and decrease back to the origin, driving the system back to the zone control. The optimization problem therefore remains feasible for the whole period, computing the optimal parameters when triggered.

These findings contribute to a new perspective on hierarchy control and MPC tuning methods presenting process benefits when the auto-tuning layer is implemented. The results named "Off" illustrate the case of the traditional RTO+MPC hierarchy control, i.e., an optimal target is set to an MPC with fixed parameters. Compared

81
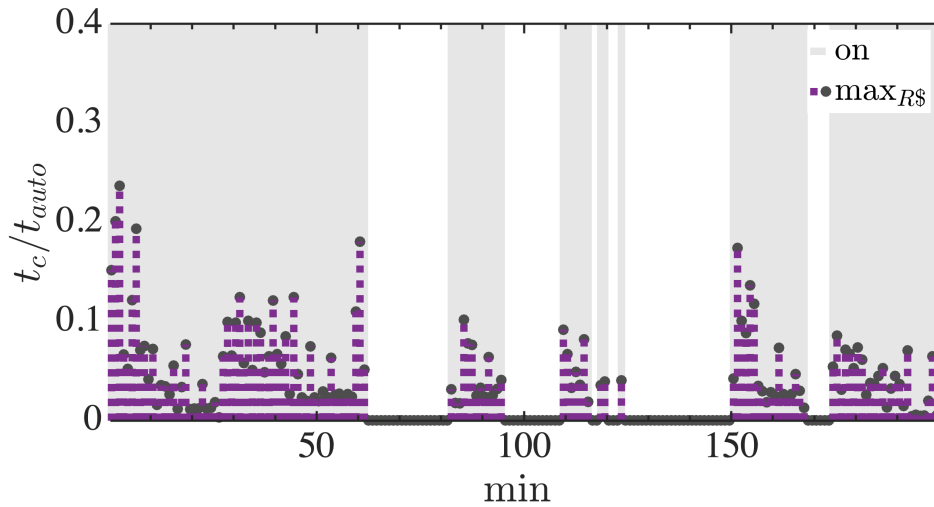
Figure 4.25: Ratio of the computational and auto-tuning sample time for $\max_{\$}$ computed when the framework is triggered (On - gray zone).

with the other results, the respective economic indicators are improved since the auto-tuning layer evaluates optimal MPC parameters, benefiting the process with the correspondent economic criterion.

Unlike Chapter 3, in this Chapter, the tuning and control layers were implemented with different sampling times, $t_{auto} = 60$ s and $T_s = t_{auto}/2 = 30$ s and, to approach an industrial application. In this case, the tuning layer was designed for the longest possible sampling time for the system.

Thus, to evaluate the impact of the mismatch between the sampling times of the layers, Figures 4.29, 4.30, 4.31 and 4.32 show the implementation of the tuning method with MPC with sampling times $T_s = t_{auto}/6 = 10$ s and $T_s = t_{auto}/3 = 20$ s using $\max_V$ tuning objective.

It is possible to observe very different responses which impact on economic performance indicators in each case as show in Table 4.4. Better indicators were obtained with $T_s = t_{auto}/2$, which the lower mismatch between the layers can explain. Since the tuning layer needs to simulate closed-loop behavior, the more similar it is to the real closed-loop, the more accurate the predictions will be, favoring better tuning results.
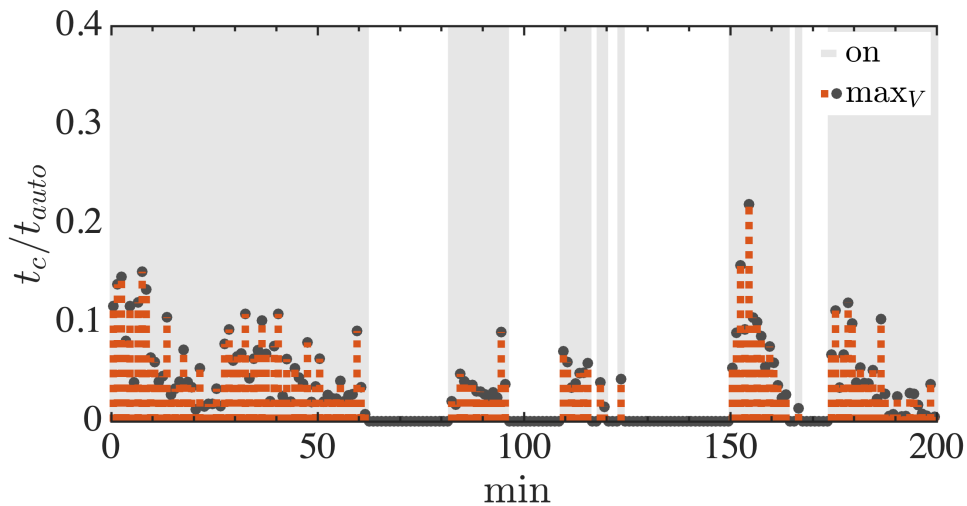
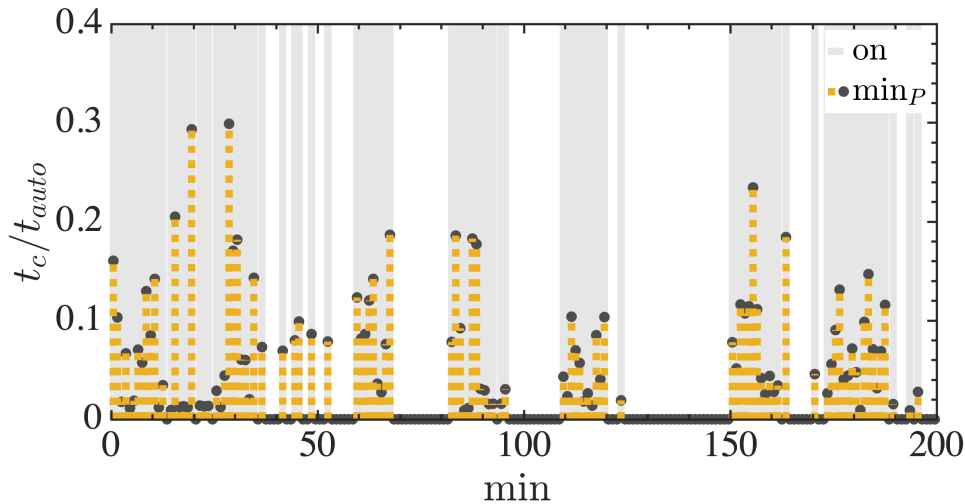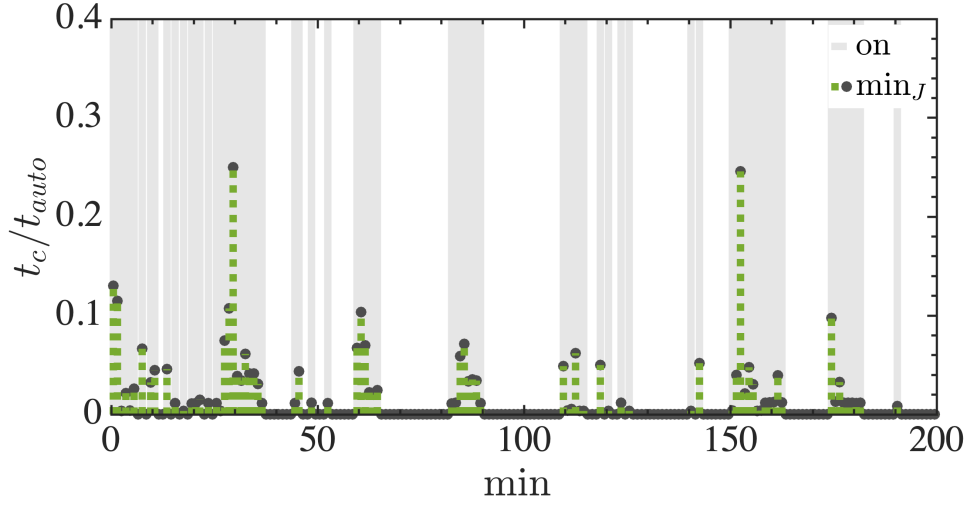Figure 4.26: Ratio of the computational and auto-tuning sample time for $\min_J$ computed when the framework is triggered (On - gray zone).
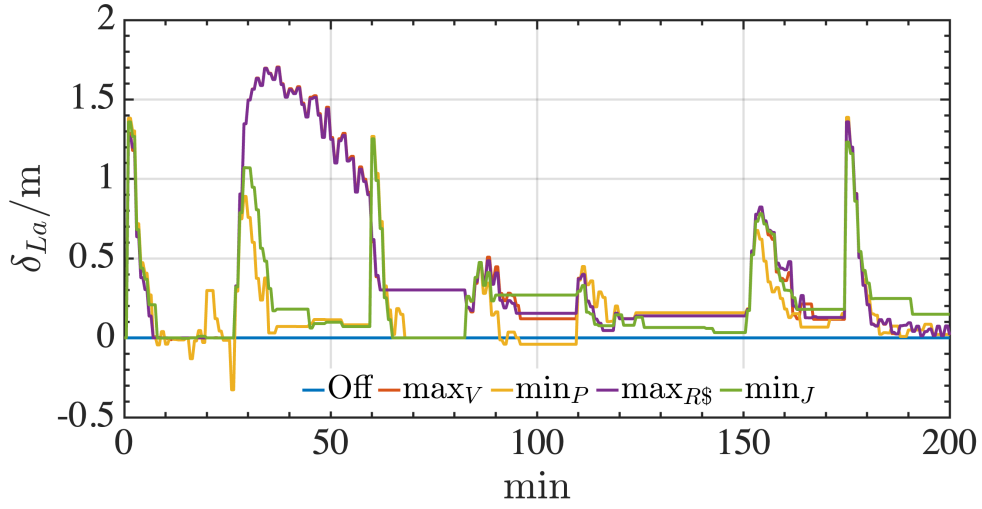
Figure 4.27: δ_{La} associated with the proposed auto-tuning framework activity.

Table 4.4: Indexes evaluated for $\max_V$ tuning objective for different sampling times.

Cases	Production (m³)	Power (kWh)	Profit (kR$)
$T_s = t_{auto}/6$	10.7	9.58	106.5
$T_s = t_{auto}/3$	11.0	10.1	109.3
$T_s = t_{auto}/2$	11.1	10.4	110.8
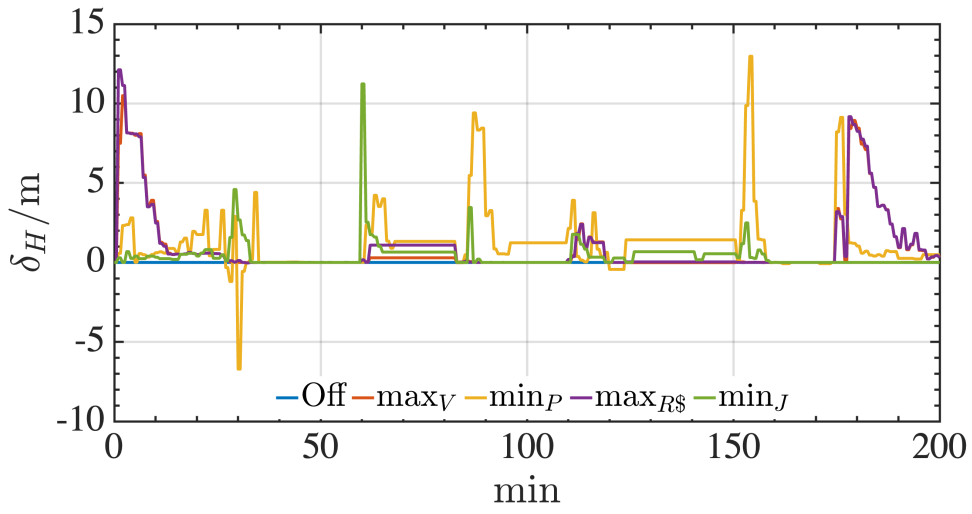
Figure 4.28: δ_H associated with the proposed auto-tuning framework activity.
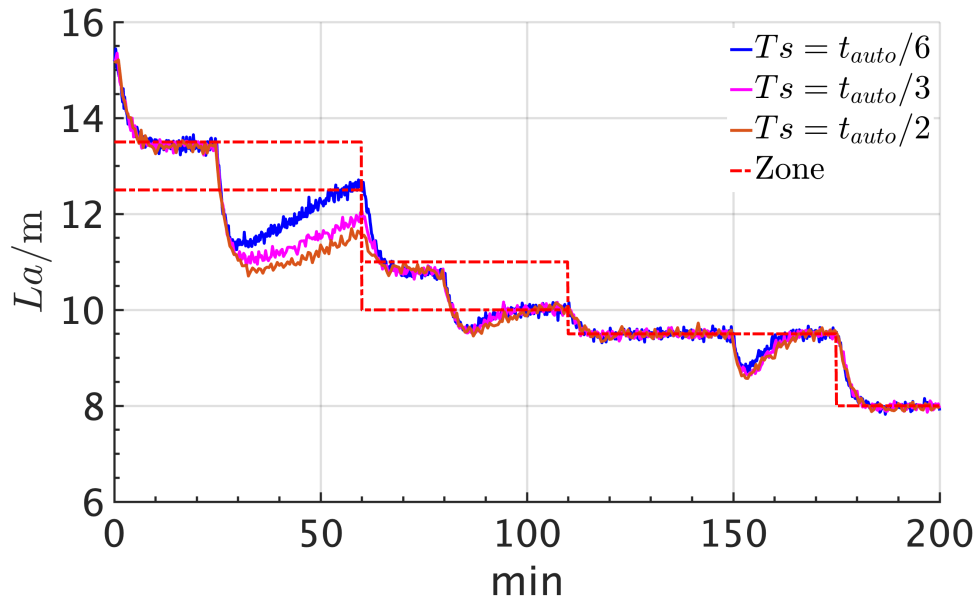
Figure 4.29: $L_a(t)$ behavior for $\max_V$ tuning objective for different sampling times.
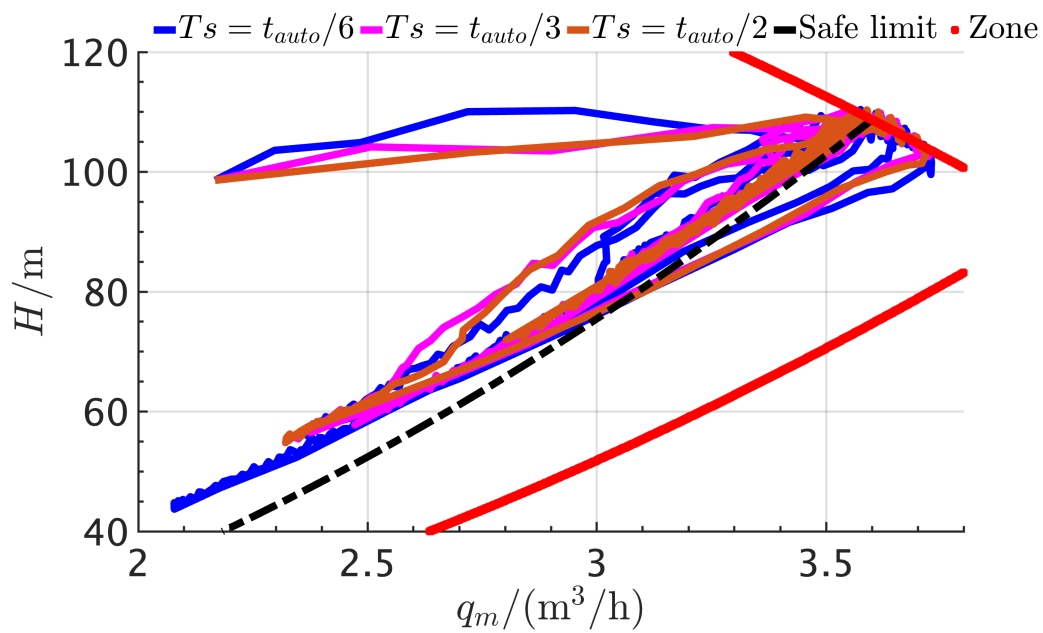
Figure 4.30: $H(t)$ vs. $q_m(t)$ behavior for $\max_V$ tuning objective for different sampling times.
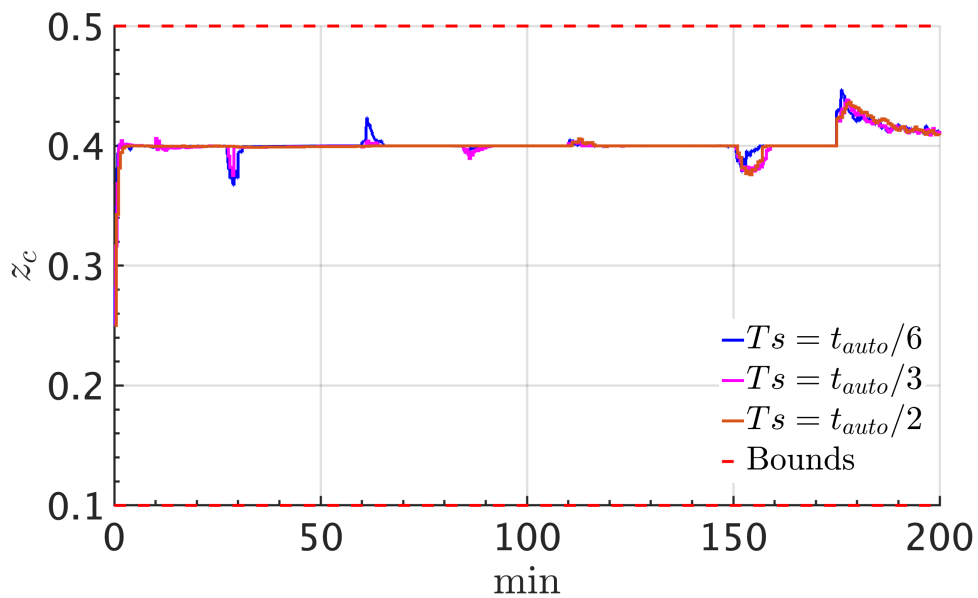
Figure 4.31: $z_c(t)$ behavior for $\max_V$ tuning objective for different sampling times.
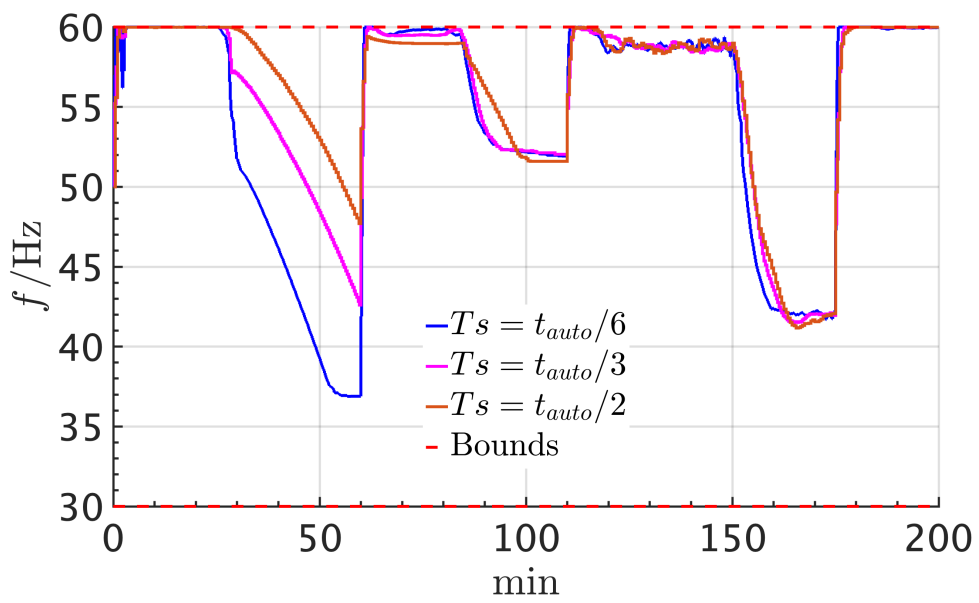
Figure 4.32: $f(t)$ behavior for $\max_V$ tuning objective for different sampling times.

Chapter 5

Conclusions

In conclusion, this thesis has achieved its objectives of tracking the economic requirements of oil wells lifted by ESP (Electric Submersible Pump) and proposing an economic-oriented Model Predictive Control (MPC) auto-tuning strategy:

First, the closed-loop simulations with model-plant mismatch structure have shown that the proposed auto-tuning framework can accommodate different processes and MPC implementations, including DMC, IHMPC, and zone IHMPC. The tuning criterion based on the objective function has facilitated better adaptation to desired criteria, resulting in smoother tuning, improved system performance with reduced control effort, and economic gains for the process.

Second, the proposed auto-tuning approach computes MPC parameters in an optimal sense, adhering to the defined tuning objectives within a reasonable computational time. The resulting optimization problem is feasible, ensuring practical implementation.

Third, the computed optimal parameter values prioritize economic goals, leading to enhanced economic gains compared to control performance requirements. The auto-tuning framework has addressed the trade-off between performance and economic criteria.

Fourth, the case study presented in Chapter 4 has demonstrated the adaptability of the proposed framework to different economic goals. The framework has achieved the desired economic objectives by optimizing the MPC parameters while ensuring the ESP operates within the operational envelope and maintains process safety.

Finally, the research findings validate the applicability of the proposed auto-tuning method in various scenarios, including those with unmeasured external disturbances and measurement noise. The flexibility of the receding optimization structure allows for the incorporation of distinct features in different cases, showcasing the versatility and robustness of the proposed framework.

In summary, this thesis has contributed to MPC auto-tuning and ESP efficiency research. The research findings demonstrate the effectiveness and flexibility of the proposed framework, which incorporates economic criteria into the MPC tuning problem and enables online implementation. The proposed economic-oriented auto-tuning framework has been developed and applied, optimizing ESP-lifted wells' performance and economic gains. The research findings have practical implications for the oil industry, providing valuable insights and tools to enhance the efficiency and profitability of oil production.

5.1 Thesis limitations and direction of future works

This work has yet to address specific issues, but they could be considered possible areas for future research. These include:

- Incorporating the steady-state economic target into a one-layer structure along with the MPC parameters: As shown in Chapter 3, some MPC are designed to drive the system towards a steady-state economic target. The steady-state economic target is incorporated into the MPC framework in such cases. However, uncertainties or disturbances may affect the system's behaviour, and the given steady state could be unreachable. One approach could be implementing a steady-state equalize layer between RTO and MPC to recompute a new reachable economic target. Given the flexible structure of the auto-tuning proposal, the steady-state economic target recomputing could be integrated as a decision variable of the auto-tuning optimization problem. In this manner, it would help improve the MPC's performance by regulating the system towards the desired steady-state economic target.

- Adapting the MPC model to match the process measurements: MPC relies on accurate process models to predict the system's behaviour. However, external

disturbances and different operating conditions affect the system's behaviour, impacting its model representation. One way to address this issue is to adapt the MPC and auto-tuning models to match the process measurements using various techniques, such as machine learning. By incorporating more precise models into the closed-loop simulation, the auto-tuning can make more accurate predictions, resulting in better process performance.

- Employing a multiphase ESP model: Electrical Submersible Pumps (ESPs) are widely used in the oil and gas industry for artificial lift. However, many oil wells produce multiphase fluids, including oil, gas, and water. In such cases, it is crucial to use a multiphase ESP model to predict the ESP system's performance accurately. The multiphase ESP model would consider the different phases in the fluid and their interactions with the pump system. Using a multiphase ESP model, the auto-tuning can make more accurate predictions of the fluid flow rate and pressure, leading to better control performance and increased efficiency of the ESP system.

- Implementing the proposed auto-tuning framework in an ESP-lifted oil well: The proposed framework may have been developed and tested in a simulation environment. However, implementing the framework in a real-world oil well, particularly one that uses ESP, could provide valuable insights into the framework's performance under practical conditions, which involve installing the necessary sensors, instrumentation, and computer to enable the auto-tuning to interact with the MPC and the ESP system. By implementing the framework in an ESP-lifted oil well, the controller's performance can be evaluated under realistic operating conditions, leading to potential improvements in the overall performance of the ESP system.

- Improving th algorithm: In this thesis, the values of the tuning actions boundary were assumed based on the author's knowledge. However, choosing these constraint values in automatic tuning algorithms is a delicate balance between achieving desired performance improvements and ensuring system stability/convergence. Small constraint values provide smoother and more incremental adjustments, whereas larger values allow aggressive actions. The appropriate

constraint values ultimately depend on the specific application, system dynamics, and performance requirements. In this manner, it must be cautious before defining the constraint values, which can be evaluated with the help of simulation tests.

- Noise presence: In this thesis, Chapter 4 shows the implementation of the proposed auto-tuning method under noise measurement. An Extend Kalman Filter technique was used to address the noise issue, which filtered the signal and provided an estimate of an unmeasured disturbance, enabling the auto-tuning implementation.

  The presence of noise can have significant effects on the solution of the tuning optimization problem. Noisy signals can distort measurements and introduce errors in the calculations used for parameter adjustments, which can result in imprecise or inefficient tuning, negatively impacting the overall performance of the control system.

  It is common to employ filtering and robust control techniques to mitigate the effects of noise. However, the use of robust control techniques can increase the computational cost of the controller itself, which could make the implementation of online tuning unfeasible. In addition, the robust control formulations are more conservative, harming the closed loop's performance. Therefore, the configuration of the auto-tuning layer has to be in sync with the robustness requirements so that the system can evaluate the controller parameters to avoid conflicting objectives, making the system unfeasible.

- Stability guarantee: Varying controller parameters over time does not automatically guarantee system stability. However, adding a restriction ensuring stability in the tuning layer can make an online implementation unfeasible, being more recommended for offline methods. It is therefore recommended that the controller design consider a region for which the controller will remain stable regardless of the tuning parameters, which are responsible only for improving the behavior of the control system.

Addressing these topics would provide additional insights and improve the overall effectiveness of the approach.

References

Abrashov, S., Airimitoaie, T. B., Lanusse, P., Aioun, F., Malti, R., Moreau, X. & Guillemard, F. (2017), 'Model Predictive Control Tuning: Methods and Issues. Application to steering wheel position control', *IFAC-PapersOnLine* **50**(1), 11331–11336.

Al-Ghazzawi, A., Ali, E., Nouh, A. & Zafiriou, E. (2001), 'On-line tuning strategy for model predictive controllers', *Journal of Process Control* **11**(3), 265–284.

Alhajeri, M. & Soroush, M. (2020), 'Tuning Guidelines for Model-Predictive Control', *Industrial & Engineering Chemistry Research* **59**(10), 4177–4191.

Ali, E. (2001), Automatic Tuning of Model Predictive Controllers Based on Fuzzy Logic, *in* 'Proc of IASTED Conference on Control and Applications', Banff, Canadá, pp. 136–142.

Ali, E. (2003), 'Heuristic on-line tuning for nonlinear model predictive controllers using fuzzy logic', *Journal of Process Control* **13**(5), 383–396.

Ali, E. & Al-Ghazzawi, A. (2008), 'On-line Tuning of Model Predictive Controllers Using Fuzzy Logic', *The Canadian Journal of Chemical Engineering* **81**(5), 1041–1051.

Ali, E. & Zafiriou, E. (1993), 'Optimization-based tuning of nonlinear model predictive control with state estimation', *Journal of Process Control* **3**(2), 97–107.

Binder, B. J. T., Kufoalor, D. K. M. & Pavlov, J. (2014), 'Embedded Model Predictive Control for an Electric Submersible Pump on a Programmable Logic Controller', *IEEE Conference on Control Applications (CCA)* (2), 579 – 585.

Binder, B., Johansen, T. & Imsland, L. (2019), 'Improved predictions from measured disturbances in linear model predictive control', *Journal of Process Control* **75**, 86–106.

Cairano, S. D. & Bemporad, A. (2010), 'Model predictive control tuning by controller matching', *IEEE Transactions on Automatic Control* **55**(1), 185–190.

Costa, E. A., de Abreu, O. S., Silva, T. d. O., Ribeiro, M. P. & Schnitman, L. (2021), 'A Bayesian approach to the dynamic modeling of ESP-lifted oil well systems: An experimental validation on an ESP prototype', *Journal of Petroleum Science and Engineering* **205**(April), 108880.

Darby, M. L., Nikolaou, M., Jones, J. & Nicholson, D. (2011), 'RTO: An overview and assessment of current practice', *Journal of Process Control* **21**(6), 874–884.

De Carvalho, R. F. & Alvarez, L. A. (2020), 'Simultaneous Process Design and Control of the Williams-Otto Reactor Using Infinite Horizon Model Predictive Control', *Industrial and Engineering Chemistry Research* **59**(36), 15979–15989.

De Schutter, J., Zanon, M. & Diehl, M. (2020), 'TuneMPC—A Tool for Economic Tuning of Tracking (N)MPC Problems', *IEEE Control Systems Letters* **4**(4), 910–915.

Delou, P. A., Azevedo, J. P., Krishnamoorthy, D., De Souza, M. B. & Secchi, A. R. (2019), 'Model predictive control with adaptive strategy applied to an electric submersible pump in a subsea environment', *IFAC-PapersOnLine* **52**(1), 784–789.

Delou, P. A., de Souza, M. B. & Secchi, A. R. (2020), 'Addressing the lack of measurements in the subsea environment by using a model scheduling Kalman filter coupled with a robust adaptive MPC', *Brazilian Journal of Chemical Engineering* .

Elsisi, M., Mahmoud, K., Lehtonen, M. & Darwish, M. M. (2021), 'Effective Nonlinear Model Predictive Control Scheme Tuned by Improved NN for Robotic Manipulators', *IEEE Access* **9**, 64278–64290.

Engell, S. (2007), 'Feedback control for optimal process operation', *Journal of Process Control* **17**(3), 203–219.

Exadaktylos, V. & Taylor, C. J. (2010), 'Multi-objective performance optimisation for model predictive control by goal attainment', *International Journal of Control* **83**(7), 1374–1386.

Fan, J. & Stewart, G. E. (2009), Automatic tuning method for multivariable model predictive controllers, *in* 'U.S. Patent: 7 577 483 B. Aug. 18, 2009', Honeywell ASCA Inc.

Fontes, R. M., A. Costa, E., S. L. Abreu, O., A. F. Martins, M. & Schnitman, L. (2020), On application of a zone IHMPC to an ESP-lifted oil well system, *in* 'Anais do Congresso Brasileiro de Automática 2020', SBA, Florianoópolis-SC.

Fontes, R. M., Martins, M. A. F. & Odloak, D. (2019), 'An Automatic Tuning Method for Model Predictive Control Strategies', *Industrial & Engineering Chemistry Research* **58**(47), 21602–21613.

Francisco, M., Álvarez, H., Vega, P. & Revollar, S. (2010), Stable model predictive control tuning considering asymmetric bounded signals, *in* S. Pierucci & G. Ferraris Buzzi, eds, '20 th European Syposium on Computer Aided Process Enginerring', Vol. 28, pp. 493–498.

Franklin, T. S., Souza, L. S., Fontes, R. M. & Martins, M. A. (2022), 'A Physics-Informed Neural Networks (PINN) oriented approach to flow metering in oil wells: an ESP lifted oil well system as a case study', *Digital Chemical Engineering* p. 100056.

Garriga, J. L. & Soroush, M. (2010), 'Model Predictive Control Tuning Methods: A Review', *Industrial & Engineering Chemistry Research* **49**(8), 3505–3515.

Giraldo, S. A., Melo, P. A. & Secchi, A. R. (2022), 'Tuning of Model Predictive Controllers Based on Hybrid Optimization†', *Processes* **10**(2).

Haapanen, B. E. & Gagner, M. G. (2010), Remote Monitoring and Optimization of Electrical Submersible Pumps Utilizing Control Algorithms, *in* 'Canadian Unconventional Resources and International Petroleum Conference', Society of Petroleum Engineers, pp. 19–21.

Han, K., Zhao, J. & Qian, J. (2006), A Novel Robust Tuning Strategy for Model Predictive Control, *in* '2006 6th World Congress on Intelligent Control and Automation', IEEE, pp. 6406–6410.

He, N., Jiang, Y. & He, L. (2020), 'Analytical tuning method of MPC controllers for mimo first-order plus fractional dead time systems', *Processes* **8**(2).

Hernes, S. B. (2020), Practical NMPC of electrical submersible pumps based on echo state networks, Master's thesis, NTNU.

Ho, Y. K., Yeoh, H. K. & Mjalli, F. S. (2014), 'Generalized Predictive Control Algorithm with Real-Time Simultaneous Modeling and Tuning', *Industrial & Engineering Chemistry Research* **53**(22), 9411–9426.

Hoffmann, A. & Stanko, M. E. (2016), Real-Time Production Optimization of a Production Network with ESP-Boosted Wells: A Case Study, *in* 'Day 1 Wed, November 30, 2016', number 1, SPE, pp. 1–22.

Ira, A. S., Shames, I., Manzie, C., Chin, R., Nesic, D., Nakada, H. & Sano, T. (2018), A Machine Learning Approach for Tuning Model Predictive Controllers, *in* '2018 15th International Conference on Control, Automation, Robotics and Vision (ICARCV)', IEEE, pp. 2003–2008.

Jabbour, N. & Mademlis, C. (2018), 'Online Parameters Estimation and Auto-Tuning of a Discrete-Time Model Predictive Speed Controller for Induction Motor Drives', *IEEE Transactions on Power Electronics* **8993**(c), 1–1.

Khalid, A.-D., Rachapudi, R. R., Al-Mutairi, T., Haider, B. & Mohammed, A.-Y. (n.d.), Automated Real Time ESP Performance Monitoring and Optimization Case Study, *in* 'All Days', SPE, pp. 697–708.

Klopot, T., Skupin, P., Metzger, M. & Grelewicz, P. (2018), 'Tuning strategy for dynamic matrix control with reduced horizons', *ISA Transactions* **76**, 145–154.

Krishnamoorthy, D., Bergheim, E. M., Pavlov, A., Fredriksen, M. & Fjalestad, K. (2016), 'Modelling and Robustness Analysis of Model Predictive Control for Electrical Submersible Pump Lifted Heavy Oil Wells', *IFAC-PapersOnLine* **49**(7), 544–549.

Krishnamoorthy, D., Fjalestad, K. & Skogestad, S. (2019), 'Optimal operation of oil and gas production using simple feedback control structures', *Control Engineering Practice* **91**(August), 104107.

Li, S. & Du, G. (2002), Online tuning scheme for generalized predictive controller via simulation-optimization, *in* '2002 IEEE World Congress on Computational Intelligence.', Vol. 2, IEEE, pp. 1381–1386.

Martins, M. A., Yamashita, A. S., Santoro, B. F. & Odloak, D. (2013), 'Robust model predictive control of integrating time delay processes', *Journal of Process Control* **23**(7), 917–932.

Matos, V. S., Santana, B. A., Chagas, T. P. & Martins, M. A. (2022), 'Embedded predictive controller based on fuzzy linear parameter-varying model: a hardware-in-the-loop application to an ESP-lifted oil well system', *Digital Chemical Engineering* **5**(August), 100054.

Mohammadzaheri, M., Tafreshi, R., Khan, Z., Franchek, M. & Grigoriadis, K. (2016), 'An intelligent approach to optimize multiphase subsea oil fields lifted by electrical submersible pumps', *Journal of Computational Science* **15**, 50–59.

Mohammadzaheri, M., Tafreshi, R., Khan, Z., Ghodsi, M., Franchek, M. & Grigoriadis, K. (2020), 'Modelling of petroleum multiphase flow in electrical submersible pumps with shallow artificial neural networks', *Ships and Offshore Structures* **15**(2), 174–183.

Nebeluk, R. & Ławryńczuk, M. (2021), 'Tuning of multivariable model predictive control for industrial tasks', *Algorithms* **14**(1).

Nery, G. A., Martins, M. A. F. & Kalid, R. (2014), 'A PSO-based optimal tuning strategy for constrained multivariable predictive controllers with model uncertainty', *ISA Transactions* **53**(2), 560–567.

Noorbakhsh, A. & Khamehchi, E. (2020), 'Journal of Petroleum Science and Technology Field Production Optimization Using Sequential Quadratic Programming (SQP) Algorithm in ESP-Implemented Wells , A Comparison Approach', *Journal of Petroleum Science and Technology* **10**, 54–63.

Odloak, D. (2004), 'Extended robust model predictive control', *AIChE Journal* **50**(8), 1824–1836.

Osnes, I. (2020), Recurrent neural networks and nonlinear model-based predictive control of an oil well with esp, Master's thesis, NTNU.

Patel, K. M., Bakhurji, A. S., Salloum, H. S., Kim, H. K., Winarno, M. B. & Mubarak, S. (2019), 'Use of Advanced Process Control for Automating Conventional Oilfield Operations', *SPE Production & Operations* **34**(04), 678–692.

Pavlov, A., Krishnamoorthy, D., Fjalestad, K., Aske, E. & Fredriksen, M. (2014), Modelling and model predictive control of oil wells with Electric Submersible Pumps, *in* '2014 IEEE Conference on Control Applications (CCA)', number 3905, pp. 586–592.

Rani, K. & Unbehauen, H. (1997), 'Study of predictive controller tuning methods', *Automatica* **33**(12), 2243–2248.

Santana, B. A., Fontes, R. M. & Martins, M. A. (2022), 'An implementable zone NMPC applied to an ESP-lifted oil well system: Handling the lack of measurements with nonlinear state estimator coupling', *Journal of Petroleum Science and Engineering* **216**(June), 110816.

Santana, B. A., Fontes, R. M., Schnitman, L. & Martins, M. A. (2021), 'An adaptive infinite horizon model predictive control strategy applied to an ESP-lifted oil well system', *IFAC-PapersOnLine* **54**(3), 176–181.

Santos, J. E. W., Trierweiler, J. O. & Farenzena, M. (2021), 'Model Update Based on Transient Measurements for Model Predictive Control and Hybrid Real-Time Optimization', *Industrial and Engineering Chemistry Research* **60**(7), 3056–3065.

Shah, G. & Engell, S. (2011), Tuning MPC for desired closed-loop performance for SISO systems, *in* 'American Control Conference', pp. 628–633.

Sharma, R. & Glemmestad, B. (2013), 'Optimal control strategies with nonlinear optimization for an Electric Submersible Pump lifted oil field', *Modeling, Identification and Control: A Norwegian Research Bulletin* **34**(2), 55–67.

Short, M. (2016), 'Move Suppression Calculations for Well-Conditioned MPC', *ISA Transactions* **67**, 371–381.

Shridhar, R. & Cooper, D. (1997), 'A tuning strategy for unconstrained SISO model predictive control', *Industrial & Engineering Chemistry Research* **5885**(860), 729–746.

Shridhar, R. & Cooper, D. J. (1998), 'A Tuning Strategy for Unconstrained Multivariable Model Predictive Control', *Industrial & Engineering Chemistry Research* **37**(98), 4003–4016.

Souza, L. D. F., Torres, L. H. S. & Schnitman, L. (2014), Adaptive control applied to an electric submersible pumping system to operate in the best efficiency point, *in* 'SPE Latin American and Caribbean Petroleum Engineering Conference Proceedings', Vol. 3, Society of Petroleum Engineers (SPE), pp. 2369–2377.

Suzuki, R., Kawai, F., Nakazawa, C., Matsui, T. & Aiyoshi, E. (2012), 'Parameter optimization of model predictive control by PSO', *Electrical Engineering in Japan* **178**(1), 40–49.

Tran, Q. N., Scholten, J., Ozkan, L. & Backx, A. C. P. M. (2014), A model-free approach for auto-tuning of model predictive control, *in* '19th IFAC World Congress', Vol. 19, Cape Town, South Africa, pp. 2189–2194.

van der Lee, J., Svrcek, W. & Young, B. (2008), 'A tuning algorithm for model predictive controllers based on genetic algorithms and fuzzy decision making', *ISA Transactions* **47**(1), 53–59.

Waschl, H., Alberer, D. & del Re, L. (2012), Automatic Tuning Methods for MPC Environments, *in* 'Computer Aided Systems Theory - Eurocast 2011, Pt Ii', 13 edn, Vol. 6928, Las Palmas de Gran Canaria, Spain, pp. 41–48.

Weber dos Santos, J. E., Trierweiler, J. O. & Farenzena, M. (2019), 'Robust tuning for classical MPC through the Multi-Scenarios Approach', *Industrial & Engineering Chemistry Research* p. acs.iecr.8b05485.

Weber dos Santos, J. E. W., Trierweiler, J. O. & Farenzena, M. (2017), 'Model Predictive Control Tuning Strategy for Non-Square Systems and Range Controlled Variables Based on Multi-Scenarios Approach', *Industrial & Engineering Chemistry Research* **56**(40), 11496–11506.

Wojsznis, W., Gudaz, J., Blevins, T. & Mehta, A. (2003), 'Practical approach to tuning MPC.', *ISA transactions* **42**(1), 149–162.

Wood, R. K. & Berry, M. W. (1973), 'Terminal composition control of a binary distillation column', *Chemical Engineering Science* **28**(9), 1707–1717.

Yamashita, A. S., Zanin, A. C. & Odloak, D. (2016), 'Tuning of model predicitve control with multi-objective optimization', *Brazilian Journal of Chemical Engineering* **33**(2), 333–346.

Yu, D., Deng, F., Wang, H., Hou, X., Yang, H. & Shan, T. (2022), 'Real-Time Weight Optimization of a Nonlinear Model Predictive Controller Using a Genetic Algorithm for Ship Trajectory Tracking', *Journal of Marine Science and Engineering* **10**(8).

Zarkogianni, K., Vazeou, A., Mougiakakou, S. G., Prountzou, A. & Nikita, K. S. (2011), 'An Insulin Infusion Advisory System Based on Autotuning Nonlinear Model-Predictive Control', *IEEE Transactions on Biomedical Engineering* **58**(9), 2467–2477.

Appendix A

Discrete-time state space model based on analytical expression of the step response

The IHMPC presented by Odloak (2004) is based on the analytical expression of the system's step response composed of distinct stable poles. Assuming a MIMO stable system with n_u inputs and n_y outputs with distinct poles, where the transfer function relating the input u_j with output y_i is given by

$$G_{i,j}(s) = \frac{b_{i,j,0} + b_{i,j,1}s + \cdots + b_{i,j,n_b}s^{n_b}}{1 + a_{i,j,1}s + \cdots + a_{i,j,n_a}s^{n_a}} \tag{A.1}$$

where $n_a > n_b$ are the order of the numerator and the denominator. The discrete-time state space model, based on the analitycal expression of the step response, can be described as follows:

$$\begin{cases} \begin{bmatrix} \mathbf{x}^s(k+1) \\ \mathbf{x}^d(k+1) \end{bmatrix} = \begin{bmatrix} \mathbf{I}_{n_y} & \mathbf{0} \\ \mathbf{0} & \mathbf{F} \end{bmatrix} \begin{bmatrix} \mathbf{x}^s(k) \\ \mathbf{x}^d(k) \end{bmatrix} + \begin{bmatrix} \mathbf{D}^0 \\ \mathbf{D}^d\mathbf{FN} \end{bmatrix} \Delta\mathbf{u}(k) \\ \\ \mathbf{y}(k) = \begin{bmatrix} \mathbf{I}_{n_y} & \Psi \end{bmatrix} \begin{bmatrix} \mathbf{x}^s(k) \\ \mathbf{x}^d(k) \end{bmatrix} \end{cases} \tag{A.2}$$

$\mathbf{x}^s = [x_1 \ldots x_{n_y}]^\top$ are the stable modes of system; $\mathbf{x}^d = [x_{ny+1} \ldots x_{n_y(n_u n_a+1)}]^\top$ represents the artificial integrating states obtained from the incremental form of inputs and corresponds to the predicted output steady-state; n_a is the order of the system; $\mathbf{I}_{n_y}$ is a $n_y \times n_y$ identity matrix; The auxiliary matrices, $\mathbf{D}^d$, $\mathbf{F}$, $\mathbf{D}^0$, Ψ, and $\mathbf{N}$ are given by:

$$\mathbf{D}^d_{n_d \times n_d} = \text{diag}\begin{bmatrix} d^d_{1,1,1} \ldots d^d_{1,1,n_a} \ldots d^d_{1,n_u,1} \ldots d^d_{1,n_u,n_a} \ldots d^d_{n_y,n_u,1} \ldots d^d_{n_y,n_u,n_a} \end{bmatrix} \tag{A.3}$$

99

$$\mathbf{F}_{n_d \times n_d} = \text{diag}\left[e^{r_{1,1,1}kT_s} \ldots e^{r_{1,1,n_a}kT_s} \ldots e^{r_{1,n_u,1}kT_s} \ldots e^{r_{1,n_u,n_a}kT_s}\right.$$

$$\left. \ldots e^{r_{n_y,n_u,1}kT_s} \ldots e^{r_{n_y,n_u,n_a}kT_s}\right] \tag{A.4}$$

$$\mathbf{D}^0_{n_d \times n_d} = \begin{bmatrix} d^0_{1,1} & \ldots & d^0_{1,n_u} \\ \vdots & \ddots & \vdots \\ d^0_{n_y,1} & \ldots & d^0_{n_y,n_u} \end{bmatrix} \tag{A.5}$$

$$\boldsymbol{\Psi}_{ny \times n_d} = \begin{bmatrix} [1 \ldots 1]_{1 \times n_u n_a} & 0 & 0 \\ 0 & \ddots & 0 \\ 0 & 0 & [1 \ldots 1]_{1 \times n_u n_a} \end{bmatrix} \tag{A.6}$$

$$\mathbf{N}_{n_d \times n_u} = \begin{bmatrix} \mathbf{J}_1 \\ \vdots \\ \mathbf{J}_{n_y} \end{bmatrix} \tag{A.7}$$

$$\mathbf{J}_{i_{n_u n_a} \times n_u} = \begin{bmatrix} 1 & 0 & \ldots & 0 \\ \vdots & \vdots & \ddots & \vdots \\ 1 & 0 & \ldots & 0 \\ & & \ddots & \\ 0 & 0 & \ldots & 1 \\ \vdots & \vdots & \ddots & \vdots \\ 0 & 0 & \ldots & 1 \end{bmatrix} \tag{A.8}$$

where $n_d = n_u n_y n_a$; $d^0_{i,j}$, $d^d_{i,j,l}$ are the partial fraction coefficients; $r^d_{i,j,l}$ are the distinct poles; T_s is the sampling time

This model structure is used to build the IHMPC present in Subsection 3.3.3 and Section 4.1 of this thesis. For CSTR case study (Subsection 3.3.3), the state

space model matrices obtained from Eq. 3.21 are given by Eq. A.9, A.10, and A.11.

$$A_{\text{cstr}} = \begin{bmatrix} 1 & 0 & 0 & 0 & 0 & 0 & 0 & 0 & 0 & 0 \\ 0 & 1 & 0 & 0 & 0 & 0 & 0 & 0 & 0 & 0 \\ 0 & 0 & 0.4721 & 0 & 0 & 0 & 0 & 0 & 0 & 0 \\ 0 & 0 & 0 & 0.5063 & 0 & 0 & 0 & 0 & 0 & 0 \\ 0 & 0 & 0 & 0 & 0.4721 & 0 & 0 & 0 & 0 & 0 \\ 0 & 0 & 0 & 0 & 0 & 0.5063 & 0 & 0 & 0 & 0 \\ 0 & 0 & 0 & 0 & 0 & 0 & 0.4721 & 0 & 0 & 0 \\ 0 & 0 & 0 & 0 & 0 & 0 & 0 & 0.5063 & 0 & 0 \\ 0 & 0 & 0 & 0 & 0 & 0 & 0 & 0 & 0.4721 & 0 \\ 0 & 0 & 0 & 0 & 0 & 0 & 0 & 0 & 0 & 0.5063 \end{bmatrix}$$

(A.9)

$$B_{\text{cstr}} = \begin{bmatrix} -0.0413 & -2.1052 \\ 0.0568 & 1.0439 \\ -0.4600 & 0 \\ 0.5142 & 0 \\ 0 & -9.6614 \\ 0 & 11.4280 \\ -0.0846 & 0 \\ 0.0620 & 0 \\ 0 & -1.7767 \\ 0 & 1.3770 \end{bmatrix}$$

(A.10)

$$C_{\text{cstr}} = \begin{bmatrix} 1 & 0 & 1 & 1 & 1 & 1 & 0 & 0 & 0 & 0 \\ 0 & 1 & 0 & 0 & 0 & 0 & 1 & 1 & 1 & 1 \end{bmatrix}$$

(A.11)

For BCS case study (Section 4.1), the state space model is obtained based on Eq. 4.1 are represented by Eq. A.12, A.13, and A.14

$$A_{\mathrm{bcs}} =
\begin{bmatrix}
1 & 0 & 0 & 0 & 0 & 0 & 0 & 0 & 0 & 0 & 0 & 0 & 0 & 0 & 0 & 0 & 0 \\
0 & 1 & 0 & 0 & 0 & 0 & 0 & 0 & 0 & 0 & 0 & 0 & 0 & 0 & 0 & 0 & 0 \\
0 & 0 & 0 & 0 & 0.3679 & 0 & 0 & 0 & 0 & 0 & 0 & 0 & 0 & 0 & 0 & 0 & 0 \\
0 & 0 & 0 & 0 & 0 & 0.8139 & 0 & 0 & 0 & 0 & 0 & 0 & 0 & 0 & 0 & 0 & 0 \\
0 & 0 & 0 & 0 & 0 & 0 & 0 & 0.3679 & 0 & 0 & 0 & 0 & 0 & 0 & 0 & 0 & 0 \\
0 & 0 & 0 & 0 & 0 & 0 & 0 & 0 & 0.8139 & 0 & 0 & 0 & 0 & 0 & 0 & 0 & 0 \\
0 & 0 & 0 & 0 & 0 & 0 & 0 & 0 & 0 & 0 & 0.3679 & 0 & 0 & 0 & 0 & 0 & 0 \\
0 & 0 & 0 & 0 & 0 & 0 & 0 & 0 & 0 & 0 & 0 & 0.8139 & 0 & 0 & 0 & 0 & 0 \\
0 & 0 & 0 & 0 & 0 & 0 & 0 & 0 & 0 & 0 & 0 & 0 & 0 & 0.3679 & 0 & 0 & 0 \\
0 & 0 & 0 & 0 & 0 & 0 & 0 & 0 & 0 & 0 & 0 & 0 & 0 & 0 & 0.8139 & 0 & 0 \\
0 & 0 & 0 & 0 & 0 & 0 & 0 & 0 & 0 & 0 & 0 & 0 & 0 & 0 & 0 & 0.3679 & 0 \\
0 & 0 & 0 & 0 & 0 & 0 & 0 & 0 & 0 & 0 & 0 & 0 & 0 & 0 & 0 & 0 & 0.8139
\end{bmatrix}$$

$$(A.12)$$

$$B_{\mathrm{bcs}} = \begin{bmatrix} -0.1866 & -0.1344 \\ 1.9634 & -0.3898 \\ 0 & 0 \\ 0 & 0 \\ -0.0177 & 0 \\ 0.1911 & 0 \\ 0 & 0 \\ 0 & 0 \\ 0 & -0.0128 \\ 0 & 0.1377 \\ 0 & 0 \\ 0 & 0 \\ -0.7201 & 0 \\ -0.0064 & 0 \\ 0 & 0 \\ 0 & 0 \\ 0 & 0.1456 \\ 0 & -0.0046 \end{bmatrix} \tag{A.13}$$

$$C_{\mathrm{bcs}} = \begin{bmatrix} 1 & 0 & 1 & 1 & 1 & 1 & 1 & 1 & 1 & 1 & 0 & 0 & 0 & 0 & 0 & 0 & 0 & 0 \\ 0 & 1 & 0 & 0 & 0 & 0 & 0 & 0 & 0 & 0 & 1 & 1 & 1 & 1 & 1 & 1 & 1 & 1 \end{bmatrix} \tag{A.14}$$

UFBA
UNIVERSIDADE FEDERAL DA BAHIA
ESCOLA POLITÉCNICA
PROGRAMA DE PÓS GRADUAÇÃO EM ENGENHARIA
INDUSTRIAL - PEI
Rua Aristides Novis, 02, 6º andar, Federação, Salvador
BACEP: 40.210-630Telefone: (71) 3283-9800
E-mail: pei@ufba.br Home page: http://www.pei.ufba.br